Dissertation
submitted to the
Combined Faculty of Natural Sciences and Mathematics
of the Ruperto Carola University Heidelberg, Germany
for the degree of Doctor of Natural Sciences

Presented by

M.Sc. Kevin Haubrich
born in Trier (Germany)
Oral examination: 15.06.2020

RNA binding regulates TRIM25-mediated RIG-I ubiquitination

Referees: Prof. Dr. Carsten Sachse
Prof. Dr. Irmgard Sinning

Abstract

TRIM25 is an E3 ligase of the tripartite motif protein family, that is best known for its function in innate immunity, where it activates the pattern recognition receptor RIG-I. More recently, it was identified as a putative RNA binding protein, though lacking domains with known RNA-binding potential. In this thesis, I present evidence that RNA binding is mediated by the coiled-coil (CC) and PRY/SPRY domain with possible contributions of the disordered linker connecting the domains. Using NMR spectroscopy and mutational analysis, I could map the RNA binding site on these domains. Small-angle X-ray scattering indicates that RNA-binding stabilizes an inherent, but weak interaction between these domains leading to a more rigid domain architecture possibly explaining the increase in ubiquitination activity in the presence of RNA observed by us and others. In line with that, mutants affecting RNA binding or the weak CC:PRY/SPRY interaction also reduced ubiquitination of the RIG-I caspase-activation and recruitment domains (CARDs). RNA binding in addition promotes phase-separation and association with RIG-I, as our results indicate that there is no direct protein-protein interaction between TRIM25 and RIG-I. This reconciles seemingly controversial results in recent studies and contributes to further unravel the mechanism behind the immune response activation upon viral infection.

Zusammenfassung

TRIM25 ist eine E3-Ligase aus der Familie der 'tripartite motif'-Proteine, die in der angeborenen Immunabwehr den intrazellulären Rezeptor für virale RNA RIG-I aktiviert. In neuerer Zeit wurde es als möglicherweise RNA-bindendes Protein beschrieben, auch wenn es keine Domänen mit bekannten RNA-Bindestellen besitzt. In dieser Arbeit zeige ich, dass die coiled-coil- (CC) und PRY/SPRY-Domänen sowie der unstrukturierten Linkers, der die Domänen verbindet, RNA bindet. Mit Hilfe von Kernspinresonanzspektroskopie und Mutationsanalyse konnten die Bindestellen dieser Domänen bestimmt werden. Röntgenkleinwinkelstreuung zeigt, dass RNA-Bindung die schwache Interaktion zwischen diesen Domänen verstärkt und dadurch zu einer weniger flexiblen Domänenanordnung führt, die möglicherweile die Zunahme der E3-Ligaseaktivität erklären kann, die wir und andere Forschungsgruppen beobachtet haben. Im Einklang damit reduzieren Mutanten, die die RNA-Bindung oder die Interaktion zwischen CC und PRY/SPRY reduzieren, auch die Ubiquitinierung der RIG-I Caspase-Aktivierungs and Recruitmentdomänen (CARDs) in Zellen. RNA-Bindung fördert auch die Assoziation mit RIG-I in durch Phasentrennung enstandenden Tröpfchen. Letzteres ist von besonderer Bedeutung, da wir keine direkte Protein/Protein-Interaktion zwischen TRIM25 und RIG-I nachweisen konnten. Wir können damit scheinbare Widersprüche aus früheren Veröffentlichungen ausräumen und zur Aufklärung dieses Mechanismus, der der angeborenen Immunabwehr gegen virale Infektionen zu Grunde liegt, beitragen.

Publications

[1] L. P. Feilen*, K. Haubrich*, P. Strecker, S. Probst, S. Eggert, G. Stier, I. Sinning, U. Konietzko, S. Kins, B. Simon, and K. Wild, "Fe65-PTB2 Dimerization mimics FE65-APP Interaction," *Frontiers in Molecular Neuroscience*, vol. 10, p. 140, 2017.

[2] M. G. Koliopoulos, M. Lethier, A. G. van der Veen, K. Haubrich, J. Hennig, E. Kowalinski, R. V. Stevens, S. R. Martin, C. Reis e Sousa, S. Cusack, and K. Rittinger, "Molecular mechanism of Influenza A NS1-mediated TRIM25 recognition and inhibition," *Nature Communications*, vol. 9, no. 1, p. 1820, 2018.

[3] F. P. Williams, K. Haubrich, C. Perez-Borrajero, and J. Hennig, "Emerging RNA-binding roles in the TRIM family of ubiquitin ligases," *Biological Chemistry*, vol. 400, p1443-1464, 2019.

* equal contribution

Contents

List of Figures

List of Tables

1. Introduction

1.1. TRIM proteins

The TRIM protein family constitutes one of the largest classes of ubiquitin E3 ligases with at least 77 members in humans and more than 200 in fish [4, 5]. They owe their name to the conserved tripartite motif (TRIM) containing a RING domain, one or two B-Box domains and a coiled-coil at their N-terminus (RBCC) (Figure 1.1 A)[6]. Within the RBCC it is the RING domain that interacts with the E2 ubiquitin conjugating enzyme and mediates the E3 ubiquitin ligase activity (section 1.2, Figure 1.2. Some TRIM proteins e.g. TRIM28 may also conjugate other small ubiquitin-like modifiers such as SUMO or ISG15 [7, 8, 9]. The coiled-coil forms anti-parallel dimers, that can act as a platform for the assembly of complexes with a variety of host and viral proteins [10, 11]. The function of the B-Box domains remains unclear with proposed functions ranging from promotion of oligomerisation, assistance in the recruitment of E2/ubiquitin conjugates to regulation of catalytic activity [12, 13, 14]. The tripartite motif is usually encoded in a single exon and the linker regions connecting individual domains show high levels of conservation, indicating that it evolved as a single structural and functional unit [15, 16]. Nevertheless, loss of individual domains of the RBCC is common. This most often affects B-Box1 or the RING domain, while B-Box2 and the coiled-coil are almost always present [15].

TRIM proteins usually feature additional domains in their C-terminal region, that enhance structural and functional diversity, allowing for a wide range of functions in cellular differentiation, innate immunity, autophagy, apoptosis, DNA maintenance and tumor progression and supression [4]. TRIM proteins have historically been sub-classified based on their C-terminal domains in 11 distinct subclasses, an approach that has been largely confirmed by sequence analysis of the tripartite motif or parts thereof [6, 18, 16, 19, 15, 20] (Figure 1.1 B). It is typically the C-terminal domain that mediates recruitment of substrates, either through direct protein-protein interaction or indirectly

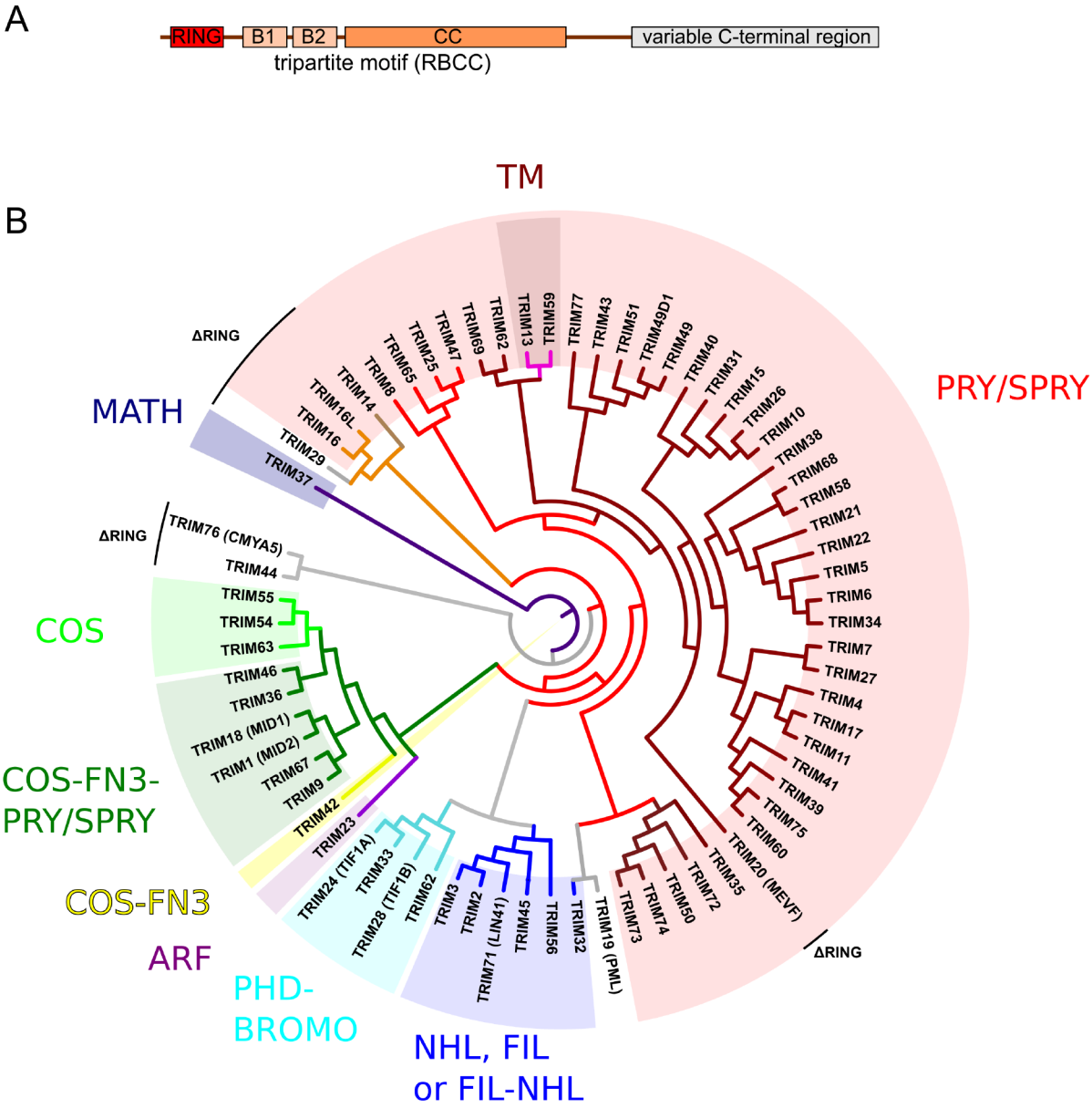

Figure 1.1.: Domain architecture and phylogeny of TRIM proteins: **(A)** TRIM proteins own their name to the tripartite motif containing a RING domain, one or two B-Boxes and a coiled-coil. In addition they have variable C-terminal regions. **(B)** A phylogenetic tree obtained by sequence analysis of the tripartite motif of the human TRIM proteins largely confirms the classification of TRIM proteins based on their C-terminal domains. A notable exception from this is TRIM32, which possibly acquired its NHL domain separately from the other NHL carrying TRIMs. The color change within the PRYSPRY domain carrying TRIMs denotes the loss of B-Box1 [17].

through protein-RNA interactions [21, 22, 23, 24, 25]. The most common C-terminal domain is the PRY/SPRY domain found in more than half of all human TRIM proteins [17]. Less common are the NCL-1, H2A, LIN-41 (NHL) domain, often associated with a filamin (FIL) domain, the C-terminal subgroup One Signature (COS) box/domain, usually associated with a Fibronectin type III (FN3) domain, and PHD finger/bromodomains [17]. Two human TRIM proteins have acquired transmembrane domains. Meprin and TRAF homology (MATH) and ADP ribosylation factor (ARF) domains are each only found in a single TRIM protein in humans [17]. Few of these groups have functions that are only defined by their C-terminal domains. Examples for this are the TRIMs with PHD-Bromo domains that act as transcriptional regulators or TRIM-NHL proteins that are generally involved in miRNA and mRNA regulation [26, 17]. The functions of the other groups are either more diverse or poorly characterized.

1.2. E3 ligases and the ubiquitin system

Ubiquitination (also ubiquitinylation) is a key post-translational modification for both proteostasis and cellular signalling [27] (Figure 1.2). Ubiquitin is a small, globular 76 amino acids long protein, that is universally conserved in all eukaryotes [27]. Via its C-terminal glycine it can be conjugated to a lysine of the target protein [27]. Conjugation of additional ubiquitins to one of the seven lysines (K6, K11, K27, K29, K33, K48, K63) or less frequently the N-terminus (M1) of the previous ubiquitin leads to the formation of poly-ubiquitin chains [27]. The biological roles of different ubiquitin chains vary with K11 and K48 being the main signals for proteasomal degradation, while the K27, K63 and M1 are involved in various signalling processes, e.g. in DNA damage response and innate immunity [27]. K63-linked chains in addition also regulate bulk autophagy and through interaction with autophagy receptors, such as p62, allows for selective autophagy [28, 29]. Mixed and branched chains are also common [30].

This diversity of chain topologies and biological functions is achieved by a cascade of enzymes called E1, E2 and E3 ligases. The E1 ligases, of which only two genes exist in humans, are ubiquitin activating enzymes that couple ATP hydrolysis to the linkage of the C-terminal carboxy-group of ubiquitin to a catalytic cysteine side chain of the E2 ligase forming a thioester [31]. About 38 different E2 ligases exist in humans and they are the key regulators of chain topology and therefore function of the ubiquitin chain in the following step [32]. The last step of the catalytic cascade is catalysed by E3 ligases,

a diverse group of enzymes with around 600 members in humans [33]. E3 ligases can be categorized in three main groups according to their catalytic domains: Really Interesting New Gene (RING), Homologous to the E6-AP Carboxyl Terminus (HECT) and RING-between-RING (RBR) ligases [33]. While HECT and RBR ligases form an intermediate with the ubiquitin bound via a catalytic cysteine, RING domains, such as those found in TRIM proteins, have no intermediates and merely act as a scaffold to bring together the ubiquitin-charged E2 and the substrate [33, 34]. Binding of the E2-ubiquitin conjugate by the RING domain orients the thioester for nucleophilic attack by the amino group of one of the target protein's lysines leading to isopeptide bond formation [34]. Repetition of this cycle leads to the formation of poly-ubiquitin chains. Many, but not all, RING domains require oligomerisation for their activity [34].

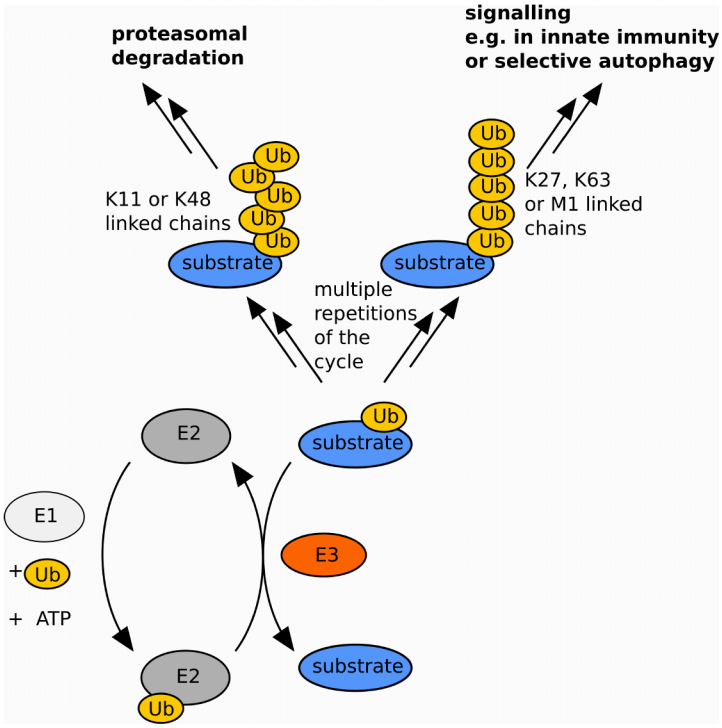

Figure 1.2.: Mechanism and outcome of ubiquitination: The ubiquitination machinery consists of the ubiquitin-activating E1, that conjugates ubiquitin to the E2 ubiquitin-conjugating enzyme via a labile thioester. This conjugate binds the E3 and the ubiquitin is transferred to the lysine or N-terminus of the substrate. In RING E3 ligases this happens in a single step, whereas HECT and RBR ligases have thioester intermediates. Depending on the topology of ubiquitin chains the substrate is either targeted for degradation by the proteasome (K11, K48) or autophagosomes (K63) or is activated in a signalling cascade (K27, K63, M1) [30, 27].

1.3. RNA binding E3 ligases and TRIM proteins

A small subset of E3 ubiquitin ligases are also RNA binding proteins [35]. Members of this group include the Mex-3 RNA Binding Family and Roquins [36, 37]. The recent discovery of direct RNA binding of several TRIM proteins discussed in the following paragraphs has considerably extended this list [38, 17]. So far very little is known about how E3 ligase activity and RNA binding are connected in these proteins. A notable exception from this is Roquin-2, where RNA binding was shown to regulate auto-ubiquitination in a E2-specific manner [37].

It was long known that some TRIM proteins, especially members of the TRIM-NHL family, such as human TRIM32, *Drosophila melanogaster* brain tumor (BRAT) and *Caenorhabditis elegans* lin41, are part of pathways that involve RNA[39, 40, 41], but only recently the rise of genome-wide approaches to find novel RNA-binding domains suggested that several TRIM proteins directly bind RNA [42, 43, 38]. Among the identified RNA-binding TRIM proteins were not only TRIM-NHL proteins, such as TRIM71 and TRIM56, but also PHD-bromodomain carrying TRIM28, 33, 44 and the PRY/SPRY-carrying TRIM25 [42, 43, 38, 44]. Further studies have also identified TRIM26 and 65 as potentially new RNA-binding TRIM-PRY/SPRY proteins [45, 46].

By now it is well established that the RNA-binding TRIM-NHL proteins are involved in translational regulation of protein expression and miRNA processing through direct RNA-binding [47, 48, 49, 50, 51, 52, 53, 46, 54]. TRIM-NHL proteins usually show specific RNA-binding to a well defined RNA motif via their C-terminal NHL domain [48, 54, 55, 56]. The central role of the NHL domain for RNA specificity has been elegantly demonstrated by experiments that swapped the NHL domains of TRIM71 and TRIM32 also leading to a swap of RNA targets [47].

RNA-binding of TRIM25 and other PRY/SPRY proteins is less well understood and therefore the focus of this work will be on their study. For a more detailed description of the current knowledge on other TRIM proteins the reader is directed to a recent review [17].

1.4. PRY/SPRY domain carrying TRIMs

The Sp1A kinase and Ryanodine receptors (SPRY) domain is a globular protein-protein interaction domain that is found alone or together with COS and FN3 domains in a large number of vertebrate TRIM proteins [15]. Although originally thought to be vertebrate-specific, SPRY domain carrying TRIM proteins have recently also been identified in invertebrates [57]. Phylogenetic analysis suggests that the mammalian TRIM-SPRY proteins can be further categorised into an evolutionary more ancient group containing members such as TRIM8, 25, 65 with orthologs in all vertebrates and a younger subgroup, containing prominent members such as TRIM5 and TRIM21, that only emerged in mammals and has seen a remarkable diversification suggesting strong evolutionary pressure [15]. This latter group plays important roles in innate immunity, as exemplified by the retroviral restriction factor TRIM5α, and likely emerged from the ancient group after loss of B-Box1 [15, 58]. As example of the functions of this group TRIM5α binds retroviral capsids using its PRY/SPRY domain and then assembles as a hexagonal lattice on the capsid via its CC and B-Box2 [59]. TRIM21, another member of this group binds intracellular antibodies and targets their antigens for degradation [60]. Trim-away, a targeted degradation system for the removal of host proteins based on their interaction with an antibody specific for the target protein, utilizes TRIM21 [61].

Members of the first subgroup, such as TRIM25 are also involved in innate immunity, but they have a wider set of functions [62, 63, 37]. TRIM8 for example, acts as a tumor supressor by regulating p53 and is involved in inflammation [62]. Its close relative TRIM65 in addition to regulating p53 also ubiquitinates TNRV6, a protein crucial for miRNA mediated mRNA silencing [64].

Structurally the SPRY domain is formed by approximately 140 aminoacids (aa) forming a β-sandwich [19]. N-terminally of the SPRY domain an associated PRY motif is usually found, that folds as an integral part of the resulting PRY/SPRY domain (equivalent to B30.2 domain or RFP-like domain) [65]. Although the core fold of PRY/SPRY domains is highly conserved, four flexible loop regions termed v1-4 differ widely in length and composition allowing for the wide range of substrate specificities found in PRY/SPRY domains ranging from linear peptides to large macromolecular assemblies [66, 67, 68] (Figure 1.3).

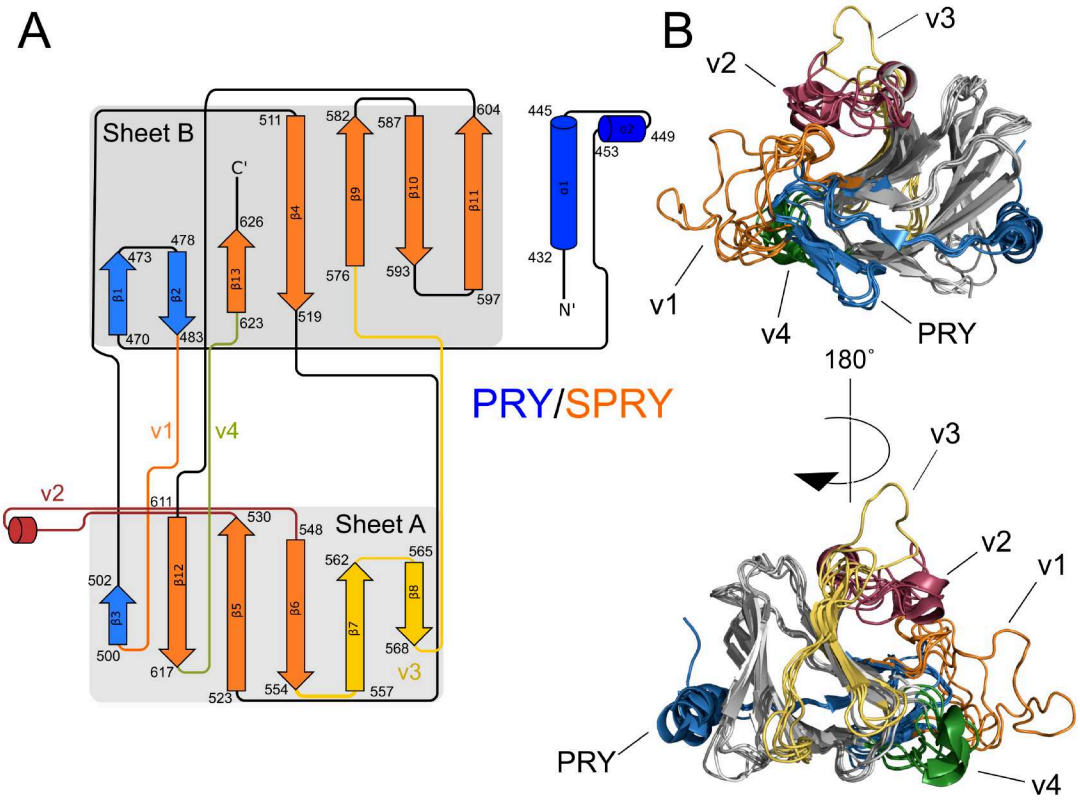

Figure 1.3.: Structure of the PRY/SPRY domain: **(A)** Topology map of the PRY (blue) and SPRY (orange) motif of the human TRIM25 PRY/SPRY domain (PDB: 6FLM). The variable loop regions v1-4 are highlighted. **(B)** Alignment of the available structures of primate PRY/SPRY domains (rhesus macaque TRIM5α (PDB:2LM3), human TRIM20(PDB:4CG4), human TRIM21(PDB:2IWG), human TRIM25(PDB:6FLM), human TRIM72(PDB:3KB5)) highlighting the variable regions v1-v4, that allow for diversity in substrate binding [17].

1.5. TRIM25 and its functions

TRIM25 was first identified as estrogen-dependent finger protein (efp), a 71 kDa protein containing a RING domain and two B-Boxes [69] (Figure 1.4). Later work also identified a coiled-coil and a C-terminal PRY/SPRY domain [70]. Historically, the first discovered functions of TRIM25 pointed towards a role in cell cycle regulation and morphogenesis: TRIM25 is highly abundant in human breast cancer samples and its expression is induced by estrogen [70, 71, 72]. TRIM25 knock-out mice are viable but have underdeveloped uteri and reduced responsiveness to estrogen [73]. TRIM25 was since shown to regulate expression levels of several important regulators of cell cycle and cell fate such as p53, MDM2, 14-3-3σ, ERG and ATBF1 [74, 75, 37, 76]. In line with this, TRIM25 was identified as one of the key regulators of tumor metastasis and its knock-down or depletion by the small molecule nitroxoline slows tumor growth [63, 77, 78].

Apart from its role in cell cycle regulation and morphogenesis TRIM25 also plays a crucial role in innate immunity. TRIM25 is one of several ubiquitin E3 ligases that activate the pattern recognition receptor RIG-I (Retinoic acid inducible gene I, alternatively called DDX58) in response to RNA virus infection [21, 79]. RIG-I features two N-terminal caspase-activation and recruitment domains (CARDs), a central RNA helicase domain and a C-terminal domain (CTD) (Figure 1.4). In the resting state the CARDs are bound and inhibited by the helicase domain, but get released when double-stranded RNA with a 5'-tri- or diphosphate binds the helicase domain and CTD [80]. TRIM25 will then attache Lysine 63-linked (K63-linked) polyubiquitin chains to K172 and other lysines in the second RIG-I CARD [21]. Ubiquitination promotes the formation of helical CARD tetramers that can subsequentially interact with the mitochondrial antiviral signalling protein (MAVS) at the surface of mitochondria and trigger MAVS filament formation [81]. MAVS filament formation activates downstream signalling pathways leading to interferon expression [82]. MAVS itself is also a ubiquitination target of TRIM25 [83]. In addition, TRIM25 releases unanchored K63-linked poly-ubiquitin chains, that can activate RIG-I [84].

Additional E3 ligases, including the RING finger protein leading to RIG-I activation (Riplet), mex-3 RNA-binding family member C (MEX3C), and TRIM4 are known to ubiquitinate RIG-I and do so at different sites in the CARDs and CTD, but their importance and possible redundancy remains controversial [85, 86, 87, 88]. A sequential ubiquitination of RIG-I first by Riplet in the CTD followed by ubiquitination of the CARDs by TRIM25 has been suggested [79]. The importance of TRIM25 in innate

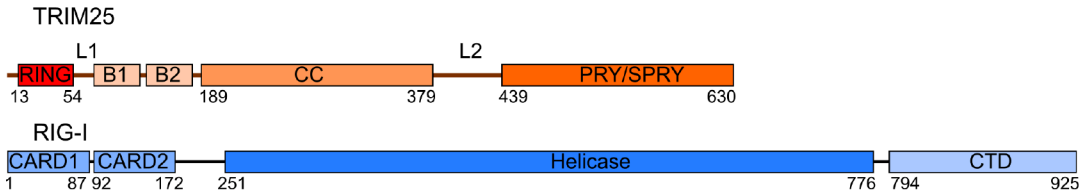

Figure 1.4.: Schematic representation of the domain arrangement of TRIM25 and RIG-I. TRIM25 contains the tripartite motif consisting of a RING domain, two B-Box domains and a coiled-coil (CC) and features a C-terminal PRY/SPRY domain. RIG-I features two caspase-activation and recruitment domains (CARDs), a helicase domain and a C-terminal domain (CTD).

immunity is however highlighted by the variety of mechanisms developed by viruses to inhibit its role in RIG-I signalling and evade innate immunity [89][90][91][92][93]. The best studied example of this is the Influenza A non-structural protein-1 (NS1) that binds the TRIM25 CC via its effector domain and prevents ubiquitination of RIG-I [89, 10].

Pull-down experiments from cells have shown that the TRIM25 PRY/SPRY and RIG-I CARDs alone are sufficient for co-purification of both proteins [21]. RIG-I T55I and mouse TRIM25 F592A and I594A/L604A were described to reduce interaction between the proteins [101, 110]. Subsequent work however showed that RIG-I T55I reduced interaction with K63-linked poly-ubiquitin chains rather than TRIM25 [84]. Despite the strong evidence for complex formation in cells so far there is no evidence for a direct interaction *in vitro*.

TRIM25's role in innate immunity is not restricted to RIG-I: It also activates the zinc-finger antiviral signalling protein (ZAP), that mediates the degradation of viral RNAs by the exosome [104]. TRIM25 interacts with ZAP via its PRY/SPRY domain, attaches mixed K48/K63-linked chains and is required for the inhibition of viral translation [104]. TRIM25 also binds ribonucleoproteins of influenza A and prevents chain elongation by restricting RNA transport into the polymerase complex [106].

In addition to its ubiquitin ligase activity, TRIM25 can also act as an E3 ligase for ISG15, a ubiquitin-like modifier expressed in response to viral or bacterial expression [98]. So far the only known target of TRIM25 ISGylation is 14-3-3σ, a negative regulator of the cell cycle. In addition, TRIM25 also autoISGylates which negatively regulates ISG15 E3 ligase activity [108].

A full list of TRIM25's known functions can be found in Table 1.1.

	function	**references**
Cell fate decision and morphogenesis	uterus development and estrogen responsiveness	[73]
	targets ERG for degradation	[76]
	stablizes p53 and MDM2	[37, 94, 95]
	regulates ZEB1	[96]
	drives adipozyte differentiation via degradation of PPARγ	[97]
	targets 14-3-3-σ for proteolysis	[74]
	ISGylates 14-3-3-σ	[98]
	promotes tumor cell's migration and invasion	[94, 63, 99, 95]
	together with lin28a and tut4 regulates let-7	[100]
Innate immunity	**activates RIG-I**	[21, 101, 102, 88]
	inhibited by Influenza A NS-1	[89, 10]
	essential co-factor of ZAP	[103, 104, 105]
	blocks RNA chain elongation in Influenza A infection by binding Ribonucleoproteins	[106]
	binds Dengue virus subgenomic RNA leading to reduced interferon expression	[90]
	localizes in stress granules	[107, 102]
	inhibited by several viral proteins	[91, 92, 93]
	auto-ISGylates	[108]
	is modified by SUMO-3, promoting ISGylation	[109]

Table 1.1.: Functions of TRIM25: TRIM25's function broadly fall in two major categories: innate immunity and cell fate decisions/morphogenesis. Functions for which there is evidence for a role of RNA binding in it are printed bold.

1.6. RNA binding of TRIM25

TRIM25 was first identified as an RNA-binding protein by mRNA interactome capture studies in murine embryonal stem cells [38]. Later work established that in addition to 3'-UTRs and exons of mRNAs it also interacts with miRNAs, viral subgenomic RNAs and viral RNPs [38, 105, 100, 90, 106]. Unlike for TRIM-NHL proteins no clear RNA-binding motif could be identified so far, although CLIP-data show a preference for G- and C-rich sequences, and *in vitro* TRIM25 binds both single- and double-stranded RNA with similar affinity [100, 102].

One of the first examples of an RNA-binding role of TRIM25 is in the regulation of the microRNA (miRNA) let-7 [100]. In pluripotent stem cells TRIM25 binds the precursor of let-7 (pre-let-7) and recruits lin28a, a pluripotency promoting factor and the terminal uridyltransferase TUT4. TUT4 then poly-uridilates the RNA, thereby marking it for degradation by the exosome. This possibly requires activation of TUT4 through ubiquitination by TRIM25 [100].

Research into the RNA-binding of TRIM25 not only uncovered its role in new pathways, but also added new understanding to previously known pathways, as mutants affecting RNA-binding also reduced ubiquitination of RIG-I and ZAP *in cells* [105, 102]. It is however not clear in these cases, if RNA binding enhances the catalytic activity of TRIM25 or rather promotes association with substrates. Enhanced auto-ubiquitination and substrate-ubiquitination in the presence of RNA have also been observed *in vitro* [105, 102]. Interestingly, one study reports, that the Dengue virus subgenomic RNA (sfRNA) binds TRIM25 to suppress interferon activation, although the exact mechanism remains unclear [90].

Controversy remains about the RNA-binding domain of TRIM25: While pull-downs hinted towards RNA-binding of the coiled-coil, the cross-linking MS based technique RBDmap identified a 40 aa long peptide in the PRY motif as responsible for RNA-binding [38, 111]. Deletion of the latter in the full-length protein abolished RNA-binding [105]. Deletion of such a long peptide in the context of a folded domain is however likely to affect not only a specific function, but also folding of the whole domain. Mutation of a lysine-rich stretch in the linker connecting CC and PRYSPRY (L2-linker) also reduced RNA-binding [102].

1.7. Macromolecular condensates and RNA-binding

RNA binding was reported to be important for the localisation of TRIM25 in membrane-less organelles through liquid-liquid phase-separation [102]. Such membrane-less organelles allow for the efficient subcellular localisation and enrichment of proteins and facilitate the interaction with their substrates and co-factors [112]. Especially relevant for TRIM proteins is that the high local concentration lead to the formation of oligomeric species, that are thought to be critical for the catalytic function of most TRIM proteins [59, 113, 114]. The best studied case for functionally relevant oligomerisation of a TRIM protein is TRIM5α, which forms hexagonal lattices on the surface of retroviral capsids using its B-Box2 and CC domains [59]. While TRIM5α so far remains the only TRIM protein known to form highly ordered, 2D crystalline oligomers, the recent focus in biology on phase-separation as a principle of cell organisation has contributed new impulses to this discussion [112]. Liquid-liquid phase-separation describes the spontaneous unmixing of a liquid mixture in two liquid phases when a miscibility gap in the phase diagram is reached[112]. The number of possible phases depends on the complexity of the mixture with only two phases allowed in a simple binary mixture, but a great number of phases possible in more complex mixtures as described by Gibb's phase rule $F = C - P + 2$, where F is the number of degrees of freedom in the system, such as temperature, pressure and volume fractions of the components, C the number of components and P the number of phases that co-exist [115]. Miscibility gaps are common for aqueous protein solutions as well and liquid-liquid phase separation therefore is a well known occurrence when handling concentrated protein solutions, e.g. for crystallisation experiments [116]. While these behaviours are usually not biologically relevant due to their high critical concentration of phase separation, multivalent interactions can lower the critical concentration to ranges more common in biological systems [117]. Indeed, many cellular structures such as P-bodies, stress granules, nuclear bodies and Cajal bodies, often collectively referred to as membrane-less organelles, exhibit characteristics of liquid-liquid phase separation [118, 119, 120, 121, 122]. Such a diversity of phase-separated structures with different compositions is expected for a complex mixture such as the cytosol as a consequence of the aforementioned phase rule. Functionally such membraneless organelles are advantageous since they allow for enrichment of lowly expressed proteins while maintaining liquid-like properties such as rapid diffusion [112, 123].

TRIM proteins with their multidomain architecture promoting diverse and often redundant interactions are an excellent example for the multivalent interactions promot-

ing phase separation and subcellular localisation in TRIM-specific, likely membrane-less compartments has been described for almost all TRIM proteins [6]. The best known case for phase-separation in TRIM proteins are the nuclear bodies formed by PML (TRIM19) [124, 119]. In addition to multivalency RNA-binding is another factor driving phase-separation and it is not surprising that the RNA-binding TRIMs TRIM25 and TRIM71 localize in RNA-containing granules likely formed by phase-separation [102, 24].

2. Aims of the Thesis

This thesis aims to elucidate the structural basis of TRIM25 RNA binding and analyse the possible interplay of RNA binding and E3 ligase activity. The latter is especially interesting in light of the reported increase in both auto- and substrate ubiquitination of TRIM25 in the presence of RNA [105, 102]. To this end in a first step the RNA binding domains need to be identified and their binding interfaces characterized at residue resolution. In a further step this will be expanded to understand how RNA targets are recognized and specificity is achieved. This will require insights into the global structure of TRIM25 as a multidomain assembly and how RNA binding affects these domain arrangement. In this context a particular importance comes to the relative position of the RING and PRY/SPRY domains, as these are mediating E3 ligase activity and substrate recognition respectively. Achieving this goal will rely on the combination of structural techniques such as nuclear magnetic resonance spectroscopy (NMR), X-ray crystallography or small angle scattering (SAS) with isothermal titration calorimetry (ITC) and related techniques to determine the thermodynamics of RNA binding and domain interactions.

This approach will allow the design of well characterized point mutants that selectively affect RNA binding or domain interactions and can therefore be used to explore the importance of these interactions in the biological function of TRIM25. A special focus here will be on its role in the ubiquitination of RIG-I.

Lastly, the interaction between TRIM25 and RIG-I is so far structurally uncharacterised. Interactions between E3 ligases and their substrates are often transient and previous attempts to reconstitute the TRIM25/RIG-I complex have failed [102]. NMR is a powerful technique to detect such weak and transient interactions. The special focus here will be on the role of RNA binding and liquid-liquid phase-separation in the TRIM25/RIG-I interaction.

3. Methods

3.1. Protein expression and purification

TRIM25 constructs covering all domains in isolation (1-60, 1-106, 100-189, 189-379, 378-630, 439-630) as well as groups of domains (1-156, 1-189, 1-379, 189-630) and the full-length protein (1-630) were designed based on secondary structure prediction and cloned into pETm22 using restriction-free cloning from a synthetic gene with codon-usage optimized for bacterial expression [125]. The constructs were expressed in BL21(DE3), BL21 Rosetta(DE3) and BL21(DE3) co-expressing bacterial chaperones KJE, ClpB and GroELS [126] with 0.2 μM Isopropyl -D-1-thiogalactopyranoside (IPTG) for 22 hours at 18 °C. The chaperone expression plasmids pBB540 and pBB542 were a kind gift from Bernd Bukau via Addgene (addgene plasmids #27393 and#27395). Cells were lysed by sonication in 50 mM Tris, pH 7.5, 300 mM $NaCl$, 10 mM imidazole, centrifuged and the protein content of pellet and supernatant analysed by denaturing poly-acrylamide gel electrophoresis (SDS-PAGE) to test for soluble protein expression [127]. Expression and purification of soluble constructs was further optimized as described below. A graphical summary of all proteins used in this study can be found in Figure A.1.

TRIM25 RING (1-60, 1-106) and CC (189-379) were cloned into pETM22 featuring a 3C protease-cleavable N-terminal His_6- and thioredoxin (trx)-tag using restriction free cloning [125]. The protein was expressed in *Escherichia coli* BL21(DE3) with 0.2 mM IPTG at 18 °C over night. Cells were lysed by sonication in 50 mM Tris, pH 7.5, 300 mM $NaCl$, 10 mM imidazole, 0.2 mM TCEP supplemented with 10 mM β-mercaptoethanol, 5 mg/ml chicken egg lysosyme and EDTA free protease inhibitor and the cleared lysate applied to a HisTrap HP immobilized metal affinity chromatography column charged with Nickel sulfate. The protein was eluted with a gradient of imidazole in the same buffer, the tag removed by 3C protease cleavage, dialysis into 50 mM Tris, pH 7.5, 300 mM NaCl, 0.2 mM TCEP (membrane cut-off 3.5 kDa) and an additional passage over the HisTrap. For Sortase-mediated ligation (see below) TRIM25 189-407 T405A

F406T and a C-terminal Sortase cleavable His_6-tag was cloned, expressed and purified as 189-379, but the tag was left intact.

TRIM25 PRY/SPRY (439-630) and CC-PRY/SPRY (189-630) were cloned into pETM22 as described before for CC. Both proteins were co-expressed in *E. coli* BL21(DE3) with bacterial chaperones KJE, ClpB and GroELS [126] with 0.2 mM IPTG at 18 °C over night. Cells were lysed and applied to a HisTrap column as CC, but the column was washed with 50 mM Tris, pH 7.5, 350 mM KCl, 5 mM $MgCl_2$ and 1 mM ATP before elution. The eluted proteins were treated with 3C protease, dialysed into 20 mM BisTris, pH 6.0, 100 mM $NaCl$, 0.2 mM TCEP and 5 % glycerol and further purified using a GE HiTrap SP HP cation exchange column to remove the tag and co-purifying chaperones. An N-terminally extended PRY/SPRY construct (407-630) was cloned into pETM20 featuring a TEV-cleavable N-terminal His_6- and thioredoxin (trx)-tag. It was expressed and initially purified as the shorter 439-630 construct. The tag was removed by TEV protease digestion and an additional passage over the HisTrap column. Enhanced monomeric green fluorescence protein (mEGFP)-tagged CC-PRY/SPRY (189-630) was cloned restriction-free into pETM11 featuring a non-cleavable His_6-tag. It was expressed and purified as trx-tagged CC-PRY/SPRY, but without protease cleavage. Mutants of CC, PRY/SPRY and CC-PRY/SPRY and truncations of CC-PRY/SPRY (Δ358-383, Δ358-400, Δ358-407) were purified as the respective wildtype protein.

All proteins were further purified by gelfiltration on a Superdex S75 16/600 (CC and PRY/PRY) or S200 16/600 (CC-PRY/SPRY) in 20 mM MES, pH 6.5, 75 mM NaCl, 0.5 mM TCEP or 20 mM sodium phosphate, pH 6.5, 150 mM NaCl, 1 mM TCEP. For long term storage samples in MES were supplemented with 20 % glycerol, flash-frozen and stored at -80 °C. For stable isotope labelling cells were grown in M9 medium supplemented with $^{15}NH_4Cl$ or $^{15}NH_4Cl$ ^{13}C-Glucose as sole nitrogen and carbon source. For additional perdeuteration a step-wise adaptation protocol was used: Cells were grown overnight in protonated M9 media. This overnight culture was used to induce a small-scale culture in deuterated M9 media to an OD_{600nm}= 0.1, that was grown at 37 °C to an OD_{600nm} of 0.6. The culture was then diluted to the final volume with deuterated M9 supplemented with ^2H-Glucose (for SANS) or $^2H/^{13}C$-Glucose (for NMR) and induced at OD(600nm)=0.8 with 0.2 mM IPTG at 18 °C.

TRIM25 RBCC (1-379) was cloned into a modified pETMBP-1a featuring an N-terminal His_6- and maltose-binding protein (MBP)-tag connected to the protein of interest by a $(GS)_5$-linker. TRIM25 1-407 T405A F406T for Sortase ligation was cloned into pETM41

featuring a TEV-cleavable N-terminal His_6- and maltose-binding protein (MBP)-tag and a C-terminal sortase cleavable His_6-tag. The proteins were co-expressed with bacterial chaperones KJE, ClpB and GroELS in *E. coli* BL21(DE3) [126] with 0.2 mM IPTG at 18 °C over night. Cells were lysed in 50 mM Tris, pH 7.5, 300 mM $NaCl$, 10 mM imidazole, 0.2 mM TCEP, 1 μM $ZnSO_4$ supplemented with 10 mM β-mercaptoethanol, 5 mg/ml chicken egg lysosyme and protease inhibitor and the cleared lysate applied to a HisTrap HP column. After wash of the column with 50 mM Tris, pH 7.5, 350 mM KCl, 5 mM $MgCl_2$ and 1 mM ATP the protein was eluted with a gradient of imidazole in the same buffer and further purified by size-exclusion chromatography (GE Superdex S200 16/600) in 50 mM Tris, pH 7.5, 250 mM NaCl, 0.5 mM TCEP (1-379) or 50 mM Hepes, pH 7.5, 500 mM NaCl, 0.5 mM TCEP.

Full-length TRIM25 for insect cell expression was cloned into a modified pFastBac HTb with a TEV-cleavable N-terminal His_6- and maltose-binding protein (MBP)-tag. The recombinant baculo virus was generated using the MultiBac protocol [128]: Briefly, 1 ng of the vector was transformed into chemically competent *E. coli* DH10MBac cells and plated on LB-agar containing 50 μg/ml kanamycin, 10 μg/ml gentamycin, 10 μg/ml tetracyclin, 100 μg/ml X-gal and 1 mM IPTG and after 48 hours white colonies were selected. This selection process was repeated once more and plasmid DNA purified from an over-night culture. *Spodoptera frugiperda* Sf9 cells grown adherent in SF900 III media were transfected with the purified plasmid DNA using Fugene and cultured in darkness at 27 °C for 48 hours. The supernatant was used for viral amplification by infection of solution cultures of Sf9 at 0.5×10^6 cells/ml. 72 hours post infection the cells were harvested and the supernatant used to infect large scale cultures at 2.5×10^6 cells/ml. The cells were harvested after 48 hours, lysed by sonication in 100 mM Hepes, pH 7.5, 500 mM NaCl, 20 mM $MgCl_2$, 5 % glycerol, 1 mM TCEP and 20 μM $ZnSO_4$. The protein was purified by Nickel affinity chromatography (1 ml GE HisTrap HP) and after TEV cleavage and dialysis overnight further purified to remove the tag by cation exchange in 50 mM Hepes, pH 7.0, 50 mM NaCl, 1 mM TCEP.

RIG-I CARDs were purified and provided by Mathilde Lethier (EMBL Grenoble). Briefly, RIG-I CARDs (1-203 or 1-208) were cloned into the NcoI and KpnI sites of pETM11, expressed in *E. coli* BL21(DE3) Rosetta 2 and induced with 250 M IPTG overnight at 16 °C. The protein was purified by Nickel ion charged nitrilotriacetic acid immobilized on agarose (Ni-NTA) in 25 mM Tris pH 7.5, 150 mM NaCl, 10 % glycerol, 0.5 mM TCEP. The column was washed with 1 M salt and eluted with 300 mM imidazole. The

His_6-tag was removed by TEV protease cleavage and an additional passage over the Ni-NTA column. As a final step the protein was purified using a GE Superdex S75 in 25 mM HEPES pH 7.5, 150 mM NaCl, 0.3 mM TCEP.

RIG-I CARDs WT and T55I (aa 2-200) fused to the red fluorescent protein dTomato and dTomato alone were cloned into pETM11 with a non-cleavable His_6-tag and expressed in *E. coli* BL21(DE3) with 0.4 mM IPTG at 18 °C. The proteins were purified by Nickel affinity chromatography and size exclusion chromatography in 20 mM Hepes, pH 7.5, 100 mM NaCl, 0.2 mM TCEP. For long term storage samples were supplemented with 20 % glycerol, flash-frozen and stored at -80 °C.

The *Staphylococcus aureus* sortase A expression vector with an N-terminal His_6- and B1 domain of protein G (GB1)-tag was a kind gift from Miriam Sonntag (TU Munich) [129]. The protein was expressed in *E. coli* BL21(DE3) overnight at 18 °C with 0.2 mM IPTG and purified using a HisTrap column in 50mM Tris, pH 8.0, 500mM NaCl, 10mM imidazole. The tag was removed by TEV protease cleavage and an additional passage over the HisTrap column. The protein was further purified by size exclusion in 50 mM Tris, pH 7.5, 150 mM NaCl, 0.5 mM TCEP and flash-frozen after addition of 20 % glycerol.

Ubiquitin was expressed from a pET15 vector kindly provided by Rachel Klevit via Addgene (Addgene plasmid #12647) in BL21(DE3) and induced overnight at 18 °C with 0.2 mM IPTG. Cells were lyzed in water and the pH of cleared lysates adjusted to 4.5 using concentrated acetic acid to precipitate most host proteins. After centrifugation the supernatant was further purified using a GE HiTrap SP HP cation exchange column in ammonium acetate, pH 5.1 and a Superdex S75 gel filtration column in 50 mM Hepes, pH 7.5, 50 mM NaCl. The expression plasmid for murine E1 ligase (mE1) in pET28 was a gift from Jorge Eduardo Azevedo (Addgene plasmid #32534) [130]. It was expressed in BL21(DE3) at 16 °C with 0.5 mM IPTG. mE1 was purified using a HisTrap column in 50 mM Hepes, pH 7.5, 150 mM NaCl, 0.5 mM TCEP and gelfiltration on a Superdex S200 in 50 mM Hepes, pH 7.5, 150 mM NaCl, 0.2 mM TCEP. UbcH5C was expressed from a pET15 plasmid provided by Wade Harper (addgene plasmid #15782) in BL21 Rosetta (DE3) with 0.4 mM IPTG for 3 hours at 37°C [31]. UbcH5C was purified using a HisTrap column in 50 mM Hepes, pH 7.5, 150 mM NaCl, 0.5 mM TCEP and gelfiltration on a Superdex S200 in 50 mM Hepes, pH 7.5, 150 mM NaCl, 0.2 mM TCEP.

Purity of all proteins was evaluated by denaturing poly-acrylamide gel electrophoresis (SDS-PAGE) [127]. The protein concentration was estimated by UV absorption at

280 nm using a Thermo Scientific Nanodrop 1000 spectrophotometer and extinction coefficients calculated from the sequence using Protparam [131].

3.2. Sortase A ligation

Sortase A ligation allows to produce segmentally isotope labelled samples for NMR and SANS (section 4.9)[129]. A site in the L2 linker (403-507) was identified that could be mutated into the *Staphylococcus aureus* Sortase A recognition site LPXTG by introducing only two point mutations (T405A F406T).

Perdeuterated His_6-trx-TRIM25 189-407 T405A F406T, natural abundance TRIM25 407-630 and Sortase A were mixed at molar ratios of 1:2:1.2 in 50 mM Tris, pH 7.5, 150 mM $NaCl$, 1 mM TCEP. After addition of 50 mM $CaCl_2$ the mixture was incubated in a 3.5 kDa cutoff Amicon centrifugal filter unit spinning at 3.000 rpm and 22 °C for 6 hours. During this concentration process the concentrator membrane allows the C-terminal cleavage product of the Sortase A reaction to escape from the reaction mixture, thereby shifting the equilibrium of the reaction towards the ligated construct. The centrifugation was stopped every 30 minutes and the mixture diluted with 50 mM Tris, pH 7.5, 150 mM $NaCl$, 1 mM TCEP, 20 mM $CaCl_2$. After the incubation the ligated protein was purified using a HisTrap column in 50 mM Tris, pH 7.5, 300 mM NaCl, 0.2 mM TCEP, 20 mM imidazole and the tag removed by treatment with 3C protease, dialysis and size-exclusion chromatography (Superdex S200 16/600).

His_6-MBP-TRIM25 1-407 T405A F406T was ligated to TRIM25 407-630 using Sortase A in 50 mM Hepes, pH 7.5, 500 mM NaCl, 5 % Glycerol, 20 mM $MgSO_4$, 0.2 mM TCEP, 10 μM $ZnSO_4$ using the same conditions as for the shorter construct. The ligated construct was purified in 50 mM Hepes, pH 7.5, 500 mM NaCl, 5 % Glycerol, 20 mM $MgSO_4$, 0.2 mM TCEP, 10 mM imidazole and the tag removed by TEV protease cleavage, HisTrap and gel filtration into 50 mM Hepes, pH 7.5, 500 mM NaCl, 0.2 mM TCEP, 5 % glycerol.

3.3. Fluorescein-labelling of Ubiquitin

To facilitate the detection of ubiquitin in ubiquitination assays it was labelled using fluorescein. To label reactive amine groups (N-terminus and lysine sidechains), ubiquitin

in 50 mM Hepes, pH 7.0, 50 mM NaCl was incubated overnight with a 5-fold molar excess of 5(6)-Carboxyfluorescein N-hydroxysuccinimide ester. The product was purified by dialysis against the same buffer and gelfiltration on a Superdex S75. N-terminally fluorescein labelled ubiquitin was purchased from Thermo Scientific.

3.4. RNA synthesis and purification

pre-let-7a-1@2 (5'-GUA UAG UUU AAA AGG AGA UAA CUA UAC -3') and DENV-SL (5- GCA GGU CGG AUU AAG CCA UAG UAC GGG AAA AAC UAU GCU ACC UG-3) were *in vitro* transcribed from DNA oligonucleotides using T7 polymerase. The oligonucleotides were designed to contain a DNA sequence complementary to the target RNA fused to a reverse T7 promotor sequence (pre-let-7a-1@2-rev: 5'-GTA TAG TTA TCT CCT TTT AAA CTA TAC TAT AGT GAG TCG TAT T-3', DENV-SL-rev: 5'-CAG GTA GCA TAG TTT TTC CCG TAC TAT GGC TTA ATC CGA CCT GCT ATA GTG AGT CGT ATT A-3'). As a forward primer the sequence of the T7 promotor was used (5'-TAA TAC GAC TCA CTA TA-3'). 2 μM forward and reverse primer, 40 mM Tris, pH 8.0, 0.2 mM MgCl2, 10 mM spermidine, 15 mM DTT, 0.01 % Triton X-100, 4 U/ml TIPP, 0.1 mg/ml T7 polymerase were incubated for 5 hours at 37 °C and extracted by chloroform/phenol treatment. Pre-let-7a-1@2 was further purified from the aqueous phase by preparative gel electrophoresis using a denaturing polyacrylamide gel (15 % acrylamide, 6 M urea), followed by electroelution from the isolated band. DENV-SL was purified by HPLC chromatography using a Thermo DNA Pac PA100 22x250mm anion exchange column at 95 °C in 50 mM Tris, pH 7.5 and eluted with a gradient of sodium perchlorate (50-500 mM). Lnczc3h7a-304-326 (5-UUUUAUCUGAGUUGGAGGUGAAG-3), pre-let-7 loop (5-UAA AAG GAG AU-3) and stem (5'-GUA UAG UUC AAC UAU AC-3') were custom-synthesized by IBA or Microsynth using solid-phase synthesis. Structured RNAs were refolded prior to use by heating to 95 ° C for 5 min and snap-cooling on ice to remove oligomers and misfolded RNAs. RNA concentration was estimated by UV absorption using a Thermo Scientific Nanodrop 1000 spectrophotometer and an absorption coefficient of 0.025 μg^{-1} cm^{-1} ml. A graphical summary of all RNAs used can be found in Figure A.6.

3.5. Circular dichroism Spectroscopy

CD spectra were aquired using a Jasco 815 circular dichroism spectrometer. Samples were measured at 25 °C in quartz cuvettes with 1 mm path length. The buffer used was 20 mM sodium phosphate, pH 6.5, 50 mM sodium chloride and 0.2 mM TCEP and protein concentration was varied between 0.1 and 0.3 mg/ml.

3.6. Nuclear Magnetic Resonance Spectroscopy

NMR spectra were acquired on 14.1, 16.4 and 18.8 T Bruker Avance III spectrometers (corresponding to proton Larmor frequencies of 600, 700 and 800 MHz) equipped with triple-resonance HCN probes. The 600 and 800 MHz spectrometers were equipped with cryogenic probes. Measurements were done in 20mM Na_2PO_4 pH 6.5, 150 mM NaCl, 2 mM TCEP at 293 K. Spectra were processed using NMRPipe[132] and analysed using CCPNMR [133] and NMRFAM-SPARKY [134]. Backbone resonances were assigned based on analysis of HNCA, HNCACB and HN(CO)CACB experiments. The assignment of TRIM25 439-630 was deposited in the BMRB (accession number: 27381). Secondary structure and order parameters were predicted from chemical shifts using TALOS and Sparta+ [135, 136]. Longitudinal and transverse relaxation and $^1H/^{15}N$ heteronuclear NOEs were analysed using PINT [137, 138, 139]. For NMR titrations natural abundance RNA or protein at 1-10 mM initial concentration was stepwise added to 100 μM protein and at each point a $^1H/^{15}N$-HSQC was collected. Changes in peak position and intensity were tracked manually using NMRFAM-SPARKY and analysed for statistical significance using R. Chemical shift perturbations or signal loss were plotted as modified B-factors on the structure of the TRIM25 CC:PRY/SPRY domain (PDB: 6FLN) using Pymol [140].

3.7. Isothermal titration calorimetry

ITC measurements were done in 20 mM MES, pH 6.5, 75 mM NaCl, 0.5 mM TCEP at 20 °C on a Malvern MicroCal PEAQ-ITC. Different RNAs at 20-860 μM were titrated into TRIM25 CC, PRY/SPRY and CC-PRY/SPRY WT or mutant solution at 2-150 μM while stirring at 750 rpm. The DENV-SL RNA was kept in the cell at 15 μM and titrated by TRIM25 189-630 at 110 μM. Experiments were repeated at least three times

and experimental data was fitted using the MicroCal PEAQ-ITC analysis software using the simplest binding mode capable of fully explaining the data (single site or two-site sequential).

3.8. Small Angle X-ray Scattering

SAXS data were collected at the beamlines BM29 at ESRF, Grenoble and P12, operated by EMBL Hamburg at the PETRA III storage ring (DESY, Hamburg, Germany)[141, 142]. Measurements were done at 20°C in 20 mM MES, pH 6.5, 75 mM NaCl and 0.5 mM TCEP in flow cell mode. For each sample and buffer 10 frames of 1 s exposure time (ESRF) or 20-40 frames with 0.05-0.195 s exposure time (DESY) were acquired. Frames were manually checked for radiation damage, averaged and buffer subtracted using PRIMUS [143]. The Guinier approximation was used to estimate the radius of gyration in PRIMUS. Pair-wise distribution functions were calculated by indirect Fourier transform using GNOM (Svergun et al. 1992). Theoretical scattering curves from PDBs were calculated and fitted to experimental data using CRYSOL [144]. SAXS statistics are summarized in Supplementary Table B.2 according to community guidelines [145].

3.9. Small Angle Neutron Scattering

SANS data was collected at ILL D22 [doi:10.5291/ILL-DATA.8-03-956]. Samples were measured in 20 mM MES, pH 6.5, 75 mM NaCl and 0.5 mM TCEP at the RNA matching point in Helma 100QS quartz cuvettes with 1mm path length. The matching point for RNA was calculated using SASSIE to be 63 % D2O [146]. Scattering data and transmission was measured for thermal neutrons of 6 Åwavelength at a detector and collimator distance of 4 m (centered detector) for the sample and buffer, a water reference sample, empty cell, empty and blocked beam. The sample was exposed for 120 min and transmission measured for 2 min. Data was reduced using GRASP and analysed using the ATSAS package [147].

3.10. Structural modelling

Models of the CC-PRY/SPRY with the disordered linker were generated using restricted MD simulations in CNS [148, 149]. A structure of the CC-PRY/SPRY with the extended 73 aa L2 linker was generated and the linker disordered by randomization of the Ψ and Φ backbone angles. The resulting structures were energy-minimized by a 3-step Cartesian dynamics simulated annealing protocol with 40,000 steps at 20,000 K followed by cooling steps from 2000 to 1000 K and 1000 K to 50 K. Separate pools of 5000 structures each were generated in which either only the L2 linker was allowed to move freely, while the CC-PRY/SPRY interface remained fixed, or in addition also one or both PRY/SPRY domains were released from the CC. The pool was fitted against the experimental SAXS data using CRYSOL [144]. Modelling was done jointly with Bernd Simon.

A model of the position of TRIM25 RING on the CC was obtained by alignment of the CC-PRY/SPRY structure (PDB: 6FLN) with the RBCC of TRIM28 (PDB: 6QAJ) in Pymol [150, 140]. The structure of TRIM25 RING bound to UbcH5-ubiquitin conjugate (PDB: 5FER) was aligned to the RING of TRIM28.

3.11. Macromolecular Crystallography

TRIM25 CC-PRY/SPRY was mixed with a 1.2 molar excess of pre-let-7a-1@2 in 20 mM MES, pH 6.5, 75 mM NaCl, 0.5 mM TCEP at 10 μM concentration and concentrated to a final absorption A(280 nm) = 8.4 (absorption rather than concentration is given as the absorption coefficient of the complex was found to differ significantly from the sum of absorptions coefficients of protein and RNA, making a reliable estimation of the concentration difficult). Crystallisation conditions were screened by Brice Murciano at the EMBL Heidelberg crystallization platform at 7 and 20 °C. Crystals grew in Tris, pH 7.5, 20 % ethanol within 24 hours and were further optimized by additive screens. Crystals were cryoprotected by adition of 20 % D-glucose in the reservoir buffer and diffraction data collected at beamline ID30B at ESRF [151]. Data was processed using XDS and molecular replacement was tried using the published structure of human TRIM25 PRY/SPRY and CC in phaser (PDB: 6FLN, 6FLM, 4LTB) [152, 153]. Search models were optimized using CHAINSAW [154]. Collection statistics are summarized in Supplementary Table B.3.

To confirm the presence of RNA in the crystals, they were harvested by centrifugation,

washed twice with reservoir solution and dissolved in loading dye. Samples of the supernatant, wash steps and dissolved crystals were analysed by denaturing polyacrylamide gel (15 % acrylamide, 6 M urea) and stained for nucleic acid using GelRed Nucleic Acid Gel Stain.

For microseeding the complex was crystallized in batch, crystals were smashed, resuspended in reservoir solution and stocks frozen at -80 ° C and different dilutions (1:10 to 1:1000). A suspension diluted 1:100 was used to seed fresh crystallisation plates.

TRIM25 TRIM25 CC-PRY/SPRY and DENV-SL were directly mixed at molar ratios of 1:1.2 on the crystallisation plate (5.4 or 2.7 mg final protein concentration). TRIM25 CC-PRY/SPRY was mixed with a 1.3 molar excess Lnczc3h7a-304-326 and concentrated to final absorption A(280 nm) = 5.5. TRIM25 CC-PRY/SPRY constructs with truncated L2 linker (Δ358-383, Δ358-400, Δ358-407) in complex with pre-let-7 were crystallized as described for the wildtype.

Crystals were cryoprotected using 25 % glycerol, fished and tested for diffraction at various beamlines at ESRF and DESY [155].

20 μM TRIM25 PRY/SPRY (439-630) in 20 mM MES, pH 6.5, 500 mM NaCl, 0.2 mM TCEP was diluted with 100 μM pre-let-7 in 20 mM MES, pH 6.5, 75 mM NaCl, 0.2 mM TCEP to a final salt concentration of 100 mM and an RNA excess of 1.3 fold. The mixture was concentrated by ultra-filtration to an absorption A(280 nm)=17.6 and crystallized in 0.2 M KCl and 20 %(w/v) PEG 3350. Crystals were cryo-protected using 40 % PEG400 and data collected at P13 operated by EMBL Hamburg at the PETRA III storage ring (DESY, Hamburg, Germany)[156]. Data was processed using XDS and the phase problem solved by molecular replacement using the published structure of human TRIM25 PRY/SPRY in phaser (PDB: 6FLM) [152, 153]. The solution was refined using REFMAC and manually edited using COOT [157, 158]. Collection and refinement statistics are listed in Supplementary Table B.3.

MBP-TRIM25 RBCC (1-379) was concentrated to 45 mg/ml in 50 mM Tris, pH 7.5, 250 mM NaCl, 0.5 mM TCEP, 10 mM Maltose. Crystals grew in 100 mM Tris, pH 8.5, 10 % Isopropanol and were cryoprotected by 30 % Glycerol, 150 mM Tris, pH 8.5, 15 % Isopropanol and tested for diffraction at ID30A at ESRF [155].

3.12. Filter binding assays

Prior to filter binding, RNAs were refolded by heating to 95°C and rapid cooling on ice in 20 mM MES, pH 6.5, 75 mM NaCl, 0.5 mM TCEP to ensure proper folding. Increasing concentrations of TRIM25 CC-PRY/SPRY were incubated with 150 pM 5'-^{32}P-labelled RNA for 10 min on ice and the sample filtered through a nitrocellulose membrane retaining only the complex. Activity of the membrane was detected using scintillation counting and binding curves fitted using SciDavis:

$$A(c_{protein}) = \frac{A_{max} * c_{protein}}{K_D + \frac{c_{RNA}}{2} + c_{protein}} \tag{3.1}$$

Where $A(c_{protein})$ is the measured activity at protein concentration $C_{protein}$ and A_{max} is the saturation activity. Filter binding assays were done jointly with Pawel Masiewicz.

3.13. In vitro ubiquitination assays

In vitro ubiquitination assays were performed with samples containing 50 nM murine E1, 2.5 μM UbcH5C, 1 μM TRIM25 (wild type and mutants) and 10 μM fluorescein-labelled ubiquitin. The sample was incubated in 50 mM Hepes, pH 7.5, 150 mM NaCl, 0.2 mM TCEP, 10 mM MgCl2 and 10 mM ATP at 37°C for 5-60 minutes. The reaction was quenched by addition of SDS loading dye and boiling at 95° C. The samples were then analysed by SDS-PAGE and ubiquitinated products were detected by fluorescence imaging or Western blotting against TRIM25 (ab167154, Abcam, 1:2000) or ubiquitin (P4D1, Santa-Cruz Biotechnology, 1:500) [10].

3.14. In cell ubiquitination assays

For in cell ubiquitination assays of RIG-I CARDs, HEK293T cells were cultured in DMEM with 10 % FBS and 24 hours prior to transfection seeded in 6 well plates at 5×10^5 cells per well. pcDNA3 expression vectors for RIG-I CARDs (aa 1-200) with an N-terminal FLAG-tag and TRIM25 WT (aa 1-630) were a kind gift from Katrin Rittinger (The Francis Crick institute, London) (Figure A.7). RNA-binding deficient mutants H505E/K508E, K602E, H505E/K508E/K602E, K283A/K285A were introduced into the TRIM25 vector by site-directed mutagenesis. Cells were transfected

with 500 ng of TRIM25 vector and 1500 ng of RIG-I CARDs using Fugene transfection reagent. As negative controls one or both plasmids were replaced by the same amount of empty pcDNA3. 24 hours after transfection cells were harvested, washed with phosphate buffered saline (PBS), and lysed by sonication in lysis buffer containg 50mM Tris, 150mM NaCl, 5mM $MgCl_2$, 0.5% IGEPAL and protease inhibitors. For proteasome inhibition, increasing concentrations of carfilzomib from 100-1000 nM were applied 24 hours after transfection and the cells harvested another 24 hours later. Overexpression of TRIM25 and RIG-I CARDs in the cleared lysates was verified by Western blots against TRIM25 (ab167154, Abcam, 1:2000) and Flag-tag (ab F3165, Sigma-Aldrich, 1:10 000). Magnetic aFlag beads were used to immunoprecipitate (IP) RIG-I CARDs from the cleared lysates and eluted in 100 μL 150 ng/μL FLAG-peptide. IP samples were tested for ubiquitination of RIG-I CARDs using Western blots against FLAG-tag (ab F3165, Sigma-Aldrich, 1:10.000) and ubiquitin (P4D1, Santa-Cruz Biotechnology, 1:500). Experiments were done at least in triplicates and the ratios of ubiquitinated to unmodified CARDs quantified using Biorad Image Lab. Ratios for different conditions were normalized to the condition without exogenous TRIM25 expression and plotted using SciDavis. In cell assays were done jointly with Sandra Augsten.

3.15. In vitro phase separation assays

TRIM CC-PRY/SPRY or GFP-TRIM25 CC-PRY/SPRY WT or K283A/K285A/H505E/K508E/K602E pentamutant were mixed on a glass slide in equimolar ratios with RNA at concentrations between 1 and 50 μM in 20 mM sodium phosphate, pH 6.5, 100 mM NaCl, 0.2 mM TCEP and immediately imaged using bright field or differential interference contrast microscopy. To assess localisation of RIG-I CARDs into phase-separated droplets, dTomato-RIG-I CARDs (WT or T55I) or dTomato as a negative control were added at 3 μM to droplets preformed by 5 μM GFP-TRIM25 and DENV-SL and imaged using the green and red channel of an Olympus FV3000 inverted confocal microscope with an Olympus UPL SAPO 40x 2 NA 0.95 objective. Relative protein concentrations were estimated based on fluorescence intensities quantified using Fiji [159]. For each condition fluorescence intensity was measured for at least 30 droplets distributed over three frames. Intensities were averaged and plotted using SciDavis.

3.16. Negative stain electron microscopy

For negative stain electron microscopy (EM) TRIM25 CC-PRY/SPRY and DENV-SL were mixed in equimolar ratios directly on the carbon-coated EM grids in 20 mM MES, 75 mM NaCl, 0.2 mM TCEP. The grids had previously been glow discharged in Argon plasma to create a hydrophilic surface. After 30 seconds of incubation with the TRIM25/DENV-SL mixture grids were washed twice with MES buffer, once with 2 % uranyl acetate and then stained in 2 % uranyl acetate for 30 seconds. Excess stain was removed using blotting paper and the grids dried overnight. Grids were imaged on a FEI Morgagni 268 transmission electron microscope at 100 kV acceleration voltage with a SIS 1K KeenView side-mounted CCD camera.

3.17. Live cell microscopy

HeLa cells were cultured in DMEM with 10 % fetal bovine serum (FBS) and penicillin and 24 hours before the transfection allowed to attach to glass bottom plates at a density of 3×10^5 cells per plate. mEGFP-TRIM25 (1-630) and RFP-RIG-I CARDs (aa 2-200) (Figure A.7) were cloned into a pcDNA3 mammalian expression vector and transfected using Fugene transfection reagent. Oxidative stress was induced by 0.5 mM sodium arsenate for 2 hours. Cells were imaged using the 488 nm and 561 nm laser of an Olympus FV3000 inverted confocal microscope with an Olympus UPL SAPO 40x2 NA 0.95 objective and an environment box allowing for temperature and humidity control. Microscopy was done jointly with Sandra Augsten.

3.18. Sequence alignment and phylogeny

Sequences of all human TRIM proteins and Riplet were obtained from Uniprot and aligned using Clustal Omega [160]. For phylogenetic analysis the aligned sequences were cropped to the parts aligning to the TRIM25 RBCC (1-379) or PRY/SPRY domain (439-630). The phylogenetic tree was created using Simple Phylogeny and visualized using iTOL [161, 160].

4. Results

As TRIM25 full-length protein and the B-Box domains are prone to aggregation it turned out that some protein constructs are difficult to express, purify, and to obtain as stable, soluble protein. Cloning of a first series of constructs covering all domains in isolation, the tripartite motif and CC-PRY/SPRY in pETM22 containing an N-terminal thioredoxin solubility tag, resulted in soluble expression in *E. coli* BL21(DE3) only for the RING (aa 1-60, 1-106) and CC (aa 189-379).

Both RING domain constructs were prone to oligomerisation (as shown by preparative size-exclusion chromatography), which results in NMR spectra of poor quality with regards to signal overlap, linewidth and sensitivity Figure A.2. 1D T2 NMR experiments using a 1-1 echo pulse sequence with a relaxation delay varying between 0 ms and 5 ms[162], confirmed the presence of oligomeric species.

The CC construct was obtained in high yields (50 mg/l of media) and eluted from the size-exclusion chromatography column as a dimer. Despite its high solubility up to 2 mM, NMR spectra showed low spectral dispersion and only few peaks corresponding to flexible regions showed intense signals (Figure 4.1 C). Low spectral dispersion is common for dominantly helical proteins. The weak signals are due to the large size (44 kDa as a dimer) and elongated shape which leads to slow overall tumbling and therefore broad peaks. Perdeuteration did little to improve the spectra and attempts to assign the HSQC spectra failed due to low signal/noise ratios for peaks in the folded regions, small spectral dispersion and biased sequences. However, the helical fold was confirmed by circular dichroism (CD) spectroscopy (Figure A.3).

Through co-expression of bacterial chaperones KJE, ClpB and GroELS [126] for the PRY/SPRY domain (439-630) and CC-PRY/SPRY (aa 189-630) soluble protein could be obtained, albeit in low yields (1-1.5 mg/l of medium). Both constructs co-purified with the co-expressed chaperones and required incubation of the initial HisTrap column with ATP containing buffer followed by cation exchange chromatography to obtain pure proteins. After purification and removal of the solubility tag these proteins remained

soluble and stable in buffers optimized for NMR or crystallography for several days at room temperature. The PRY/SPRY construct was found to be monomeric in solution and yielded a well dispersed $^{1}H/^{15}N$-HSQC NMR spectrum. By analysis of the HNCA, HNCACB and HN(CO)CACB 3D spectra the HSQC could be assigned to 96 % with the help of additional three dimensional NMR spectra (Figure A.4). An N-terminally extended construct of the PRY/SPRY (aa 407-630) was originally cloned for segmental isotope labelling using Sortase A mediated ligation (section 4.9), but also showed increased yields and reduced co-purification with chaperones compared to the shorter construct. The HSQC of this construct could be assigned to 65 % by transfer from the existing assignment of the shorter construct and HNCA and HNCACB spectra were used to partially assign the N-terminal extension Figure A.5. We found that the expression system used did not permit deuteration as cells grew slowly (more than 2 hours doubling times) and protein expression was weak. This may be caused by the necessity of two additional antibiotics as selection markers stabilizing the helper plasmids for chaperone co-expression, which together with the slower growth in D_2O causes too much stress for the cells to efficiently produce proteins.

Several constructs containing the B-Box domains from the first vector series were initially obtained soluble from this procedure, however cleavage of the solubility tag caused complete loss of the protein due to aggregation. Improved constructs of the B-Box/CC region (100-379) and the entire tripartite motif (1-379) were obtained in pETMBP-1A by co-expression with chaperones. The tripartite motif as an MBP-fusion construct formed a well-behaved dimer, that remained stable for several weeks at concentrations up to 50 mg/ml.

Despite numerous attempts no full-length TRIM25 could be obtained from bacterial expression. Using Baculo virus infected insect cells a TEV-cleavable MBP fusion construct could be obtained in small quantities (0.5 mg/l of SF900). The construct co-purified with both endogenous proteins and RNA and was prone to degradation. Therefore no further structural characterisation was untertaken for this construct.

All successful constructs used for *in vitro* experiments in this work are shown in Supplementary Figure A.1.

4.1. TRIM25 CC and PRY/SPRY interact

A crystal structure of TRIM25 CC-PRY/SPRY was solved by Mathilde Lethier and Stephen Cusack (EMBL Grenoble) [10]. In this structure the PRY/SPRY domain is bound to the CC (Figure 4.1 A). The L2 linker connecting these domains was not resolved due to its flexibility and disorder even in the crystal. This raised the question if the CC:PRY/SPRY[1] interaction also occurs in solution and how strong it would be. NMR is an excellent method to answer this question since it is very sensitive to local structural changes upon binding and allows to assign the binding site with residue resolution. The experiment used here is a $^{1}H/^{15}N$-heteronuclear single quantum coherence (HSQC) spectrum, a two-dimensional spectrum, in which every proton directly bound to nitrogen produces a cross peak [163]. Therefore each backbone amide of a non-proline residue correspond to one peak in the spectrum and additional peaks correspond to the sidechains of asparagines, glutamines, tryptophans, arginines and rarely lysines.

When changes in the HSQC were tracked over the course of a titrations of ^{15}N-labelled PRY/SPRY domain by natural abundance CC strong loss of signal upon addition of the CC was observed (Figure 4.1 B). Using the previously established assignment of the PRY/SPRY signal loss could be quantified for each assigned residue. It was strongest for residues in the proximity of the interface observed in the crystal structure. Signal loss upon titration with a binder can be caused by two phenomena: if the rate constants of association and dissociation are of similar size as the difference in the resonance frequency between bound and unbound state of a residue, a situation known as intermediate exchange, line broadening is observed. If chemical exchange rates are faster than the difference in resonance frequencies (fast exchange) instead a movement of the peak position, known as chemical shift perturbation (CSP), is observed during the titration. In the case of much slower exchange rates peaks for both bound and unbound form can be resolved with their relative intensities changing over the course of the titration[164]. Signal loss can also occur in these exchange regimes, if the binder affects the tumbling and relaxation properties of the observed molecule, for example by formation of a larger complex with slower tumbling. Both of these phenomena indicate binding and cannot always be clearly distinguished. In this case the binding of a large (44 kDa) and rod-like molecule like the CC to the much smaller, globular PRY/SPRY

[1] In the interest of clarity the denotion CC:PRY/SPRY will be used from now on for the interaction between these domains, while CC-PRY/SPRY is used throughout for the construct containing both domains connected by the L2 linker.

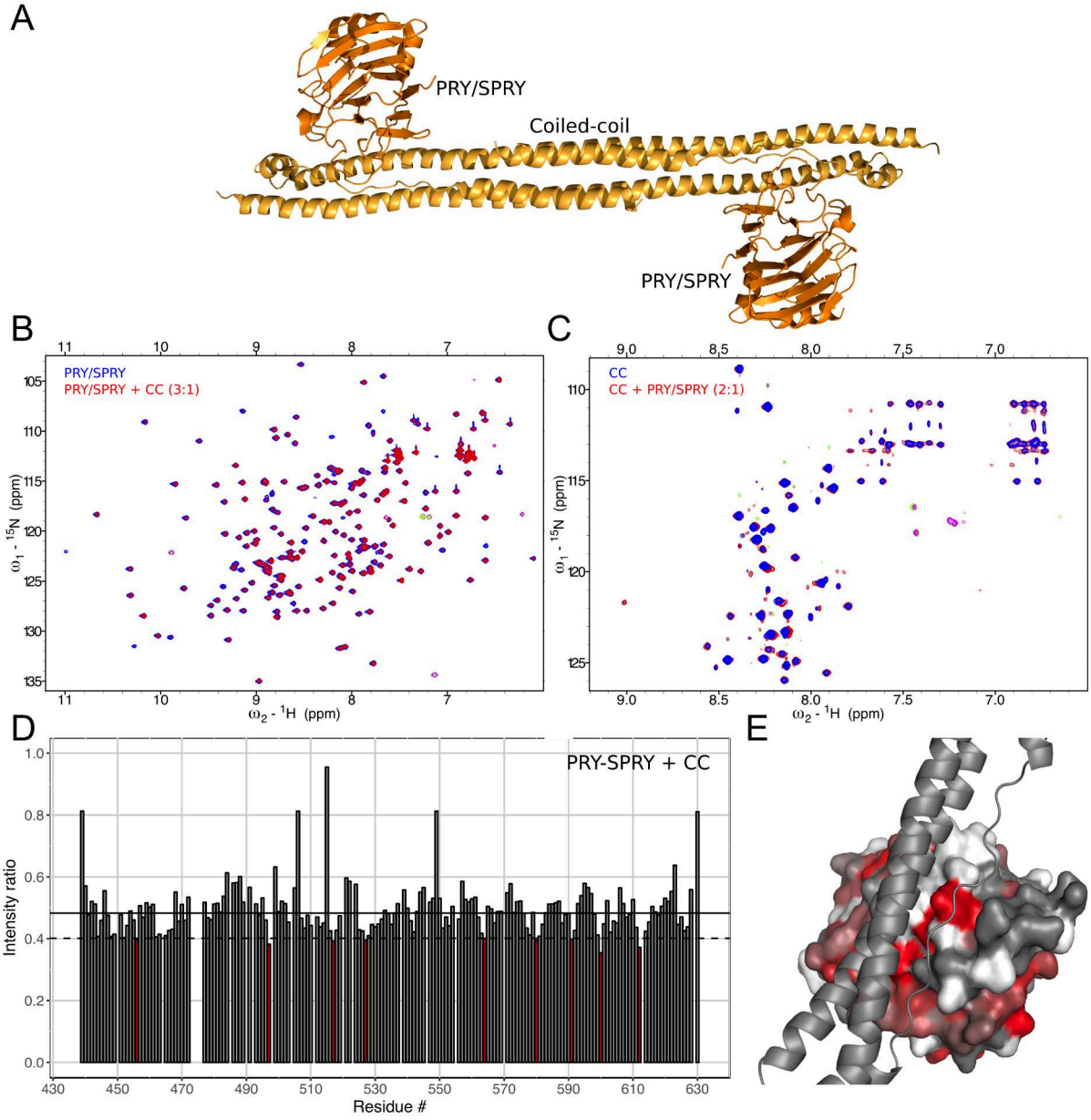

Figure 4.1.: NMR confirms the interaction between CC and PRY/SPRY domains. **A** The crystal structure of TRIM25 CC-PRY/SPRY (PDB: 6FLN) solved by Mathilde Lethier and Stephen Cusack shows an interaction between PRY/SPRY and CC [10]. The presence of this interaction in solution is confirmed by loss of signal due to peak broadening in the $^{1}H/^{15}N$-HSQC when ^{15}N-labelled PRY/SPRY is titrated by natural abundance CC **B** and clear chemical shift perturbations when ^{2}H/^{15}N-labelled CC is titrated by natural abundance PRY/SPRY **(C)**. Intensity ratios in **(B)** were assigned to the sequence **(D)**. Ratios more than one standard deviation (dashed line) below the mean (full line) are highlighted in red. **(E)**: Intensity ratios are plotted onto the structure as a gradient from gray to red for the strongest affected residues. Signal loss was strongest close to the interface observed in the crystal structure, confirming the importance of this interface for the interaction in solution [10].

(25 kDa) is likely to change the tumbling properties of the latter and therefore cause line broadening irrespective of the exchange regime.

In agreement with that a reverse titration of $^{2}H/^{15}N$-labelled CC by natural abundance PRY/SPRY showed clear chemical shift perturbations (CSPs) in fast exchange rather than line broadening (Figure 4.1 C). Due to the low signal intensity, small spectral dispersion and biased sequence of the CC these CSPs could not be assigned to the sequence.

These experiments confirmed the presence of a weak interaction between the isolated domains. In the context of the full-length protein these are connected by the about 80 amino acid long L2 linker, that might stabilise the interaction. Therefore we next characterized the CC:PRY/SPRY interaction in the context of the CC-PRY/SPRY construct with the L2 linker present. To do so, we recorded small-angle X-ray scattering curves (SAXS) of CC-PRY/SPRY and compared to the theoretical curves calculated from the crystal structure. SAXS is a technique that can obtain low resolution shape information, such as radius of gyration, molecular weight and pair-wise distance distributions from elastic scattering of X-rays by particles in solution. SAXS curves can be predicted directly from crystal structures, allowing for a direct comparison of the conformation of a macromolecule in the crystal and in solution [144]. Unsurprisingly, the curve calculated from the crystal structure did not fit the experimental data well, as the L2 linker is not resolved ($\chi^2 = 15.8$). We therefore created an ensemble of structures with a randomized linker and obtained a slightly better fit (best fit for single structure: $\chi^2 = 6.5$). However, a much better fit ($\chi^2 = 1.1$) was only obtained when one or both PRY/SPRY domains were allowed to dissociate from the CC, indicating that the PRY/SPRY in solution is mostly not bound to the CC. Thus, from NMR and SAXS data, I could confirm an interaction between both domains, but this interaction is weak and under these experimental conditions the PRY/SPRY is mostly detached from the CC.

To further confirm the observed interface, based on the crystal structure point mutants were chosen to disrupt the CC:PRY/SPRY interface and their effect on the interaction measured in NMR. The double mutant Y463S Y476S on the PRY/SPRY resulted in a weaker loss of NMR signals compared to WT PRY/SPRY when titrated by CC WT (Figure 4.3 A). The triple-mutant CC I277A I280D Y323S showed a similar but weaker effect when titrated into PRY/SPRY WT (Figure 4.3 B). This shows that both mutants reduce the CC:PRY/SPRY interaction, confirming the importance of these residues for the interaction. Despite the weakness of the interaction, in cell ubiquitination assays

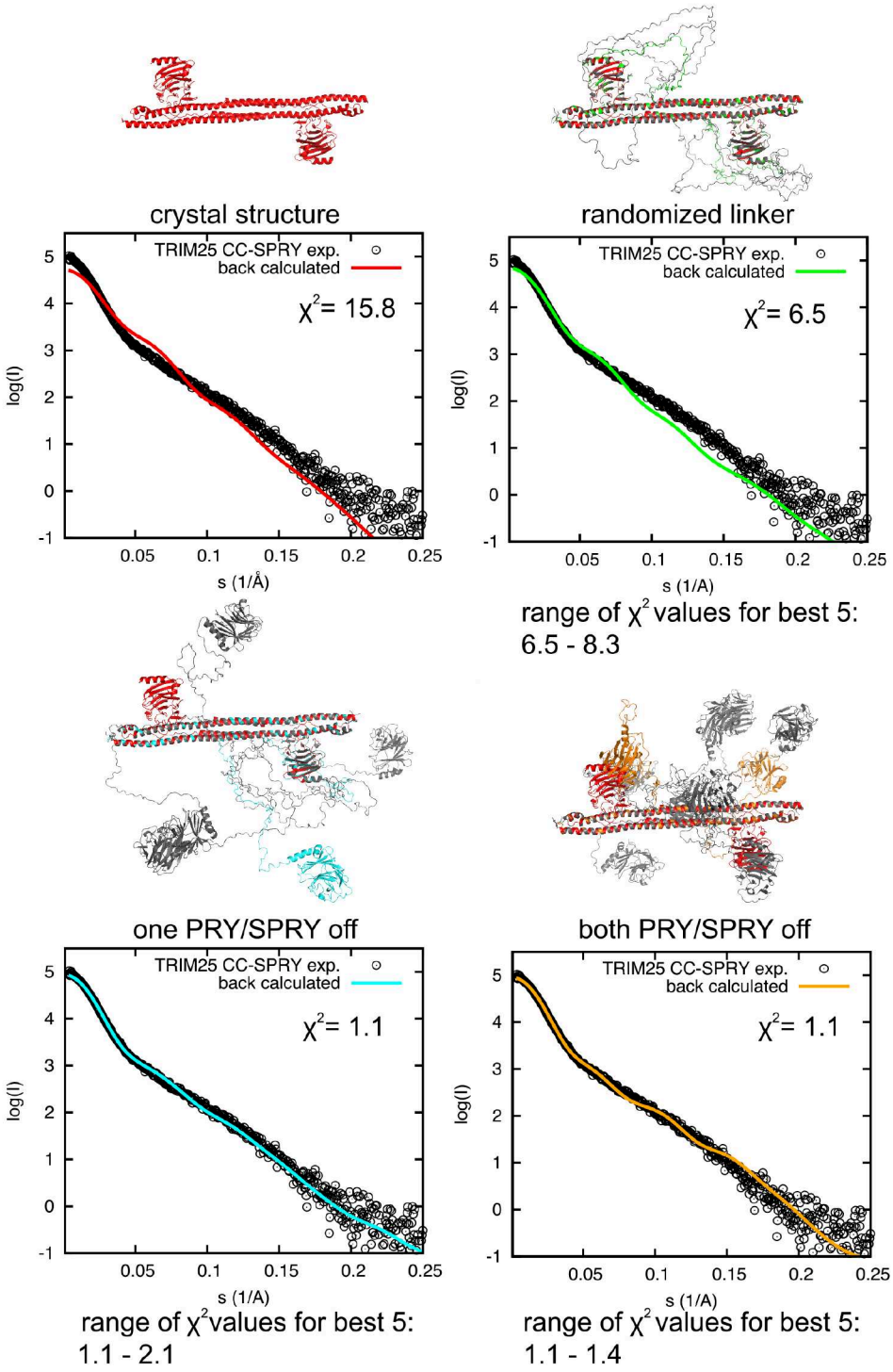

Figure 4.2.: Small angle X-ray scattering of TRIM25 CC-PRY/SPRY: A theoretical SAXS curve calculated from the crystal structure does not fit the experimental SAXS curve. Simulation of the disordered L2 linker absent from the crystal structure improves the fit, but only once one or both of the PRY/SPRY domains is allowed to dissociate a good fit is achieved [10]. Experimental data collected on a sample provided by Mathilde Lethier and fitted against structures of a CC-PRY/SPRY ensemble generated jointly with Bernd Simon [10].

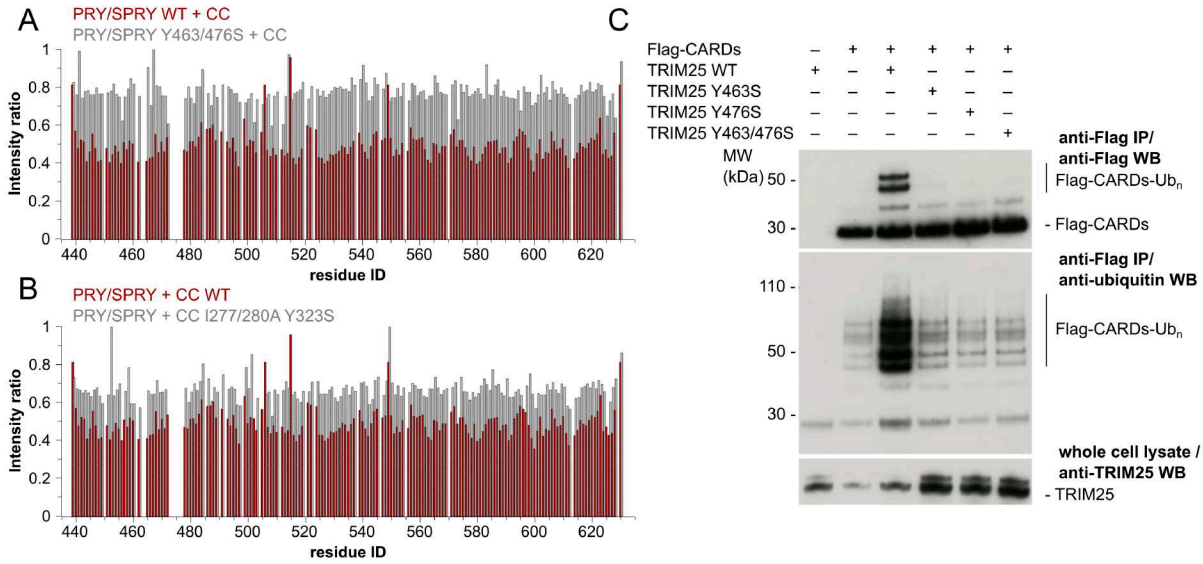

Figure 4.3.: Mutation of the CC:PRY/SPRY interface: **(A)**The mutant Y463S Y476S on the PRY/SPRY was designed based on the crystal structure of CC-PRY/SPRY and its interaction with the CC probed using NMR. Signal loss in the $^{1}H/^{15}N$-HSQC upon titration by natural abundance CC was much smaller for the mutant than WT PRY/SPRY (25 % on average vs. 55 % for WT). This indicates that the mutant reduces the interaction between PRY/SPRY and CC, but doesn't completely abolish it. **(B)** The triple mutant I277A I280D Y323S on the CC has a similar, but weaker effect. **(C)** In the context of the full-length protein the Y463S Y476S mutant dramatically reduces ubiquitination of Flag-tagged RIG-I CARDs in HEK293 cells. The in cell ubiquitination experiments were performed by Marios Koliopolous [10].

carried out by Marios Koliopoulos in the group of Katrin Rittinger (The Francis Crick Institute, London) show that the double mutant Y463S Y476S almost completely abolishes TRIM25's ability to ubiquitinate isolated RIG-I CARDs (Figure 4.3 C)[10].

4.2. RNA binding interface of the PRY/SPRY domain

TRIM25 was recently identified as an RNA-binding protein although the identity of the RNA binding domain is not clear [38, 111]. To characterize possible RNA-binding of TRIM25 the PRY/SPRY domain was titrated by pre-let-7a-1@2. This RNA was previously reported as the minimal construct of pre-let-7a-1 miRNA capable of binding TRIM25 and promoting the assembly of the lin28a/TUT4 complex [100]. We observed significant chemical shift perturbations (CSPs) of NMR resonances corresponding to

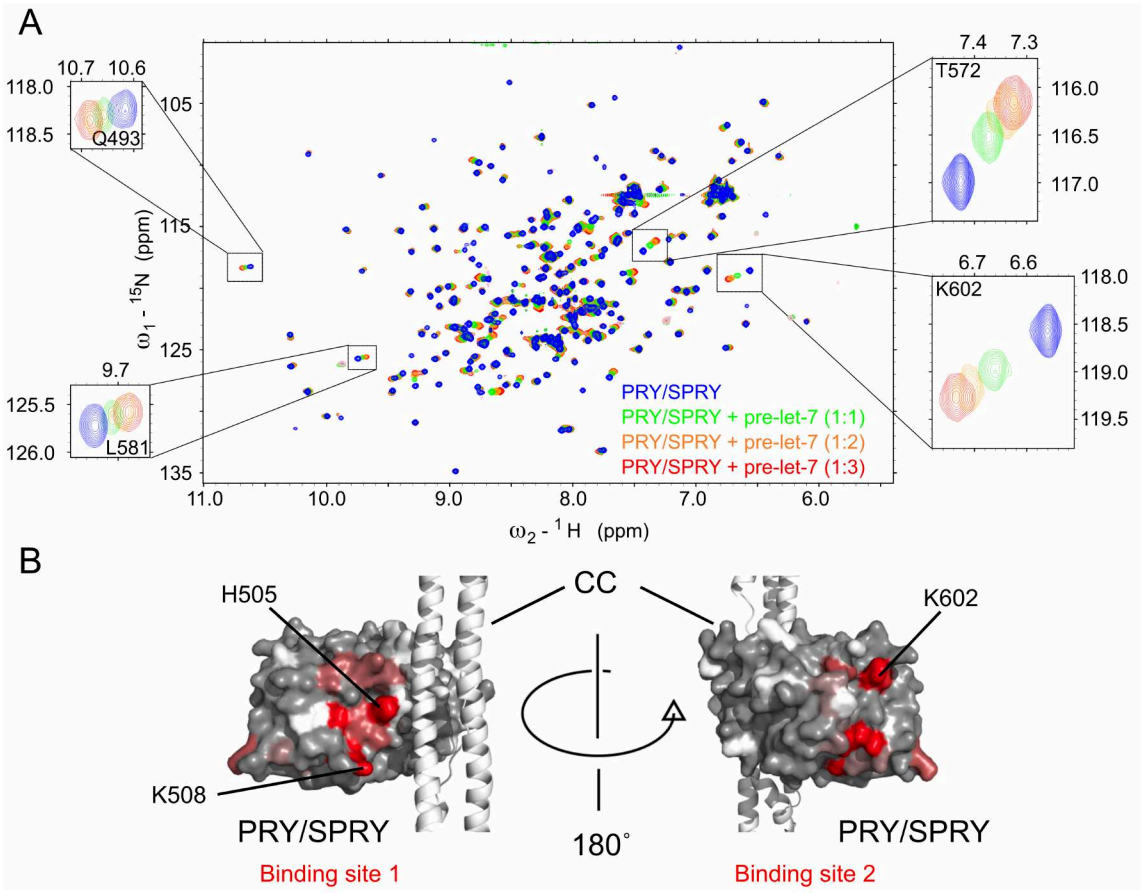

Figure 4.4.: TRIM25 PRY/SPRY titrated by pre-let-7a-1@2: **(A)** $^{1}H/^{15}N$-HSQC of TRIM25 PRY/SPRY before and after addition of a 3-fold excess of pre-let-7. **(B)** Chemical shift perturbations are plotted on the structure of CC-PRY/SPRY (PDB: 6FLN) as a gradient from gray to red. Unassigned residues are shown in white. CSPs occur in two regions, henceforth called binding site 1 and 2.

residues in the PRY/SPRY domain, clearly indicative of binding. CSPs occured on two regions of the PRY/SPRY domain (Figure 4.4). One of these regions (binding site 1) is located at the C-terminus of the PRY region. The most affected residues are found in the linker connecting β3 and β4 strand. This binding site agrees well with the RNA-binding region identified by Castello *et al.* using RBDmap (aa 470-508) [111], but allows for a more detailed analysis down to residue level resolution. Comparison with the crystal structure of CC and PRY/SPRY [10] shows that binding site 1 is located in the vicinity of the PRY/SPRY:CC interface. The second region strongly affected by RNA binding is located on the opposite side of the domain around β10 and β11 and the N-terminal helix α1. This region was previously described to play a role in binding of RIG-I, but

not in RNA binding. β-sheets are prone to propagation of CSPs due to allosteric effects so that mutational analysis was necessary to confirm direct binding for both binding sites (see section 4.4).

As previous research had not found a clear preference for binding of single or double-stranded RNA or even identified a binding motif [100, 102], we attempted to gain further insights into the specificity of the two binding sites through titrations with constructs of pre-let-7 truncated to contain only the loop or stem region (Figure 4.5). The single stranded loop region only caused CSPs in a small subregion of binding site 1 in the immediate proximity of the CC binding site, while binding site 2 was completely unaffected. By contrast the double-stranded stem strongly affected both binding sites 1 and 2. This suggests that binding site 2 is specific for double stranded RNA whereas binding site 1 binds both single and double stranded RNA, although a different subset of residues are involved in this. The identification of two binding sites with different specificity for single and double stranded RNAs suggests that RNA binding by the PRY/SPRY domain might be structure- rather than sequence-specific. To test this idea we examined reported RNA targets of TRIM25 [90, 165] and found stem-loops of similar size and loop composition as in pre-let-7 in several of them. We used isothermal titration calorimetry (ITC) to test several of them for binding to TRIM25 CC-PRY/SPRY (Table 4.1, Figure A.8, see Figure A.6 for summary of structures). Pre-let-7a-1@2 bound CC-PRY/SPRY with a $K_D = 72 \pm 33nM$ in these experiments. A stem-loop derived from the subgenomic RNA of the Dengue virus (DENV-SL) bound significantly stronger ($K_D = 15.2 \pm 3.0nM$) while the stem-loop of the long non-coding RNA Lnczc3h7a showed weaker, but still tight binding ($K_D = 486 \pm 77nM$). Using filter-binding assays we could also show binding to completely unrelated stem-loops of the *Drosophila melanogaster* lncRNA roX2 [166](Table B.1).

Analysis of the ITC data was complicated by the occurrence of additional binding events at higher concentrations. This was most pronounced for pre-let-7, that showed a very complicated calorigram indicating 3 or more binding sites, while the other stem-loops could be fitted assuming a two-site sequential binding mode (Figure A.8). To obtain interpretable data for pre-let-7, measurements had to be done a low concentrations to avoid the occurrence of additional binding sites and fit by a single binding model (Figure 4.7). This way the highest affinity binding event could be accurately estimated. The nature of the additional binding events is not clear, however they generally show low N values, indicating that they possibly represent RNA-induced oligomerisation or

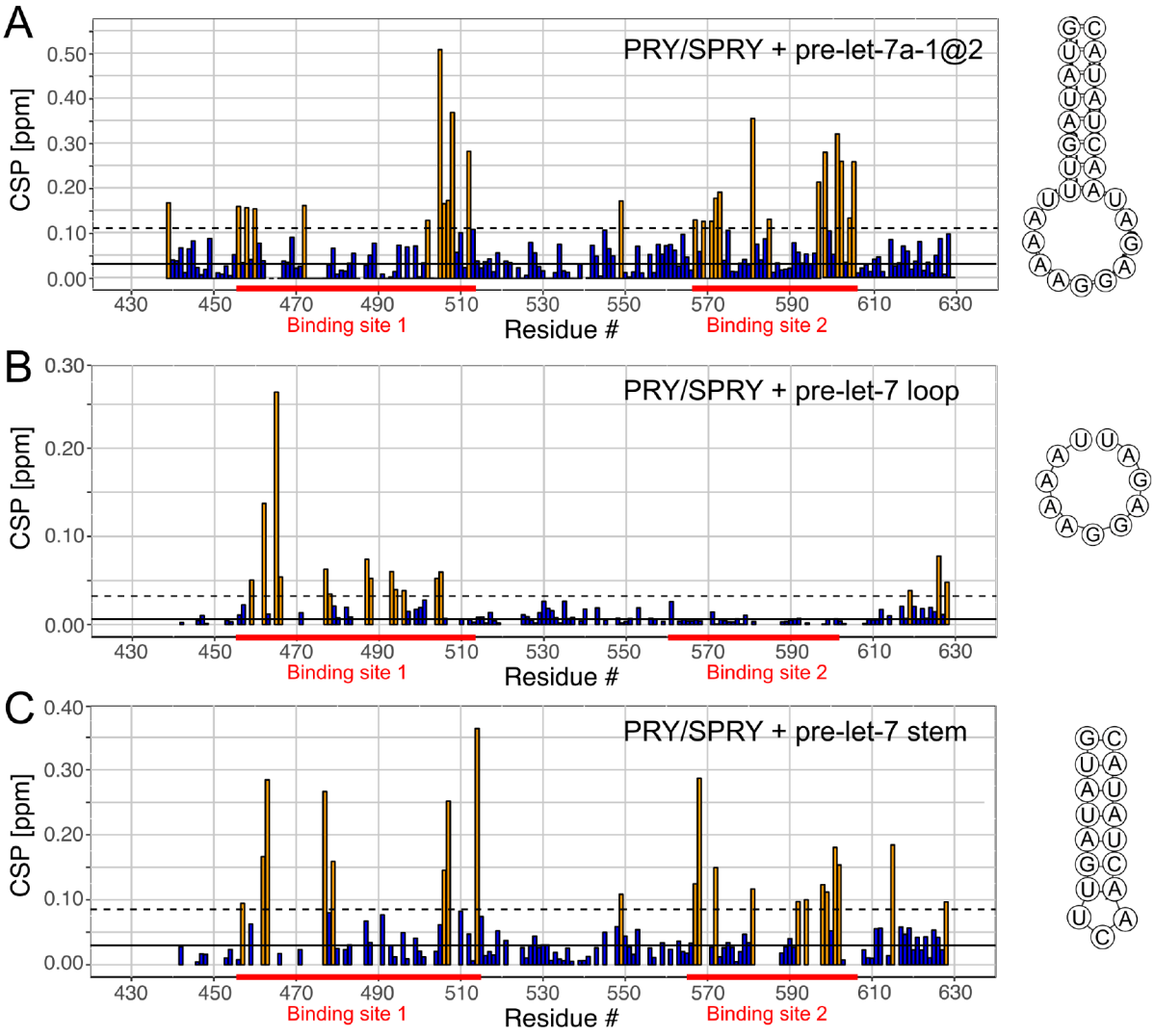

Figure 4.5.: Chemical shift perturbations in the $^{1}H/^{15}N$-HSQC for TRIM25 PRY/SPRY at 100 μM titrated by pre-let-7a-1@2 **(A)**, pre-let-7 loop **(B)** and stem **(C)** to a ratio of 1:3 each. Perturbations for the single-stranded loop are limited to a subset of binding site 1, while the stem causes perturbations also of binding site 2. CSPs more than one standard deviation (dashed line) above the mean (full line) are highlighted in yellow.

aggregation. This is in agreement with the observation of precipitation upon RNA addition with most RNAs tested. Affinities estimated from filter binding assays were up to ten-fold higher as those measured by ITC for the same protein/RNA pair, indicating that these assays are even more sensitive to aggregation (Table B.1). The effect of RNA binding on oligomerisation of TRIM25 will be revisited in more detail in section 4.8.

ITC data of the PRY/SPRY domain to pre-let-7 could be fitted using a single binding site model with a $K_D = 4.1 \pm 1.1 \mu M$ (Figure 4.7). The PRY/SPRY alone is therefore not sufficient to explain the almost 100 times stronger binding of TRIM25 CC:PRY/SPRY to RNA. This suggests that additional binding sites might be present in TRIM25.

4.3. RNA binding of the CC and PRY/SPRY stabilizes CC:PRY/SPRY interaction

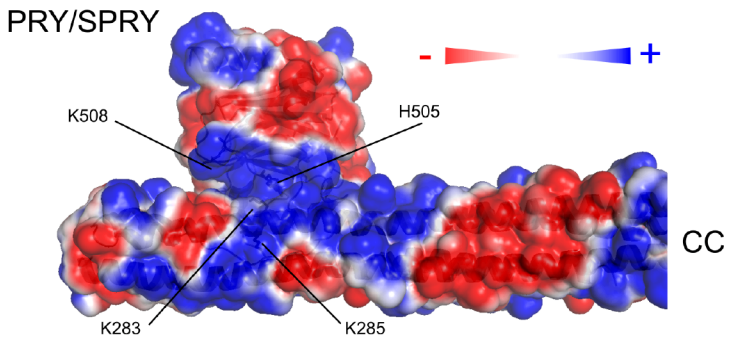

Figure 4.6.: The surface potential of TRIM25 CC-PRY/SPRY shows a joint positive surface, that could support RNA binding.

The structure of TRIM25 CC:PRY/SPRY shows a joint, positively charged interface of PRY/SPRY and CC, that on the PRY/SPRY overlaps well with our proposed binding site 1 (Figure 4.6). This gave rise to the idea that the RNA-binding interface might extend to the CC increasing affinity through cooperative binding. Indeed we observed binding of the CC to pre-let-7 with a K_D of $8.1 \pm 3.1 \mu M$ that is just slightly weaker than that of the PRY/SPRY (Figure 4.7). Both domains show low N values in ITC when titrated by pre-let-7 most likely indicating that the RNA is big enough to bind more than one domain simultaneously. The much stronger RNA binding of CC-PRY/SPRY can therefore be explained by cooperative binding through both domains, that might depend also on the weak interaction between these domains.

Table 4.1.: Thermodynamic parameters of TRIM25/RNA interactions measured by ITC. The original curves can be found in Figure 4.7, Figure A.8 and Figure A.9.

protein	**RNA**	$\mathbf{K}_D$	**N**	**ΔH (kJ/mol)**
PRY/SPRY	pre-let-7-1a@2	$5.0 \pm 1.2\ \mu M$	0.711 ± 0.020	-29.9 ± 1.6
CC	pre-let-7-1a@2	$8.1 \pm 3.1\ \mu M$	0.287 ± 0.036	-52 ± 12
CC-PRY/SPRY	pre-let-7-1a@2	$72 \pm 33\ nM$	0.750 ± 0.028	-33.0 ± 2.3
	pre-let-7-1a@2 stem-only	$> 100\ \mu M$	n.d.	n.d.
	pre-let-7-1a@2 loop-only	$4.1 \pm 1.9\ \mu M$	0.809 ± 0.062	-48.9 ± 7.6
	DENV-SL	$15.2 \pm 3.0\ nM$	0.780 ± 0.020	-32.4 ± 3.4
		$106 \pm 35\ nM$	0.080 ± 0.020	-330 ± 100
	Lnczc3h7a	$486 \pm 77\ nM$	1.25 ± 0.05	$+38.8 \pm 5.9$
		$8.9 \pm 4.5\ \mu M$	0.104 ± 0.063	-17 ± 82
CC-PRY/SPRY 381-392 7KA	pre-let-7-1a@2	$428 \pm 55\ nM$	0.765 ± 0.028	-17.0 ± 1.2
		$967 \pm 11 \mu M$	0.13 ± 0.22	-270 ± 410
CC-PRY/SPRY H505E K508E	pre-let-7-1a@2	$484 \pm 48 nM$	0.972 ± 0.030	-10.2 ± 0.76
		$4.19 \pm 0.50\ \mu M$	0.196 ± 0.043	-91 ± 18
CC-PRY/SPRY K602E	pre-let-7-1a@2	$196 \pm 22\ nM$	1.08 ± 0.03	-3.31 ± 0.53
		$2.54 \pm 0.12\ \mu M$	0.050 ± 0.043	-270 ± 230
CC-PRY/SPRY K283A K285A	pre-let-7-1a@2	$606 \pm 124\ nM$	1.36 ± 0.06	-5.53 ± 0.90
		$16.6 \pm 2.1\ \mu M$	0.12 ± 0.20	-145 ± 215
CC-PRY/SPRY H505E K508E K602E	pre-let-7-1a@2	$790 \pm 160\ nM$	0.973 ± 0.025	-2.83 ± 0.49
		$132 \pm 24\ \mu M$	0.06 ± 0.29	-300 ± 1400
CC-PRY/SPRY K283A K285A H505E K508E K602E	pre-let-7-1a@2	$1.32 \pm 0.37\ \mu M$	0.972 ± 0.030	-0.2 ± 1.7
		$124 \pm 28\ \mu M$	0.26 ± 0.12	-210 ± 130
CC-PRY/SPRY Y278A	pre-let-7-1a@2	$62.9 \pm 6.8\ nM$	1.04 ± 0.02	7.27 ± 0.74
		$491 \pm 41\ nM$	0.590 ± 0.017	-14.5 ± 1.1
CC-PRY/SPRY Y463S Y476S	pre-let-7-1a@2	$252 \pm 61\ nM$	1.42 ± 0.03	-8.6 ± 1.2
		$17 \pm 11\ \mu M$	0.05 ± 0.10	-290 ± 580

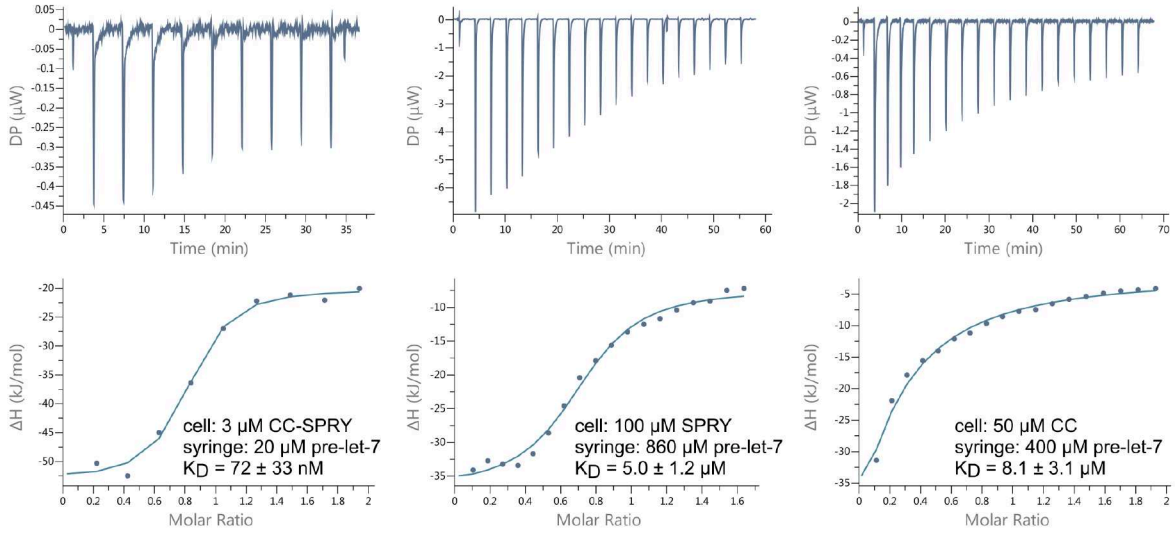

Figure 4.7.: Isothermal calorimetric titration curves for the CC and PRY/SPRY domain titrated by pre-let-7. Both domains individually bind RNA with low micromolar affinity, but the longer construct shows much higher affinity indicating cooperative binding.

Such cooperative RNA binding of the CC and PRY/SPRY could stabilize the transient interaction between these domains. Again, SAXS is a powerful technique to observe large-scale structural changes upon RNA binding. Comparison of the scattering curves of free and pre-let-7 bound CC-PRY/SPRY shows significant changes in the scattering curves (Figure 4.8). The radius of gyration of the complex ($5.69 \pm 0.02nm$) is significantly smaller than that of the free protein ($R_g = 6.83 \pm 0.05nm$). This indicates that the complex is more compact than the free protein. This finding is even more apparent from the pair-wise distance distribution P(r) obtained by indirect Fourier transform of the scattering curve. The distance distribution of the complex is more narrow than that of the free protein and has only a single peak. By comparison the free protein shows a bimodal distribution, which is in agreement with largely independent movement of the two domains as described in section section 4.1. This compaction of the complex upon RNA binding is in agreement with a stabilisation of the CC:PRY/SPRY interaction.

We attempted to confirm these results using small-angle neutron scattering (SANS). Unlike X-rays, that are scattered by electrons, neutrons are scattered by nuclei and the contrast in SANS therefore depends on the isotopic composition of buffer and scattering particles. This can be exploited to make the scattering contribution of individual parts of a complex disappear through selective deuteration and variation of the solvent's D_2O content (Contrast matching) [146]. In this case in measurements at 63 % D_2O the

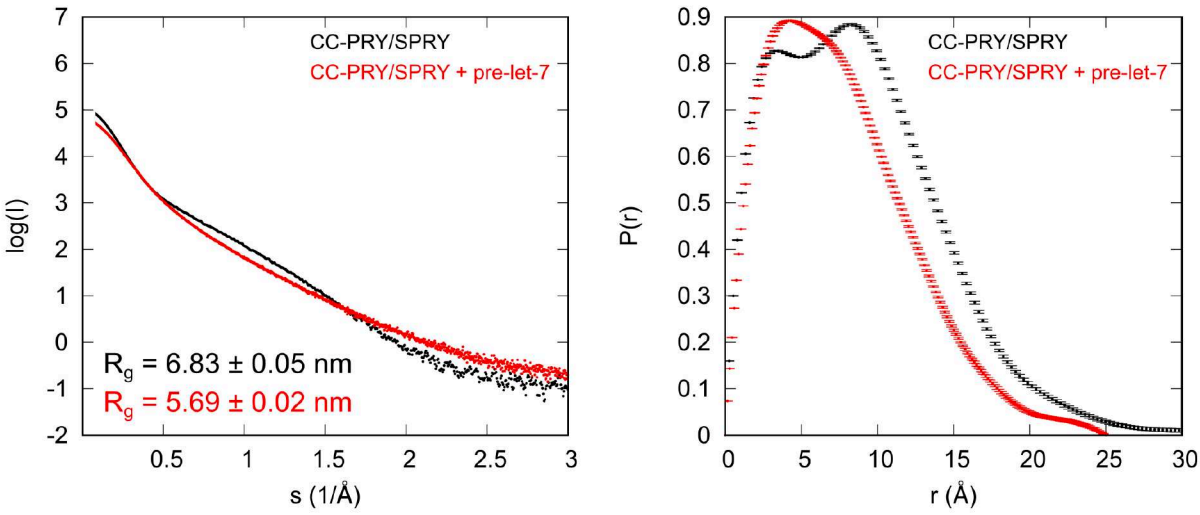

Figure 4.8.: Small angle X-ray scattering curve of TRIM25 CC-PRY/SPRY in the free form and in complex with pre-let-7 (**A**). The pair-wise distance distribution P(r) shows a broad, bimodal distribution for the free protein, indicating that the two domains are independent, while the complex shows a much narrower distribution with a single peak indicating that the complex forms a more compact, single entity.

scattering contribution of the RNA would be invisible, while the protein remains visible (albeit with negative contrast), so that any changes observed upon addition of RNA must be due to conformational changes of the protein. Scattering curves of the free protein under these conditions indicated the presence of significantly larger particles than observed in SAXS ($R_g = 8.47 \pm 0.50nm$). This is suggestive of oligomerisation in D_2O, a phenomenon occasionally observed due to the stronger hydrogen bridge network and lesser steric requirements of deuterons compared to protons [167]. No such oligomerisation was observed for the complex with pre-let-7, however its solubility in 63 % D_2O proved limiting for SANS experiments. While the R_g of $4.26 \pm 0.42nm$ is in agreement with a compaction of the complex upon RNA binding the data is of low quality and does not justify further conclusions (Figure A.10).

Taken together, these data point towards a stabilisation of the otherwise transient interaction of CC and PRY/SPRY through cooperative RNA binding, as a clear compaction is observed upon RNA binding. This may be explained by the PRY/SPRY being mostly bound to the CC in the presence of RNA, whereas it is mostly dissociated in the absence of RNA. Mutational analysis will be necessary to confirm that the same interface is responsible for the CC:PRY/SPRY interaction in the presence and absence of RNA binding.

4.4. Mutational analysis confirms cooperative RNA binding

To confirm the observed RNA binding sites on the PRY/SPRY and the proposed binding site on the CC we used mutational analysis. Mutants on the PRY/SPRY were designed based on the CSP data from NMR and tested using ITC in the context of the CC-PRY/SPRY construct ((Table 4.1, Figure A.9). Mutation of the strongest affected residues on binding site 1, H505E K508E, reduced binding to pre-let-7 almost 7-fold ($K_D = 484 \pm 48nM$). The strongest affected residues on binding site 2 were Y601 and K602. K602E bound pre-let-7 with a K_D of $196 \pm 22nM$. This confirms that both binding sites are directly involved in RNA binding. However even the combination of all three mutants on the PRY/SPRY only reduced the affinity to $790 \pm 160nM$, once more indicating the presence of additional binding sites. Unlike WT TRIM25 CC-PRY/SPRY titrated by pre-let-7, ITC data for the mutants could be fitted by a model assuming only two sequential binding sites.

In the absence of NMR data on the interaction site with the CC, we chose typical RNA binding amino acids, such as lysines, arginines or aromates, that were solvent accessible and located on the previously mentioned positive surface in the proximity of the CC:PRY/SPRY interaction. The double mutant K283A K285A in the context of the CC-PRY/SPRY had a similar effect to the mutants on the PRY/SPRY ($K_D = 605 \pm 124nM$). In close vicinity of these residues the known phosphorylation site Y278 is located, a posttranslational modification that could possibly regulate RNA-binding. However, mutation to Alanine did not significantly reduce the affinity ($K_D = 62.9 \pm 6.8nM$), although it did abolish additional binding events similarly to the other mutants. While this suggests that this residue does not contribute significantly to RNA binding, a less conservative mutant such as Y278E, that could mimic the effect of phosphorylation might still reduce RNA binding due to its close proximity to the RNA binding interface.

It should be noted, that even combination of all the mutants on the CC and PRY/SPRY domain reducing affinity resulting in the pentamutant K283A/K285A/H505E/K508E/K602E (pentamutant in the following) did not completely abolish RNA-binding, although it did reduce RNA-binding almost 20-fold ($K_D = 1.32 \pm 0.37\mu M$). An additional binding site has been reported in the L2 linker connecting CC and PRY/SPRY: The mutation of seven lysines to alanines in a lysine rich region (381-392 7KA) reduced binding to double stranded RNA about 20-fold in electrophoretic mobility shift assays (EMSAs)

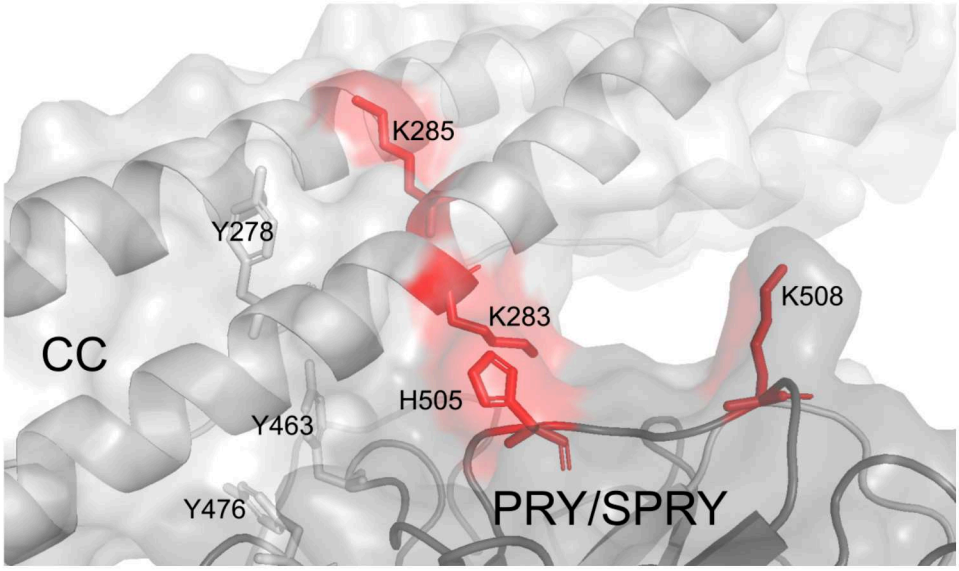

Figure 4.9.: CC and binding site 1 form a joint RNA binding surface. The putative RNA binding residues K283 and K285 on the CC identified by mutational analysis form a joint surface with binding site 1 on the PRY/SPRY containg H505, K508 and K602. Mutation of Y463 and Y476 affects RNA binding through reduction of the CC:PRY/SPRY interaction.

[102]. In our hands this mutant showed a much more modest effect, still binding pre-let-7 with a K_D of $428 \pm 55nM$.

In support of our model suggesting cooperative binding of RNA through both the CC and the PRY/SPRY, also the double mutant Y463S Y476S that reduces the interaction between these domains (see section 4.1), reduces RNA-binding moderately ($K_D = 252 \pm 61nM$). Taken together these experiments confirm that TRIM25 binds RNA cooperatively through at least four binding sites on the PRY/SPRY, CC and in the L2 linker, that each have only relatively modest contributions to RNA binding and rely on the weak CC:PRY/SPRY interaction to form a joined RNA-binding interface (Figure 4.9).

4.5. Progress towards a high-resolution structure of the TRIM25/RNA complex

The tight interaction between TRIM25 CC-PRY/SPRY and stem-loop RNAs made us optimistic that the structure of the complex could be solved by X-ray crystallography.

Initial experiments trying to isolate the complex of TRIM25 CC-PRY/SPRY and pre-let-7a-1@2 using size-exclusion chromatography yielded only very low recovery of complex as the complex was prone to aggregation and losses due to unspecific binding to the column were significant. Therefore, the TRIM25 was mixed with an excess of pre-let-7 at low concentrations to avoid precipitation, concentrated to about 1.5 mg/ml and subjected to crystallisation screens. Crystals grew within 24 hours in 0.1 M Tris, pH 8.5, 20 % ethanol. Presence of pre-let-7 in the crystals was verified by gel electrophoresis of washed crystals (Data not shown).

Additive screens were used to optimize the condition. One crystal grown in the same condition with additives 0.02 % w/v Anthrone, 2 μM Hepes, pH 6.8, 0.02 % w/v Benzidine, 0.02 % w/v N-(2-Acetamido)-2-aminoethanesulfonic acid, 0.02 %w/v Phenylurea; 0.02 % w/v beta-Alanine diffracted weakly to 5.3 Å. Due to radiation damage only a partial data set could be collected. The crystals belong to space group P 6 2 2 or a closely related space group (cell parameters: a = b = 105.6 Å, c = 282.9 Å, $\alpha = \beta = 90.00$, $\gamma = 120.00$). Due to the low resolution and incomplete data no solution of the phase problem could be found by molecular replacement with the known structures of CC and PRY/SPRY (Table B.3). Despite extensive attempts to reproduce this crystal no more diffracting crystals were obtained. Dehydration and cross-linking of crystals using glutaraldehyde did not improve diffraction. Crystals from the initial hit were therefore crushed and used for microseeding experiments. Crystals were obtained in several new conditions, but showed no diffraction.

Since I reasoned that the flexible L2 linker might interfere with crystal packing, several truncations of the L2 linker (Δ358-383, Δ358-400, Δ358-407) were screened for crystallisation conditions in complex with pre-let-7, but did not yield crystals. The PRY/SPRY domain alone was crystallized with an excess of pre-let-7 in 0.2 M potassium chloride, 20 % w/v PEG 3350. Crystals diffracted to 3.9 Å and the structure was solved by molecular replacement, but no additional density for the RNA was found (Table B.3).

The DENV-SL and the TRIM25-binding stem-loop of Lnczc3h7a were also crystallized with TRIM25 CC-PRY/SPRY. Unlike pre-let-7 these RNAs did not cause precipitation when mixed at high concentrations, even though DENV-SL phase-separated (see section 4.8). To avoid losses due to unspecific binding of this phase-separated material to tubes and pipette tipps, TRIM25 CC-PRY/SPRY and DENV-SL were mixed directly on the plate at the final concentrations. Crystals were obtained in the same condition as for the TRIM25 CC-PRY/SPRY:pre-let-7 complex and again no diffraction was observed.

To fully explain the catalytic mechanism of TRIM25 and the effect of RNA binding on it, additional information on the arrangement of the N-terminal tripartite motif (RBCC) is necessary. This was complicated by the low solubility of the tripartite motif and its high tendency to aggregate. However, an MBP-fusion construct with a short $(GS)_5$-linker was sufficiently stable for crystallisation experiments and yielded small crystals. Unfortunately, no diffraction past 20 Å was observed. Experiments to optimize diffraction of this construct were put on hold as several structures of the tripartite motif of KAP1, another TRIM protein, were reported in 2018 [150, 11].

4.6. RNA binding mutants affect RIG-I ubiquitination and auto-ubiquitination in cells

Since all our experiments point towards a stabilisation of the weak CC:PRY/SPRY interaction through RNA binding and this interaction is critical for the E3 ligase activity of TRIM25 [10], we next tested the impact of RNA binding deficient mutants on ubiquitination. As before for the CC:PRY/SPRY mutant we assessed the catalytic activity of these mutants in the context of RIG-I ubiquitination. We transiently expressed wild-type and mutant TRIM25 together with Flag-tagged RIG-I CARDs in HEK293T cells and used Western blots to probe the ubiquitination state of immunoprecipitated CARDs (Figure 4.11 A). Expression of the isolated CARDs rather than full-length RIG-I was chosen as the full-length would require a complex activation process through viral RNA and post-translational modification before it could be ubiquitinated by TRIM25 (see section 5.4 for details). We found that only expression of TRIM25 WT increased CARD ubiquitination significantly above the level observed in the control due to endogenous TRIM25 or other E3 ligases (Figure 4.11 B). In contrast, the K602E mutant, H505E/K508E double and K602E/H505E/K602E triple mutant on the PRY/SPRY almost completely abolished poly-ubiquitination of RIG-I and significantly reduced mono-ubiquitination. While the K283A/K285A double mutant on the CC did not share this dominant negative phenotype, its expression did not increase poly-ubiquitination beyond the background level observed without transient expression of TRIM25.

Expression levels of the TRIM25 mutants were compared to that of the wildtype using a Western blot of the cell lysates. While transient transfection of wild-type TRIM25 or K283A/K285A only caused a modest increase in TRIM25 levels, the mutants on the PRY/SPRY domain showed dramatically increased expression levels (Figure 4.11

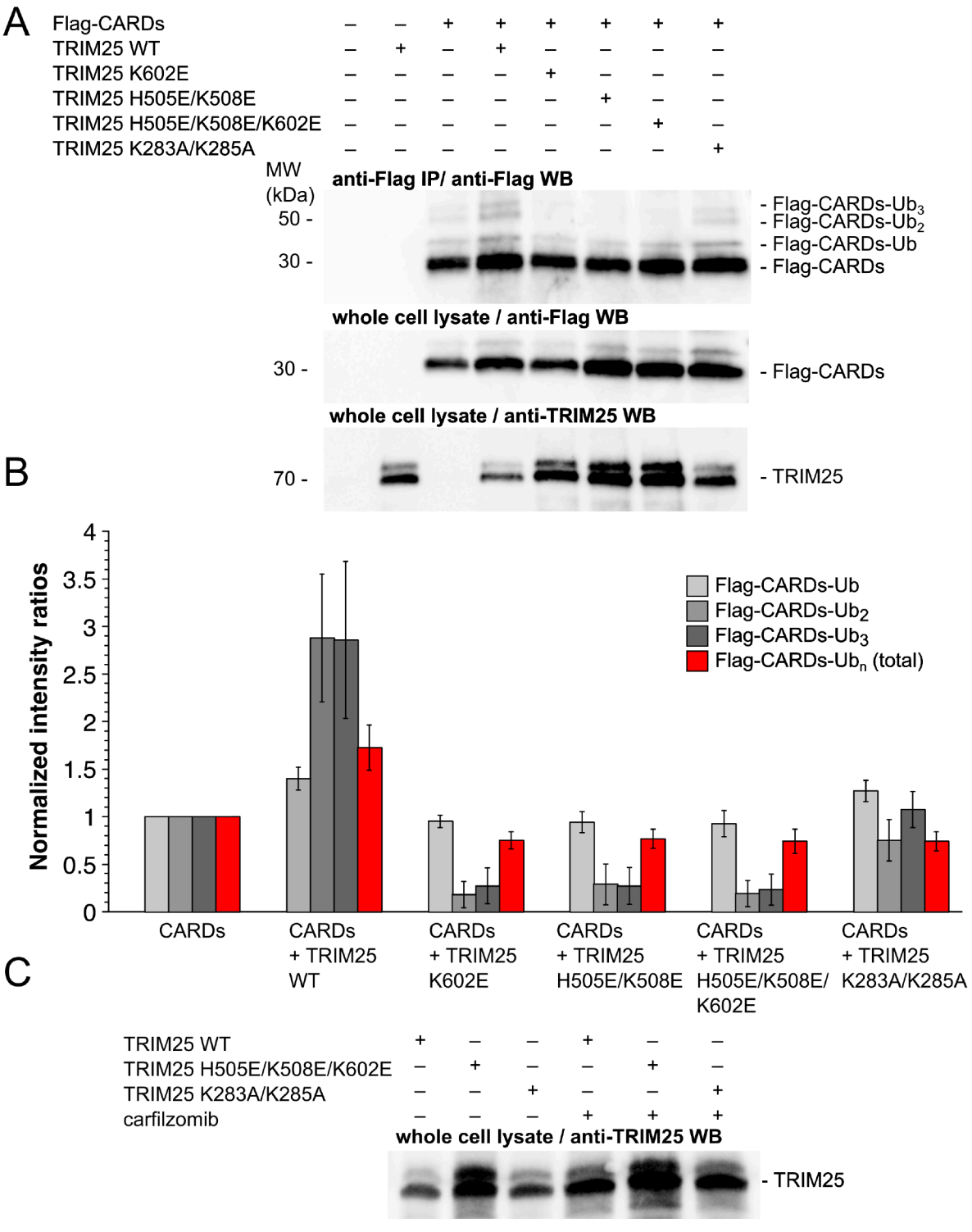
A
Flag-CARDs
TRIM25 WT
TRIM25 K602E
TRIM25 H505E/K508E
TRIM25 H505E/K508E/K602E
TRIM25 K283A/K285A
MW (kDa)
anti-Flag IP/ anti-Flag WB
50 -
30 -
- Flag-CARDs-Ub3
- Flag-CARDs-Ub2
- Flag-CARDs-Ub
- Flag-CARDs
whole cell lysate / anti-Flag WB
30 -
- Flag-CARDs
whole cell lysate / anti-TRIM25 WB
70 -
- TRIM25
B
Normalized intensity ratios
Flag-CARDs-Ub
Flag-CARDs-Ub2
Flag-CARDs-Ub3
Flag-CARDs-Ubn (total)
CARDs
CARDs + TRIM25 WT
CARDs + TRIM25 K602E
CARDs + TRIM25 H505E/K508E
CARDs + TRIM25 H505E/K508E/ K602E
CARDs + TRIM25 K283A/K285A
C
TRIM25 WT
TRIM25 H505E/K508E/K602E
TRIM25 K283A/K285A
carfilzomib
whole cell lysate / anti-TRIM25 WB
- TRIM25

Figure 4.11.: The RNA binding interface is critical for ubiquitination activity **(previous page)**: **(A)** RIG-I CARD ubiquitination assays for TRIM25 mutants. Flag-tagged CARDs are transiently expressed in HEK293 cells together with TRIM25 WT or mutants. The CARDs are immunoprecipitated and probed for ubiquitination. **(B)** Quantification of ratios of ubiquitinated to unmodified CARDs shows that only WT TRIM25 enhances ubiquitination of CARDs. The mutants on the PRY/SPRY (K602E, H505E/K508E) have a dominant negative effect and reduce ubiquitination even below the level observed without exogenous TRIM25 expression. Each band was normalized to its counterpart in the lane without exogenous TRIM25 expression. **(C)** As apparent from **A** the mutants on the PRY/SPRY show higher expression levels than the WT. In the presence of the proteasome inhibitor carfilzomib these differences are strongly reduced as the WT is stabilized. This suggests that this effect is at least in parts due to reduced auto-ubiquitination and proteasomal degradation. Data produced jointly with Sandra Augsten.

A). As increased auto-ubiquitination of TRIM25 in the presence of RNA *in vitro* has been reported earlier [105, 102], we hypothesized that the increase in expression levels is due to reduced auto-ubiquitination of the mutants and therefore reduced proteasomal degradation. We therefore used the proteasome inhibitor carfilzomib to prevent degradation of auto-ubiquitinated TRIM25 and compared expression levels of wildtype and H505E/K508E/K602E triple mutant. While both proteins were stabilized by proteasome inhibition the effect was stronger for the wildtype and at the highest inhibitor concentrations expression levels for the wildtype reached similar levels as for the triple-mutant (Figure 4.11 C). While this shows that the changes in expression levels are at least partially due to a reduced ability of the PRY/SPRY mutants to auto-ubiquitinate, it is unclear if this is due to reduced catalytic activity or removal of preferred ubiquitination sites, as all the mutants affect lysines. This phenotype of increased expression levels and dramatically reduced CARD poly-ubiquitination is shared with the Y463S/Y476S mutant reducing the CC:PRY/SPRY interaction, further supporting the hypothesis that RNA binding stabilizes this interaction. The mutant on the CC K283A/K285A did not show increased expression levels relative to wildtype TRIM25.

In summary, these experiments show that the full RNA binding interface is required for the catalytic activity of TRIM25 in RIG-I ubiquitination. It is also clear that the RNA binding residues on the PRY/SPRY are critical for auto-ubiquitination, but it remains unclear if this is due to a mechanistic effects or because the RNA binding

lysines themselves are targets of ubiquitination.

This question could be answered by *in vitro* ubiquitination assays, that allow to study rates of auto-ubiquitination in the presence of defined RNA concentrations. Such *in vitro* assays have been reported earlier and found an increase of ubiquitination activity in the presence of RNA [105, 102]. In these assays the ubiquitination machinery of E1, E2 and E3 ligase is reconstituted in the presence of ATP and magnesium, the reaction is quenched after defined times and analysed using SDS-PAGE. Ubiquitinated products can be detected by Western blotting or detection of ubiquitin labelled with a fluorescent dye. Despite numerous attempts these assays were found unreliable and poorly reproducible in my hands due to the failure to obtain full-length TRIM25 from insect cells without impurities of RNAs and host proteins, including components of the ubiquitination machinery, or pre-existing ubiqutination. The production of full-length TRIM25 using Sortase A mediated ligation of separately expressed RBCC and PRY/SPRY as described in section 4.9 might offer an alternative here, but requires further optimisation.

4.7. Interaction of TRIM25 and RIG-I

Although the interaction between TRIM25 and RIG-I is well characterized in cells, it could so far not be validated *in vitro* [21, 102]. We therefore attempted to use NMR spectroscopy to characterize the interaction site and measure affinities *in vitro*. Previous research has shown that the PRY/SPRY domain of TRIM25 and the CARDs of RIG-I are sufficient for efficient interaction in cells. We therefore titrated the ^{15}N-labelled PRY/SPRY domain with natural abundance RIG-I CARDs and collected ^{1}H/^{15}N-HSQCs at every titration point (Figure 4.12 A). No changes that would be indicative of direct binding such as CSPs, line broadening or occurrence of new peaks, was observed even at excesses as high as 3:1. This suggests that if a direct interaction between the PRY/SPRY and CARDs exist, it is extremely weak with a K_D in the millimolar range.

A more recent publication [110] suggested a rather unusual mechanism for the interaction of the PRY/SPRY domain with the CARDs. This mechanism would involve a large conformational change of the N-terminal α1-helix of the PRY motif freeing up its interaction site on the PRY/SPRY domain, that could then be replaced by a similar helix of the CARDs. The authors of the original study observed elevated b factors for the α1-helix in a crystal structure, supporting its increased flexibility. We attempted to test

this mechanism by probing the dynamics and secondary structure of this helix in solution by NMR spectroscopy (Figure 4.12 B-D). Chemical shifts of the backbone carbons are sensitive probes for the backbone conformation and therefore secondary structure of a residue, as they experience characteristic shifts in helices or β-strands relative to their random coil chemical shifts [168, 135]. Secondary structure prediction from chemical shifts and order parameters calculated using TALOS clearly demonstrated the helical propensity of α1 in solution, ruling out a mechanism in which this helix would unfold spontaneously. This is also supported by $^{1}H/^{15}N$ heteronuclear NOEs (HetNOEs) that show strong correlation of the backbone orientations in solutions, indicating that the residues forming α1 are lying in a region with strong secondary structure. This would however still allow for a mechanism in which the entire α1-helix flips out. Such dynamical processes can be observed using NMR relaxation measurements. Two forms of relaxation occur in NMR after excitation of spins from the Z axis (axis of the magnetic field) into the XY plane by electromagnetic pulses. Both are sensitive to the dynamics of the nuclei involved: Longitudinal or T1 relaxation refers to the decay of magnetisation in the XY plane after excitation due to re-orientation of spins with the magnetic field. It is therefore also referred to as spin-lattice relaxation. Transverse relaxation, T2 relaxation or spin-spin relaxation refers to a decay of magnetisation due to loss of coherence of spins precessing in the XY plane. This is caused by minuscule differences in the precession frequency of the spins (Larmor frequency). T1 relaxation is more sensitive to dynamics at high frequencies ($10^{-8} - 10^{-11} s^{-1}$), while T2 relaxation is sensitive to slower dynamics [139]. Analysis of both longitudinal (T1) and transverse (T2) relaxation rates of the PRY/SPRY domain show no significant deviation for α1 with respect to the core domain. This suggests that α1 behaves as an integral part of and does not show strong dynamics independent of that of the PRY/SPRY domain, ruling out a spontaneous detachment of α1 from the domain. This obviously does not rule out any process that would only happen when induced by the CARDs, although such a process would likely be observed in the NMR titrations.

Together these experiments suggest the absence of any direct interaction between TRIM25 and RIG-I. This is in apparent contradiction to reports of mutants on both TRIM25 PRY/SPRY and RIG-I CARDs affecting this interaction [21, 110]. As for the mutants on the PRY/SPRY we noticed however that many of them cluster in the vicinity of our binding site 2, suggesting a role of RNA-binding in the binding of RIG-I.

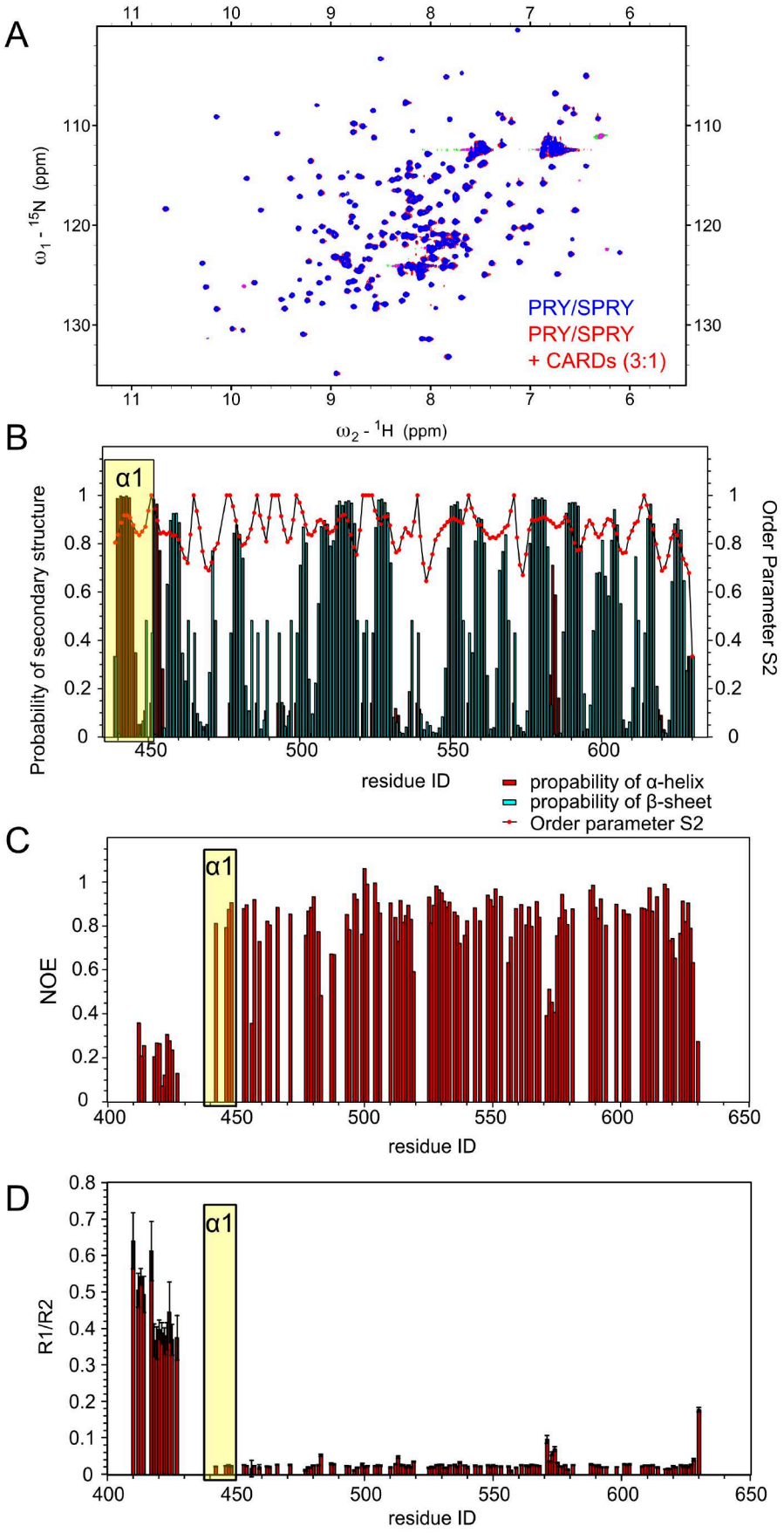
A
ω_1 - ^{15}N (ppm)
ω_2 - ^{1}H (ppm)
PRY/SPRY
PRY/SPRY
+ CARDs (3:1)
B
α1
Probability of secondary structure
Order Parameter S2
residue ID
propability of α-helix
propability of β-sheet
Order parameter S2
C
α1
NOE
residue ID
D
α1
R1/R2
residue ID

Figure 4.12.: RIG-I interaction and dynamics of the PRY/SPRY **(previous page)**: **(A)** $^{1}H/^{15}N$-HSQCs of ^{15}N-labelled PRY/SPRY titrated by natural abundance CARDs. No signs of interactions, such as CSPs, line broadening or signal loss were observed. **(B)** D'Cruz *et al.* described a role of dynamics of helix $\alpha 1$ in CARD binding [110]. Secondary structure and order parameters predicted from chemical shifts indicate that $\alpha 1$ is structured. This is supported by heteronuclear NOEs, that report on correlation of the backbone orientation of adjacent residues **(C)**. Relaxation measurements also do not report stronger dynamics of $\alpha 1$ compared to the core domain **(D)**. Our findings therefore do not support the mechanism proposed by D'Cruz *et al.* and furthermore show no evidence for a direct interaction between these domains.

4.8. RNA binding induces phase-separation

During crystallisation trials we noted that TRIM25 CC-PRY/SPRY phase-separated in the presence of DENV-SL (Figure 4.13 A). More systematic exploration of this phenomenon showed that RNA-induced phase-separation occured at concentrations as low as 1 μM in low salt buffer (100 mM NaCl). Phase-separation possibly still occurs at lower concentrations, but due to the rarity, size and uneven distribution of droplets and the risk of confusing them with other low abundant particles, e.g. aggregated proteins or dust, it gets difficult to unambiguously identify them at low concentrations. Even the pentamutant reducing RNA binding approximately 20-fold did not affect phase-separation at this concentrations. This can possibly be explained by the extremely strong binding of DENV-SL ($K_D = 15.2 \pm 3.0 nM$), so that these concentrations are much higher than the K_D even for the pentamutant. Interestingly none of the other RNAs tested in this study induced phase-separation with TRIM25. To gain further insights into the structural basis of these interactions, the phase-separated droplets were imaged using negative stain electron microscopy (EM). This showed the formation of irregular, filamentous structures of several hundred nanometers in length and about 10-15 nm in width (Figure A.11).

TRIM25 has been described to localize in membrane-less organelles also in cells and several studies have described co-localisation of TRIM25 and RIG-I in stress granules [169, 170, 171, 107]. We were therefore wondering if phase-separation could account for the TRIM25/RIG-I interaction *in vitro*. To test that, we added dTomato-RIG-I CARDs fusion protein to preformed TRIM25/DENV-SL condensates. We observed a more than

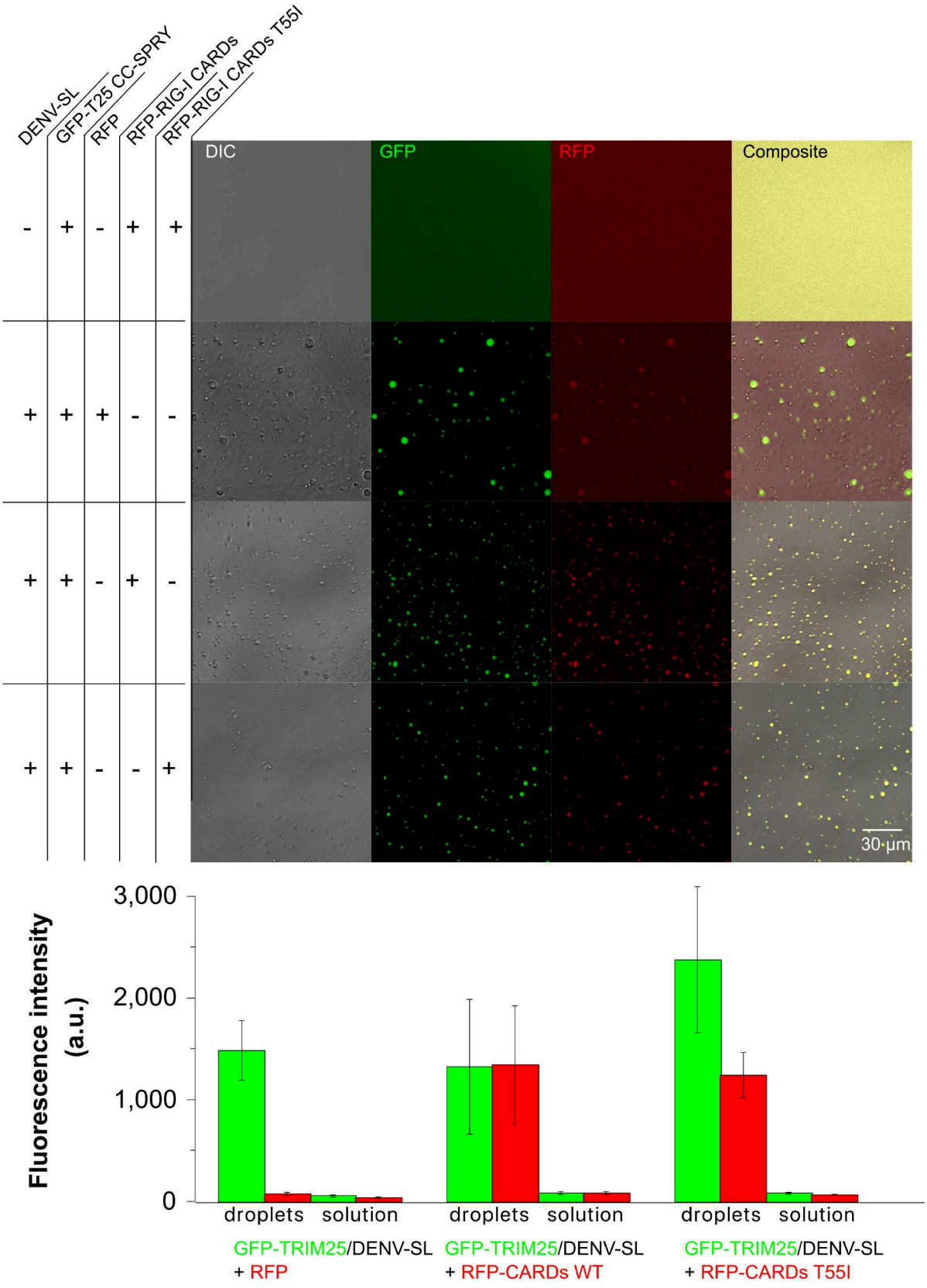
DENV-SL
GFP-T25 CC-SPRY
RFP
RFP-RIG-I CARDs
RFP-RIG-I CARDs T55I
DIC
GFP
RFP
Composite
30 µm
Fluorescence intensity (a.u.)
3,000
2,000
1,000
0
droplets
solution
GFP-TRIM25/DENV-SL + RFP
GFP-TRIM25/DENV-SL + RFP-CARDs WT
GFP-TRIM25/DENV-SL + RFP-CARDs T55I

Figure 4.13.: TRIM25 CC-PRY/SPRY phase-separates with RNA (**previous page**): **(A)** Laser scanning confocal microscopy of GFP-TRIM CC-PRY/SPRY in the absence and presence of DENV-SL. GFP-TRIM25 forms a homogenous solution in the absence of DENV-SL, but phase-separates in droplets in the presence of DENV-SL. Both RIG-I CARDs fused to red fluorescent protein dTomato (RFP-CARDs) and dTomato alone (RFP) enrich in these droplets **(B)** Quantification of fluoresence intensity as a measure of protein concentrates shows approximately 20-fold enrichment of RFP-CARDs in the droplets over the surrounding solution compared to less than 2-fold enrichment of dTomato alone. The RIG-I T55I mutant, that was reported to reduce the TRIM25/RIG-I interaction in cells [101], does not significantly change enrichment.

20-fold enrichment of CARDs in the droplets (Figure 4.13 B). dTomato alone under the a same conditions enriched less than 2-fold in the droplets. No significant change between WT CARDs and the T55I mutant, that was reported to reduce interactions with TRIM25, was observed [101].

To validate our findings in cells we transfected GFP-TRIM25 and dTomato-RIG-I CARDs into HeLa cells and assessed their subcellular localisation using confocal microscopy (Figure 4.14). Unlike previous researchers [101, 102] we found only sporadic localisation of TRIM25 WT in granules. RIG-I CARDs showed a diffuse localisation in nearly all cells and co-localisation with TRIM25 was only observed in a handful of cells. The triple mutant H505E/K508E/K602E showed elevated expression levels as judged from the stronger fluorescence intensity. It also showed more TRIM25-containing granules, especially in and around the nucleus, however it is not clear if this is an effect of reduced RNA-binding, higher expression or reduced auto-ubiquitination.

In summary, these experiments for the first time show interactions between TRIM25 and RIG-I CARDs *in vitro*, possibly giving insights into their interaction in cells. It is not clear whether this interaction is due to binding of both proteins to the same RNA or induced protein/protein interactions and additional studies will be necessary to solve this question. However, so far there is no evidence for RNA-binding of the CARDs nor could I find any direct interaction between PRY/SPRY and RIG-I CARD domains.

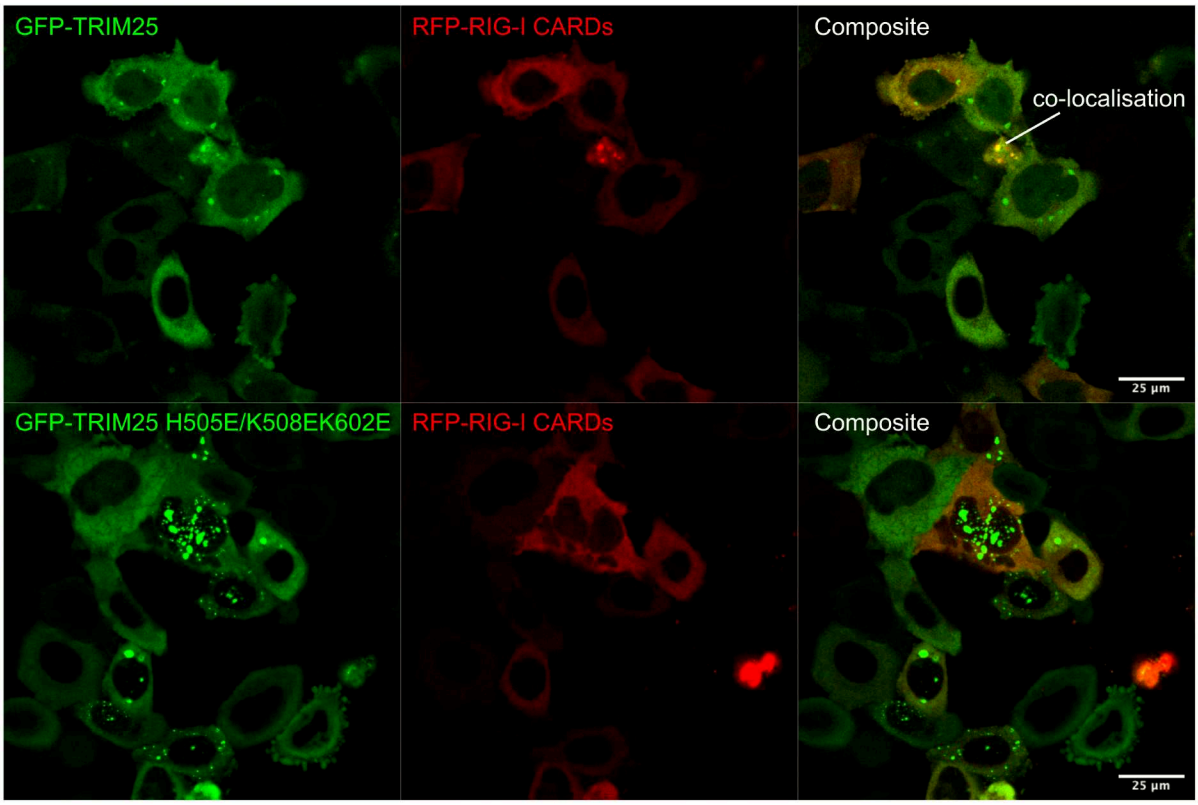

Figure 4.14.: Localisation of TRIM25 and RIG-I CARDs in HeLa cells: Confocal microscopy shows that GFP-TRIM25 WT localizes in cytosolic granule structures in many cells. RIG-I CARDs fused to the red fluorescent protein dTomato show a diffuse localisation in many cells and only rarely co-localize in the same granules as TRIM25. The triple mutant TRIM25 H505E/K508E/K602E shows higher expression levels and localizes strongly to both cytosolic and nuclear granules. Note that excitation intensities had to be lowered for the mutant to avoid overexposure. Data produced jointly with Sandra Augsten.

4.9. Development of a segmental labelling scheme for further NMR and SANS studies of TRIM25

The bacterial enzyme *Staphylococcus aureus* Sortase A allows to ligate two separately expressed proteins *in vitro* (Figure 4.15 A). Requirement for this is that one of the proteins carries a C-terminal Sortase recognition site LPXTG, while the other starts with a glycine [129]. The recognition site could be introduced into the L2 linker between CC and PRY/SPRY using only two mutations (T405A F406T). TRIM25 189-407 T405A

F406T was cloned into pETM22 and expressed in BL21(DE3). The purified product could then be linked with the N-terminally extended PRY/SPRY (aa 407-630) using Sortase A. Reaction times and reagent concentrations needed careful optimisation, but in the end the ligated CC-PRY/SPRY construct could be obtained with a yield of up to 20 %. This approach allowed segmental labelling of TRIM25 CC-PRY/SPRY with the CC being perdeuterated and the PRY/SPRY natural abundance (Figure 4.15 B). The opposite labelling scheme with the PRY/SPRY perdeuterated is currently not possible, since the used expression system did not allow expression of perdeuterated PRY/SPRY in sufficient quantities (see chapter 4). This construct was planned for use in SANS, but suffered from similar oligomerisation issues as the natural abundance protein in D_2O.

A similar approach was used to obtain full-length TRIM25. The tripartite motif with the L2 linker extended to the recognition site (aa 1-407 T405A F406T) could be expressed as a MBP-fusion construct and ligated with the extended PRY/SPRY. The reaction was significantly slower than for the CC-PRY/SPRY and never proceeded to more than about 50 % completion. Purification of the ligated protein therefore proved difficult and the final product contained significant amounts of unreacted RBCC (Figure 4.15 C). The solubility tag could not be cleaved efficiently and therefore remained in the final construct. Because of these limitations additional work is necessary before this construct may be used in structural experiments or in vitro ubiquitination experiments. Ultimately, it may allow for studies of the interaction of the N-terminal domains of TRIM25 with the PRY/SPRY and how this is affected by RNA-binding.

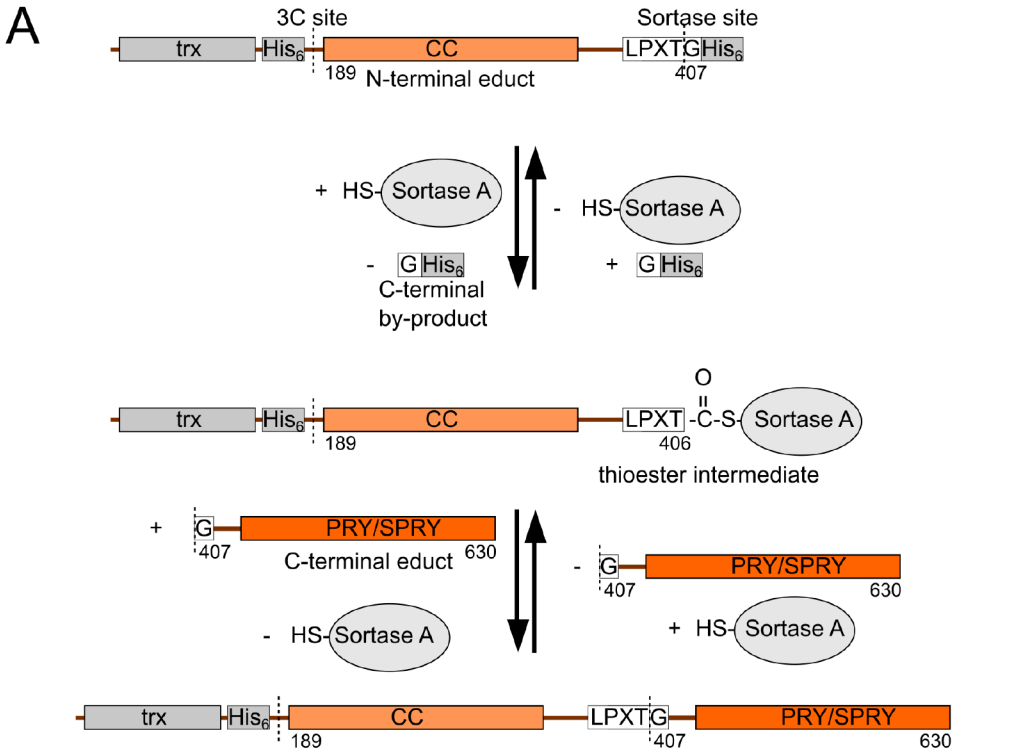
A
3C site
Sortase site
trx
His6
CC
LPXTGHis6
189
N-terminal educt
407
+ HS-Sortase A
- G His6
C-terminal
by-product
- HS-Sortase A
+ G His6
O
trx
His6
CC
LPXT -C-S- Sortase A
189
406
thioester intermediate
+ G
PRY/SPRY
407
C-terminal educt
630
- HS-Sortase A
- G
PRY/SPRY
407
630
+ HS-Sortase A
trx
His6
CC
LPXTG
PRY/SPRY
189
407
630

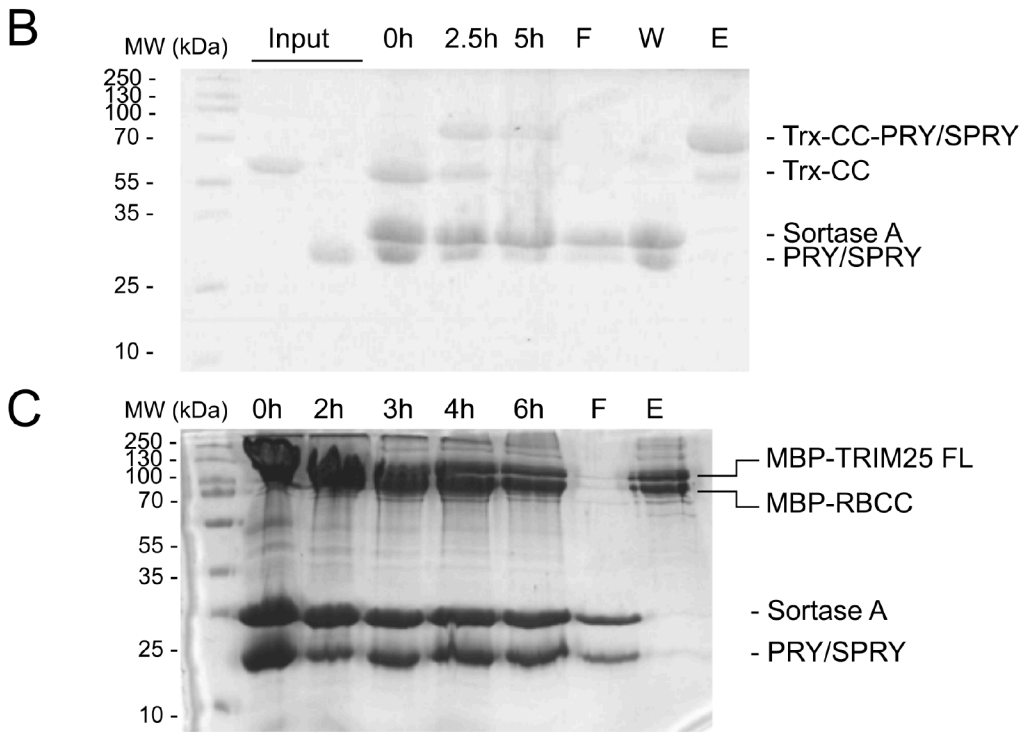
B
MW (kDa)
Input
0h
2.5h
5h
F
W
E
250 -
130 -
100 -
70 -
55 -
35 -
25 -
10 -
- Trx-CC-PRY/SPRY
- Trx-CC
- Sortase A
- PRY/SPRY
C
MW (kDa)
0h
2h
3h
4h
6h
F
E
250 -
130 -
100 -
70 -
55 -
35 -
25 -
10 -
MBP-TRIM25 FL
MBP-RBCC
- Sortase A
- PRY/SPRY

Figure 4.15.: Sortase A allows for segmental isotope labelling **(previous page)**: **(A)**Schematic representation of the Sortase A mediated reaction: Sortase A binds the recognition site LPXTG and cleaves it, forming a thioester intermediate via a catalytic cysteine. The nucleophilic amino group of the N-terminal glycine of the C-terminal educt attacks the intermediate and forms a peptide bound, leading to the desired ligation product. All steps of the reaction are fully reversible. Therefore the small C-terminal by-product has to be continuously removed from the reaction mixture by ultra-filtration or dialysis to drive the reaction towards the desired product, which after completion of the reaction can be purified by Nickel affinity chromatography. **(B)**Perdeuterated Trx-CC is ligated to PRY/SPRY using Sortase A. The product of about 70 kDa builds up over time and is purified using Nickel affinity chromatography. Sortase A and left-over PRY/SPRY is found in the flow-through (F) and wash (W) of the column, while the product remains bound to the column until eluted with 300 mM imidazole (E). **(C)** A similar approach using MBP-fused RBCC produces full-length protein, but the efficiencies are lower and the product does not separate from the MBP-RBCC on the Nickel affinity column.

5. Discussion

5.1. The CC:PRY/SPRY interaction

Data from multiple structural and biophysical techniques support the presence of a transient interaction between the CC and PRY/SPRY of TRIM25 in solution. The importance of this interaction is highlighted by the near complete loss of function in RIG-I ubiquitination upon mutation of the interface (Y463S Y476S). This can be understood by comparison with recent structures of the tripartite motif of TRIM28 (KAP1) [150, 165]. In these structures the RING domain binds to the ends of the CC just outside the equivalent position to the CC:PRY/SPRY interaction side in TRIM25 (Figure 5.1 A). This allows to propose a model of near full-length TRIM25 with the RING domain and PRY/SPRY in close proximity and possibly interacting. Structures of the TRIM25 RING with E2-ubiqutin conjugates have been reported [173, 113] and by incorporation of these structure in the model further insights into the mechanism of TRIM25 ubiquitination were gained. In such a model, the E2 bound by the RING is positioned in the broad cleft between PRY/SPRY and CC (Figure 5.1 B). Ubiquitin is clamped between the E2 and CC, with its C-terminal peptide passing below the E2 and contacting the PRY/SPRY domain. The C-terminus of ubiquitin is positioned close to K508 on the PRY/SPRY domain, a residue that is possibly prone to auto-ubiquitination, as the H505E K508E mutation strongly reduces auto-ubiquitination in cells. It should however be noted that this model does not agree with earlier proposed models [113] that suggest a position of the RING closer to the middle of the CC and allow for intramolecular RING dimerisation. Additional structural work will be necessary to decide which model describes the true state of TRIM25.

Intriguingly, together with recent structures of TRIM25 CC bound to Influenza A NS-1 solved in the lab of Katrin Rittinger this can explain the mechanism of TRIM25 inhibition by NS-1 [10]. The effector domain (ED) of NS-1 binds the TRIM25 CC opposite to the PRY/SPRY binding site. While this causes only minor clashes, NS-1

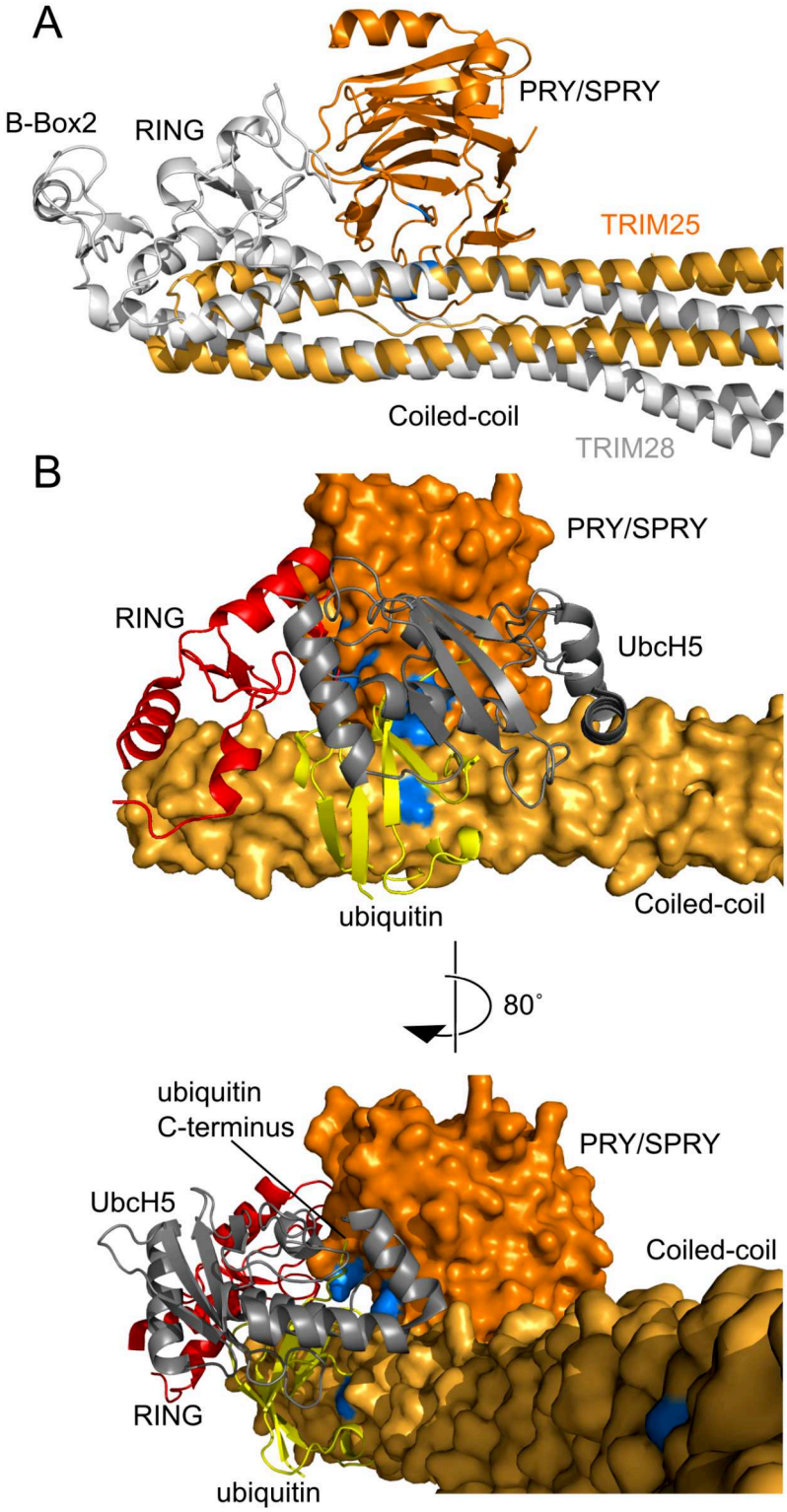
A
B-Box2
RING
PRY/SPRY
TRIM25
Coiled-coil
TRIM28
B
PRY/SPRY
RING
UbcH5
ubiquitin
Coiled-coil
80˚
ubiquitin
C-terminus
PRY/SPRY
UbcH5
Coiled-coil
RING
ubiquitin

Figure 5.1.: Model of the full-length TRIM25 **(previous page)**: **(A)** The recent structures of the tripartite motif of TRIM28 allow to construct a model of near full-length TRIM25 (the B-Box1 is lacking in these structures) [150, 165]. The ends of the CCs of TRIM25 and TRIM28 align well and allow for speculation on the position of RING and B-Box2. The RING domain in this model is found just outside the PRY/SPRY binding site and would be close enough to interact with the PRY/SPRY. **(B)** Inclusion of a crystal structure of the TRIM25 RING in complex with the E2 UbcH5 conjugated to ubiquitin (5FER) shows that the E2-Ub conjugate fits between the PRY/SPRY and CC with minimal clashes. The C-terminus of ubiquitin in this model runs between the E2 and CC and contacts the PRY/SPRY near the residue K508, that in cell assays is critical for auto-ubiquitination. It is noteworthy that in this model the E2 obstructs the RNA binding interface on PRY/SPRy and CC (shown in blue) and RNA binding therefore requires a huge conformational change of the N-terminus of TRIM25.

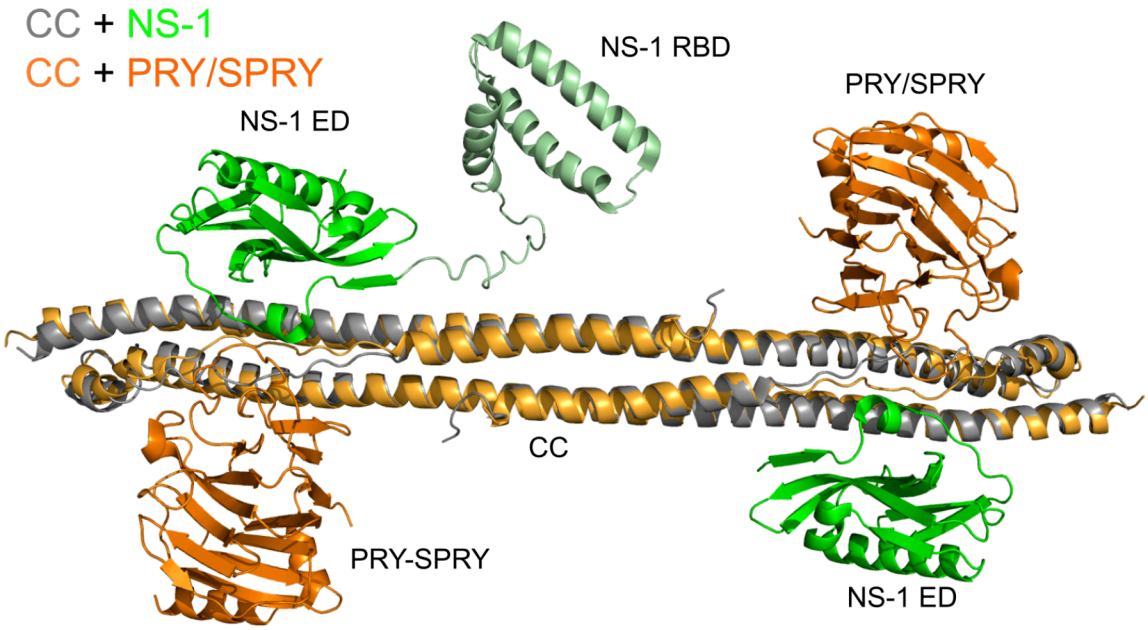

Figure 5.2.: The CC:PRY/SPRY interaction explains the mechanism of Influenza A NS-1: The alignment of structures of TRIM25 CC-PRY/SPRY (orange) and CC (gray) bound by NS-1 (green) shows that binding of the NS-1 effector domain (ED) prevents simultanous binding of the PRY/SPRY domain by distorting the CC. Note the presence of the additional RBD in close proximity to the RNA-binding interface of TRIM25. This could allow for a mechanism were binding of NS-1 and TRIM25 to the same RNA facilitates their interaction. A similar mechanism was recently proposed for DHX30, another target of NS-1 [172].

binding to the α 2 and 3 helices of the CC leads to distortions of the structure that prevents simultaneous binding of the PRY/SPRY (Figure 5.2).

An interaction between CC and PRY/SPRY was also reported earlier for Pyrine (TRIM20) [174]. The interface of this interaction found in the crystal structure differs significantly from that found in TRIM25 and the interaction appears to be much more stable in solution [174]. However, the authors report a second conformation of the protein dominant in solution, that involves a rotation of the PRY/SPRY along the CC. This conformation is possibly closer to the interaction observed for TRIM25. Irrespectively, the interaction between CC and PRY/SPRY might be more common among TRIM proteins.

5.2. Mechanism of RNA binding and catalytic activation

RNA binding of TRIM25 depends on several, in isolation weakly interacting binding sites, that together achieve remarkable affinity and structure specificity. We could confirm and refine a previously reported binding site on the PRY/SPRY [111] and find additional binding sites on the PRY/SPRY and CC. This second binding site on the PRY/SPRY specifically binds double-stranded RNA and overlapps with a previously reported binding site for RIG-I [110]. The presence of several binding sites with different specificities for single- or double-stranded RNA likely explains the failure of previous studies to report a clear RNA motif for TRIM25 [100]. We suggest that TRIM25 binds RNA with structure rather than sequence specificity, which is supported by the presence of very similar stem-loops in the reported RNA targets. In such a model binding site 2 and parts of binding site 1 on the PRY/SPRY bind the stem, while the remaining surface of binding site 1 and the CC bind the loop. Sanchez *et al.* [102] described an additional lysine-rich sequence in the L2 linker to be critical for double-stranded RNA-binding. Albeit much weaker , I could confirm a contribution of this sequence to stem-loop binding.

In order to achieve structure specific binding, the binding sides have to be rigidly assembled. This is achieved through the weak CC:PRY/SPRY interaction that is stabilized by RNA binding (section 5.1). In agreement with this the mutant reducing the CC:PRY/SPRY interaction also reduces affinity to RNA. Stabilisation of this interaction brings the PRY/SPRY domain in close proximity to the RING, allowing for more efficient ubiquitination of substrates bound by the PRY/SPRY. This mechanistically explains the enhanced auto-ubiquitination of TRIM25 in the presence of RNA reported

earlier [105, 102].

This mechanism is similar to that of Roquin2, another RNA-binding E3 ligase [37]: Roquins bind RNA through two multi-domain subunits, that are connected by a flexible linker. RNA-binding happens at the interface of the two subunits and removes flexibility from the system. This forces the N-terminal RING domain into a conformation that restricts its ability to bind some E2s, leading to a selective activation of K63-linked, but not K48-linked ubiquitination. Such a selective activation is plausible also for TRIM25, as in the model of full-length TRIM25 with the E2-ubiquitin conjugate in place, RNA and the E2 compete for space (Figure 5.1). This crowding could explain the reduced RNA binding of full-length TRIM25 compared to CC-PRY/SPRY reported earlier [102].

5.3. RNA assisted substrate recruitment and phase-separation

In addition to directly increasing ubiquitination activity of TRIM25 through stabilisation of a more active conformation, RNA binding may also participate in the recruitment of substrates. In line with this many of the reported substrates of TRIM25, including RIG-I, ZAP, TuT4, p53, MDM2 have confirmed or putative RNA binding activity [21, 104, 100, 175, 176]. This might be especially relevant in the case of RIG-I for which we found no evidence for a direct protein/protein interaction. This case is discussed in more detail in the next section.

The co-localisation of TRIM25 with its substrate can be further enhanced through phase-separation. Localisation of TRIM25 and other TRIMs to membrane-less organelles in cells was reported early on [6], but the mechanism by which this happened remained unclear. Our observation that the DENV-SL RNA can induce phase-separation of TRIM25 *in vitro* can give new insights into this mechanism. Since the CC-PRY/SPRY is sufficient for phase-separation in the presence of RNA, two mechanisms are likely (Figure 5.3): a large enough RNA might be able to bind two or more TRIM25 dimers simultanously thereby leading to the formation of a linear polymer. Alternatively, RNA-binding might stabilize the interaction of the PRY/SPRY of one molecule with the CC of another dimer, thereby potentially leading to the formation of gel-like structures with each dimer interacting with up to four other dimers. The observation that only DENV-SL, but not the smaller RNAs tested in this study promoted phase-separation might give a hint,

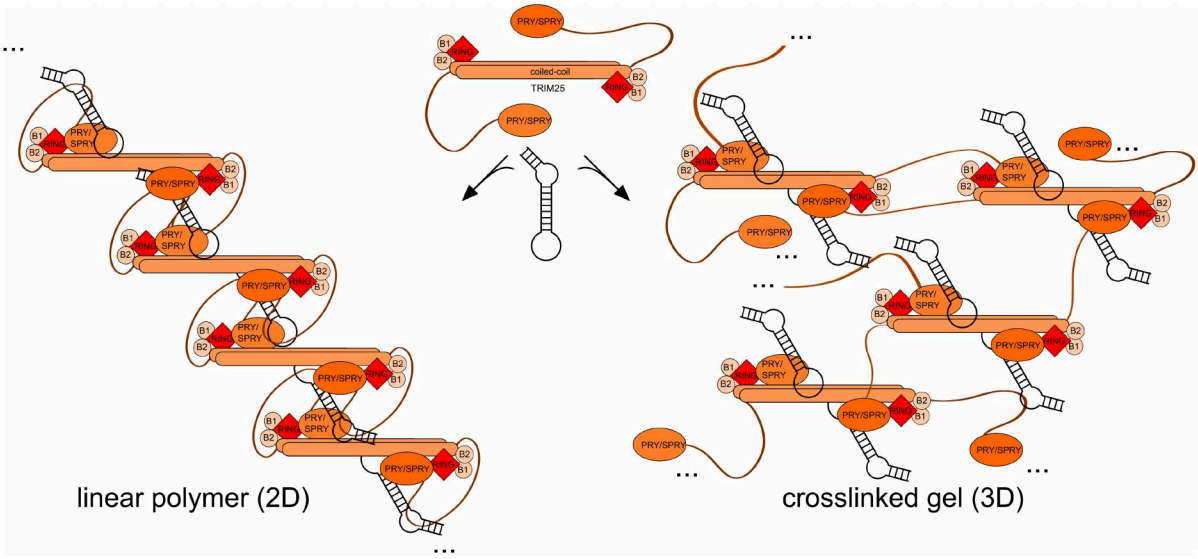

Figure 5.3.: Possible mechanisms of RNA-induced phase-separation of CC-PRY/SPRY: Binding of two or more TRIM25 dimers to a sufficiently large RNA can lead to the formation of a linear polymer of polymers (left). Alternatively, stabilisation of the CC:PRY/SPRY interaction may occur intermolecularly, so that binding of the PRY/SPRY of one dimer to the CC of another dimer can be stabilised. In this case every dimer can interact with up to four neighbours leading to a heavily cross-linked gel-like structure. In either case the interactions are likely very dynamic and mixed forms are conceivable. In the full-length, additional, unspecific protein/protein interactions, e.g. through the B-Boxes might stabilize the interaction further.

that binding of the RNA to at least two dimers is required, however DENV-SL also shows much stronger interaction with TRIM25 than these RNAs, possibly supporting the second model. The observation of large filamentous species in negative stain EM (Figure A.11) suggests that high-resolution EM data might be able to elucidate the mechanism of phase-separation.

These models of phase-separation are also interesting since unlike the previously described cases of PML and TRIM5α [59, 177, 114], they do not rely on the B-Box or post-translational modifications, such as SUMOylation for multimerisation. It should however be possible to modify the minimal system for RNA-induced phase-separation described here so that it allows to study the impact of the various post-translational modifications of TRIM25 (phosphorylation, auto-ISGylation, auto-ubiquitination) by reconstitution of the respective pathways *in vitro* [97, 178, 108].

It is remarkable, that RIG-I CARDs strongly enrich in these granules, although they

have been reported not to bind RNA [165, 179] and in our experiments show no direct interaction with TRIM25 PRY/SPRY in the absence of RNA. This is not contradictory to previous reports [21, 110] of interactions between TRIM25 PRY/SPRY and RIG-I CARDs in cells, since these are based on co-purification experiments from cell lysates that would not be able to tell apart direct protein/protein interactions and interactions mediated by additional factors, such as RNA. In this context it is especially noteworthy that some of the mutants reported to reduce co-purification of TRIM25 and RIG-I are located in RNA binding site 2 on the PRY/SPRY, suggesting once more that this interaction is RNA dependent.

In our experiments also the RIG-I T55I mutant did not reduce enrichment of CARDs with TRIM25 in the separated phase. This at first contradicts earlier reports that this mutant abolishes the interaction with TRIM25 in cells and thereby RIG-I's ability to induce IFNβ promotor activation. However, as later *in vitro* work has shown, at least some of the effect of this mutation is due to reduced binding of K63-linked polyubiquitin chains, which is critical for oligomerisation of the CARDs and therefore downstream interferon activation [84]. A role of auto-ubiquitination of TRIM25 in RIG-I recruitment will be discussed in the next section.

In summary, the reported phase-separation and enrichment of CARDs in these droplets are the first evidence for the TRIM25/RIG-I interaction *in vitro*, although it is unclear if this interaction is due to so far unreported RNA-binding of the CARDs, an RNA-induced protein-protein interaction or an unreported contribution of the CC in CARD binding. It is to be expected that the presence of the RNA binding helicase and CTD in full-length RIG-I will further increase this interaction, which is in line with reports that full-length RIG-I strongly co-localizes with TRIM25 in cells [107], while we observed only sporadic co-localisation of RIG-I CARDs with TRIM25 in our experiments with HeLa cells.

5.4. An updated model of RIG-I ubiquitination

Taken together these results allow to update the mechanism of RIG-I ubiquitination by TRIM25 (Figure 5.4). RNA-binding of TRIM25 stabilizes the conformation of TRIM25 in which the PRY/SPRY domain is bound to the CC, bringing the PRY/SPRY in close proximity to the RING. This close proximity allows for more efficient ubiquitination of substrates bound directly to PRY/SPRY or indirectly via RNA as well as the

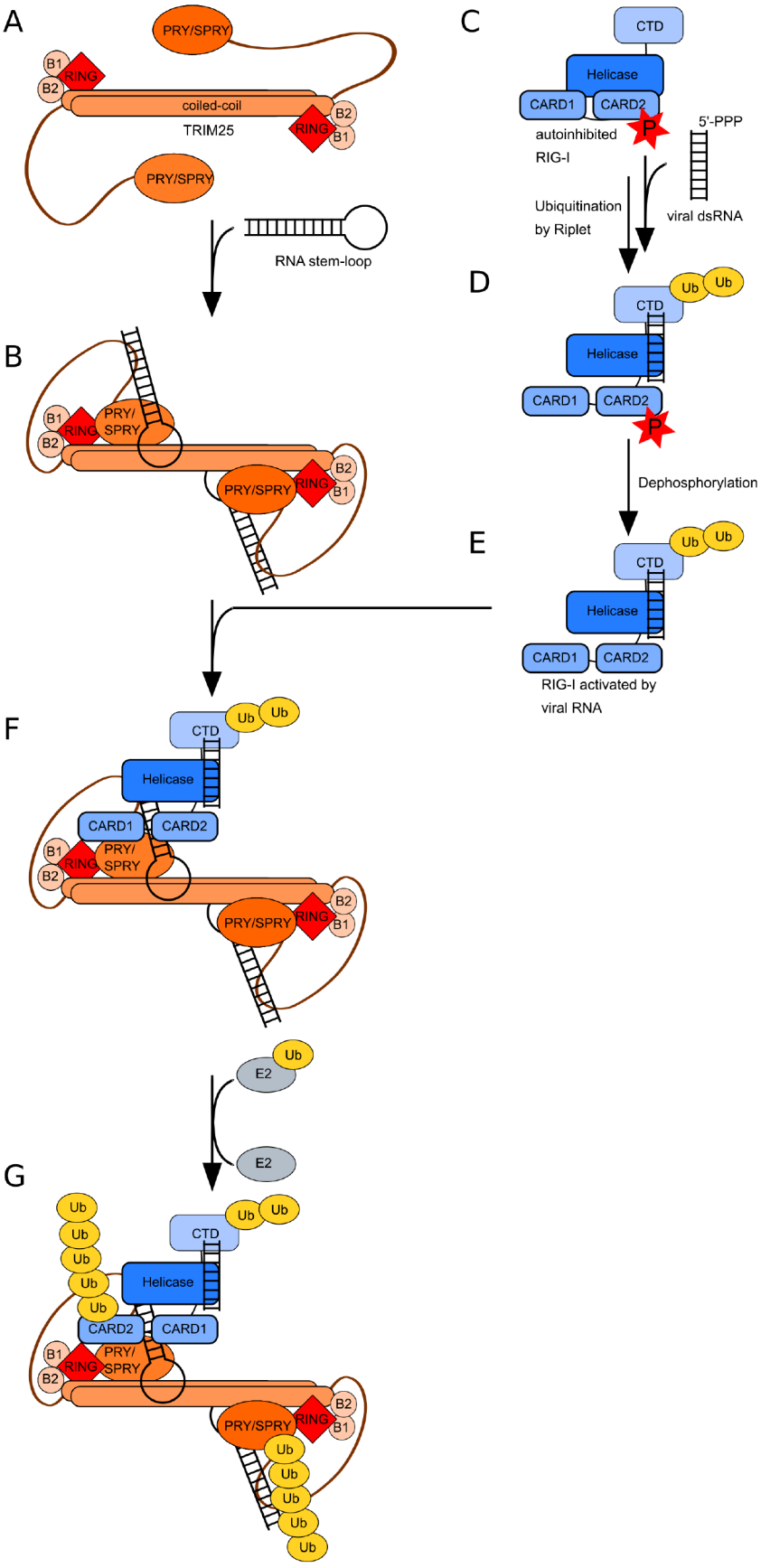
A
PRY/SPRY
B1
RING
B2
coiled-coil
TRIM25
B2
RING
B1
PRY/SPRY
RNA stem-loop
B
B1
RING
B2
PRY/
SPRY
PRY/SPRY
RING
B2
B1
C
CTD
Helicase
CARD1
CARD2
P
autoinhibited
RIG-I
5'-PPP
viral dsRNA
Ubiquitination
by Riplet
D
Ub
Ub
CTD
Helicase
CARD1
CARD2
P
Dephosphorylation
E
Ub
Ub
CTD
Helicase
CARD1
CARD2
RIG-I activated by
viral RNA
F
Ub
Ub
CTD
Helicase
CARD1
CARD2
B1
RING
B2
PRY/
SPRY
PRY/SPRY
RING
B2
B1
G
Ub
E2
E2
Ub
Ub
Ub
Ub
Ub
Ub
Ub
CTD
Helicase
CARD2
CARD1
B1
RING
B2
PRY/
SPRY
PRY/SPRY
RING
B2
B1
Ub
Ub
Ub
Ub
Ub

Figure 5.4.: Proposed mechanism of RNA-dependent RIG-I ubiquitination **(previous page)**: **(A)** In the absence of RNA CC and PRY/SPRY interact only transiently. This interaction is stabilized by cooperative RNA binding of the CC, L2 linker and PRYSPRY, bringing the PRY/SPRY in close proximity to the RING **(B)**. RIG-I meanwhile remains in the auto-inhibited resting state **(C)**. Autoinhibition is removed by binding of viral, double-stranded RNA with a triphosphate overhang at the 5'-end and possibly ubiquitination of the C-terminal domain through Riplet, a close relative of TRIM25 [80, 85] **(D)**. This leads to release of the CARDs from the helicase domain, which require de-phosphorylation by C-Src for full activation [180] **(E)**. The activated RIG-I can now bind the same stem-loop RNA as TRIM25 **(F)**. After this activation and recruitment process TRIM25 ubiquitinates the RIG-I CARDs **(E)**. TRIM25 also auto-ubiquitinates under these conditions, which possibly has regulatory functions.

PRY/SPRY itself (auto-ubiquitination). Since we found no evidence of a direct interaction between TRIM25 and RIG-I, we propose that binding of both proteins to the same RNA is required to bring them in close proximity. This idea is further supported by the recent discovery of lncRNAs promoting the TRIM25/RIG-I interaction [165, 181]. These RNAs are, however, not able to break the auto-inhibited state of RIG-I, which requires binding of additional viral, double-stranded RNA to the helicase and CTD of RIG-I and additional post-translational modifications [80, 180, 79]. While the exact sequence of events of activation of TRIM25 by lncRNA binding, association with RIG-I through binding to the same lncRNA and release of auto-inhibition of RIG-I by binding to viral RNA is not clear yet, all these processes are required for ubiquitination of RIG-I by TRIM25. Ubiquitination of RIG-I K172 by ubiquitin K63-linked chains then promotes tetramerisation of RIG-I and association with MAVS.

Mutants affecting RNA binding on the PRY/SPRY, but not on the CC also affected auto-ubiquitination in cells. This is in line with *in vitro* experiments that show an increase in auto-ubiquitination of TRIM25 in the presence of RNA [105, 102]. This effect in cells might however be partially due to removal of preferentially ubiquitinated lysines (K508 and K602). The role of auto-ubiquitination of TRIM25 is not completely understood yet. It might have a a regulatory function as auto-ubiquitination leads to proteasomal degradation and therefore facilitates removal of the protein when not needed. It might also play a role in substrate recruitment since RIG-I CARDs non-covalently interact with poly-ubiquitin chains [84], possibly assisting in recruitment to auto-ubiquitinated TRIM25. This would also explain the effect of the RIG-I T55I mutant, that was origi-

nally reported to abolish direct TRIM25/RIG-I interaction in cells, but later shown to reduce interaction with poly-ubiquitin chains *in vitro* [101, 84].

Additional E3 ligases including several TRIMs (TRIM4, 15, 40) and the closely related Riplet have been described to ubiquitinate RIG-I [85, 182, 86, 87, 183] . Recently the importance of TRIM25 for RIG-I signalling was questioned as knock-out of Riplet, but not of TRIM25 reduced RIG-I activation and NF-κB expression in different cell lines [88]. It is, however, not clear how Riplet could functionally replace TRIM25 as it ubiquitinates the CTD rather than the CARDs [85] and therefore is likely not involved in promoting CARD oligomerisation. The region around the ubiquitination sites of Riplet on the CTD are however important for the formation of the auto-inhibited resting state of RIG-I and ubiquitination could therefore be important for release of the CARD domains, allowing for downstream ubiquitination of the CARDs by TRIM25 or potentially redundant E3 ligase [184, 79]. Such potentially redundant E3 ligases are TRIM4 and MEX3C that both ubiquitinate the CARDs. A sequential ubiquitination model where Riplet is essential to break the auto-inhibited state which in turn allows for CARD ubiquitination by additional, redundant E3 ligases, such as TRIM25, explains the observation of Hayman *et al.* [88]. Regulation of TRIM25 activity through ubiquitination might also be more direct since ubiquitination of K508 and K602 likely abolishes RNA-binding and therefore down-regulates ubiquitination activity.

A potential redundancy of TRIM25 and related proteins such as TRIM4 and Riplet raises the question if the proposed mechanism of RNA activated ubiquitination is conserved in these proteins as well. This will be discussed later (section 5.6).

5.5. RNA binding in TRIM25 inhibition

Despite the strong evidence for activation of TRIM25 by RNA, there is the case of the Dengue virus subgenomic RNA (sfRNA), that appears to inhibit interferon production through binding of TRIM25 [90]. Although it has been proposed that sfRNA inhibits the TRIM25/RIG-I interaction or RIG-I ubiquitination by competing with hostRNAs that promote RIG-I ubiquitination [185] this explanation is not in agreement with the original reports, as they found co-purification of TRIM25 and RIG-I unimpaired in the presence of sfRNA [90]. This finding is however in agreement with our observation that a stem-loop originating in the Dengue sfRNA promotes phase-separation of TRIM25 and interaction with RIG-I. The exact mechanism of TRIM25 inhibition by sfRNA remains

therefore unclear. It is noteworthy, that DENV-SL binds TRIM25 much stronger than the host RNAs we tested in this study, suggesting that it is able to out-compete these.

Also other mechanisms of viral inhibition of TRIM25 might rely on RNA binding. Influenza A NS-1 binding of TRIM25 in cells was found to depend on both effector domain (ED) and RBD [89]. In contrast *in vitro* the ED alone is sufficient to explain binding of NS-1 to TRIM25 [10]. This suggests that RNA could act as a platform for the assembly of TRIM25/NS-1 complexes as well. A very similar mechanism was recently proposed for DHX30, another target of NS-1 [172].

Two other viral RBPs, the paramyxovirus protein V and protein N of the coronaviruses SARS and MERS, inhibit TRIM25 [93, 91]. Both proteins interact with the TRIM25 PRY/SPRY via their C-terminal domains, which also bind RNA [93, 91, 186, 187].

5.6. Conservation of RNA binding in TRIMs

A broader conservation of RNA binding in TRIM-PRY/SPRY has been first proposed by Choudhury *et al.* [105] based on the observation that full-length TRIM25 retains RNA binding and auto-ubiquitination when the the "RNA-binding peptide" (470-508) was replaced by homologous sequences of TRIM5α, 21, 27 and 65, but not when this region was deleted. The interpretation that this points towards conservation of RNA binding in these TRIM proteins does however not hold true in the light of our results. The deleted region contains binding site 1 reported here, but also parts of the CC:PRY/SPRY interaction site and therefore likely completely abolishes the CC:PRY/SPRY interaction required for auto-ubiquitination. This interaction is, as discussed in section section 5.1, likely conserved in other TRIM proteins. Replacement of this region with homologous sequences therefore restores the CC:PRY/SPRY interaction, so that RNA can interact with the additional binding sites on the PRY/SPRY, CC and the L2 linker. Deletion of this integral part of the domain on the other hand likely causes miss-folding of the PRY/SPRY explaining the lack of RNA-binding.

More reliable evidence for RNA binding exists for two other TRIM-PRY/SPRY proteins: TRIM65 was found in the interactome of miRNAs, although this was attributed to its interaction with the RBP TNRC6 rather than direct RNA binding by the authors [45]. TRIM26 was found to specifically bind the miRNA miR-18b [46, 44]. Despite their similar functions these proteins are evolutionary far apart with TRIM65 being a close

relative of TRIM25 with homologue in all vertebrates, while TRIM26 is part of the mammalian specific subgroup of TRIM-PRY/SPRY proteins [15].

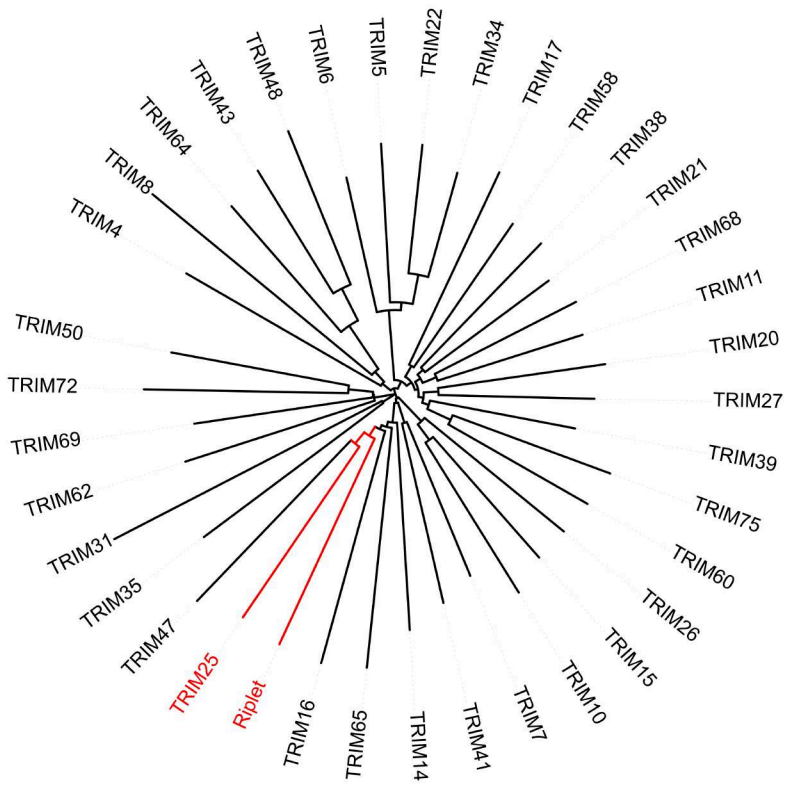

Figure 5.5.: Phylogenetic tree of TRIM-PRY/SPRY domains: The sequences of all human TRIM-PRY/SPRY domains were used for phylogenetic analysis. Riplet, despite not commonly treated as a TRIM protein is a very close relative of TRIM25 with which it also shares RIG-I as a substrate of ubiquitination.

To gain a more general insight into conservation of RNA binding in TRIM-PRY/SPRY proteins we aligned the sequences of all human members of this group and analysed for conservation of the RNA-binding residues identified by Sanchez *et al.* [102] and us (see Figure C.1). We found little conservation of the binding sites on the PRY/SPRY domain. Only the critical residues of binding site 2 Y601 and K602 show some conservation in TRIM16, 5, 22 and 34. The residues identified on the CC were even less conserved and the surrounding region is enriched in glutamates in many TRIMs. Notable exeptions from that are TRIM47 (the closest relative of TRIM25 in the TRIM group) and TRIM15 (a more distant relative sharing RIG-I as a target), which feature aromatic or positively charged residues more suitable for RNA binding in this region. Lysine and arginine-rich regions in the L2 are common in several TRIM proteins, including TRIM5, 6, 22, 34,

although they generally have fewer of these amino acids than TRIM25.

A particularly interesting case to consider is Riplet, which although not commonly seen as a TRIM protein due to its lack of B-Box domains, likely originated from this family. Phylogenetic analysis of the PRY/SPRY domains of all human TRIMs shows that the TRIM25 PRY/SPRY is the closest relative to that of Riplet (Figure 5.5). Despite this close similarity the residues critical for RNA binding are not conserved. K602, which is a critical part of the second binding site of the TRIM25 PRY/SPRY, is a glutamate in Riplet. The CC of Riplet is truncated and therefore missing the RNA-binding region altogether and the lysine-rich region in the L2 is also absent. Taken together that suggests that despite being a closely related protein and sharing the same substrate, Riplet does not seem to share the mechanism of catalytic activation by RNA with TRIM25. This raises further interesting questions as to how the interaction between Riplet and RIG-I is mediated and what made these proteins evolve along such divergent paths.

6. Conclusion and Outlook

This work represents the first biophysical and structural characterisation of the RNA binding of TRIM25. We found that TRIM25 binding relies on at least four, each individually only weakly RNA binding sites on the CC, PRY/SPRY and L2 linker, that act together to achieve structure specific binding with high affinity. This is facilitated by an, in the absence of RNA, only transient interaction between CC and PRY/SPRY. RNA binding stabilizes this interaction and thereby a more a compact conformation critical for the E3 ligase activity. While further work on the structure of the N-terminus of TRIM25 and a possible interaction of the RING with the CC and PRY/SPRY will be necessary, this suggests a model where RNA binding by the CC and PRY/SPRY is required to bring the PRY/SPRY and substrates bound by it in close proximity to the catalytic RING. This work will be facilitated by the development of segmental isotope labelling strategies for TRIM25, that will allow to study interactions of the N- and C-terminal domains using advanced NMR techniques such as paramagnetic relaxation enhancement (PREs) and the initial crystallisation conditions for TRIM25 RBCC, that may after some optimisation lead to a high-resolution structure.

At least in the case of RIG-I, RNA-binding is also required for substrate recruitment as binding to the same RNA rather than direct protein/protein interaction seem to account for the interaction. Further experiments in collaboration with the group of Sagar Bhogaraju at EMBL Grenoble are in preparation to investigate using a proteomics approach if ubiquitination of other substrates of TRIM25 depend on RNA-binding in a similar way.

Our model system for phase-separation will allow for future studies of the determinants of RNA-induced phase-separation and can be enhanced in order to allow for studies of the impact of PTMs on the regulation of phase-separation.

Due to these developments and the controversial discussion of the different roles of TRIM25, Riplet and related proteins in RIG-I, RNA-binding of TRIM25 will remain an exciting field of research for the years to come.

Appendices

A. Supplementary figures

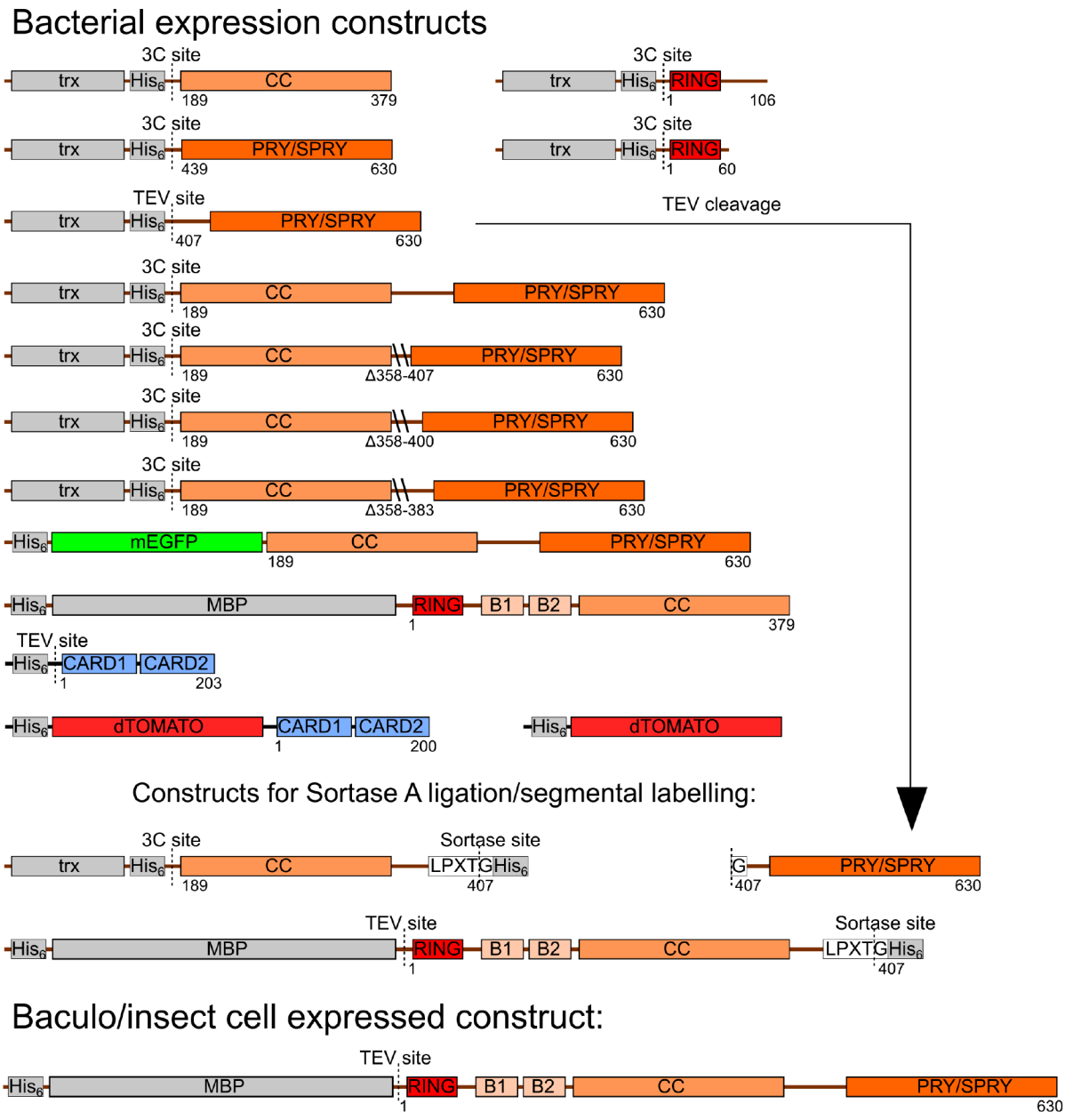

Figure A.1.: Overview of protein constructs used for *in vitro* experiments. The constructs cover all domains of TRIM25. For RIG-I only the N-terminal CARD domains were used.

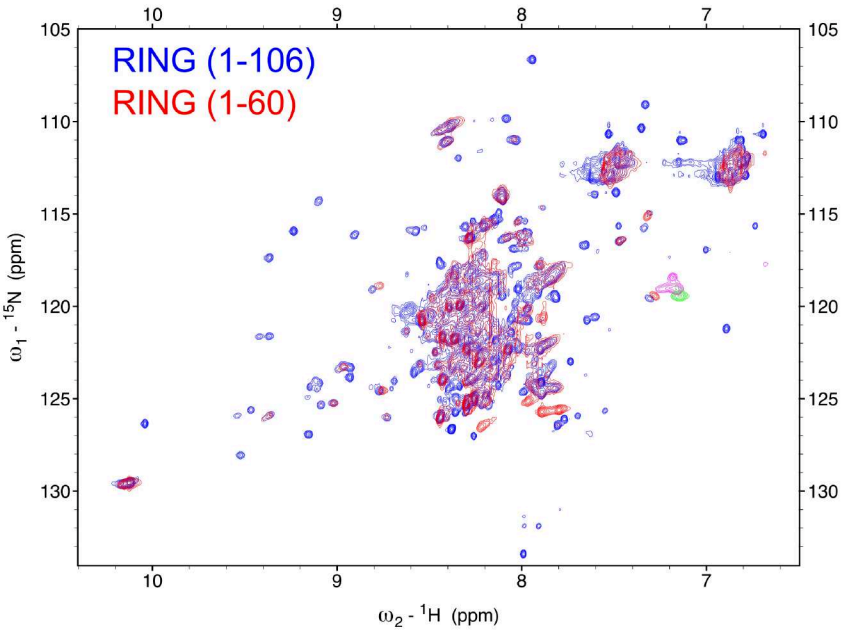

Figure A.2.: HSQCs of TRIM25 RING constructs 1-106 (blue) and 1-60 (red).

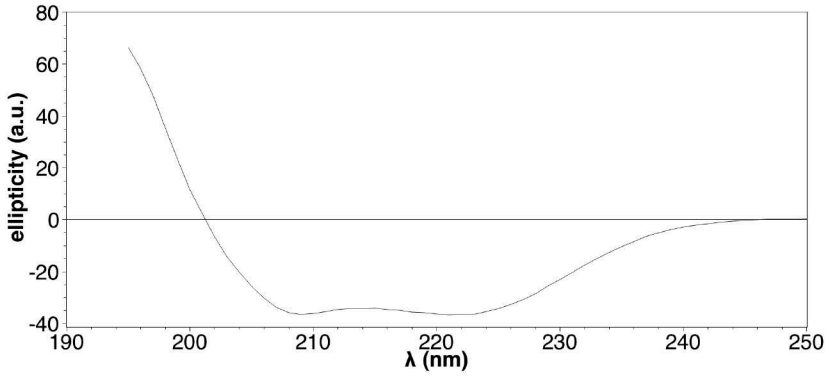

Figure A.3.: Circular dichroism spectra of TRIM25 CC (189-379). The negative bands around 208 and 222 nm are characteristic for α-helices [188].

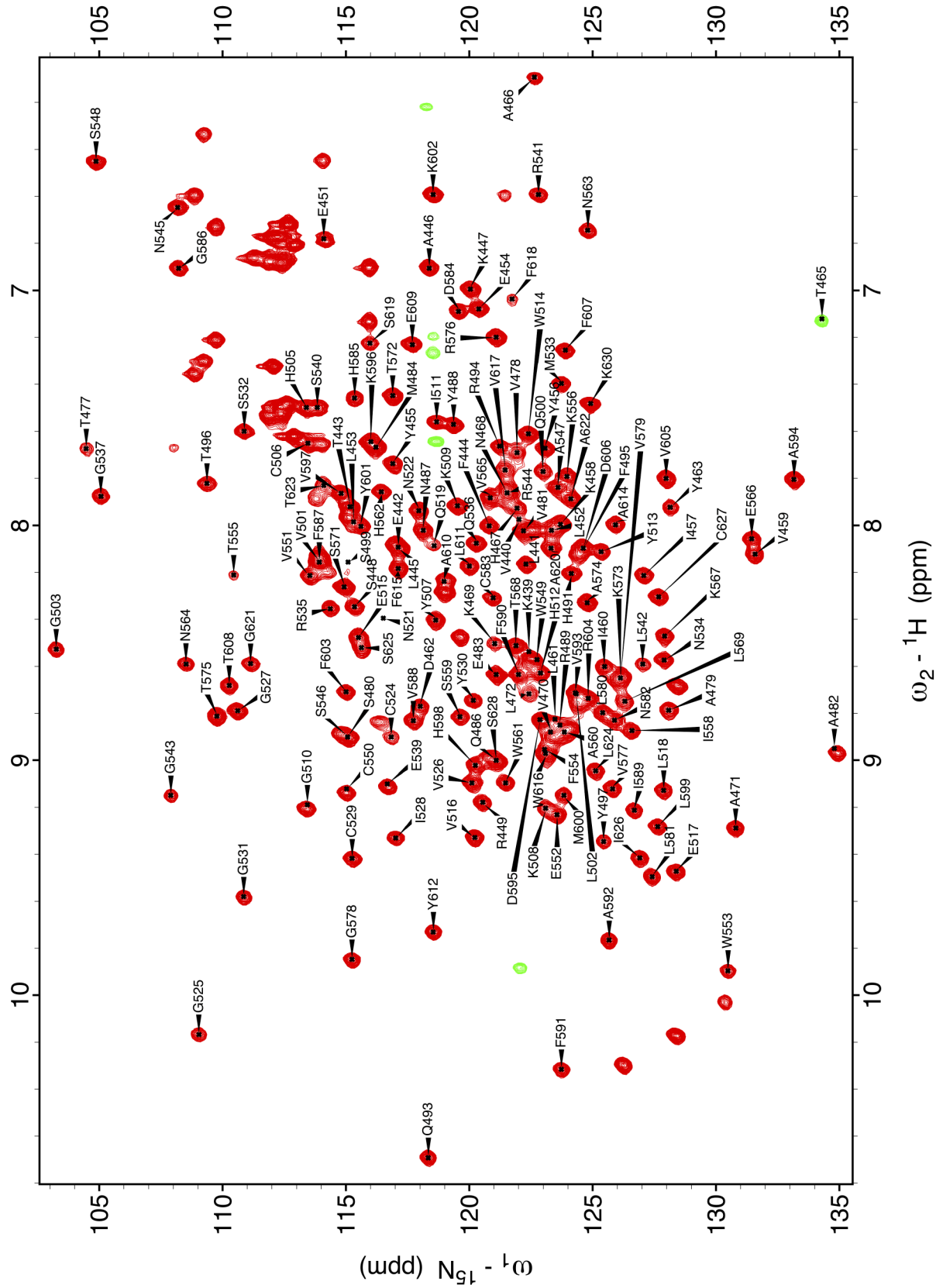

Figure A.4.: HSQC of TRIM25 439-630: 96 % of the backbone amids of the TRIM25 PRY/SPRY domain were assigned to the sequence using 3D experiments. The assignment is deposited in the BMRB under accession number: 27381.

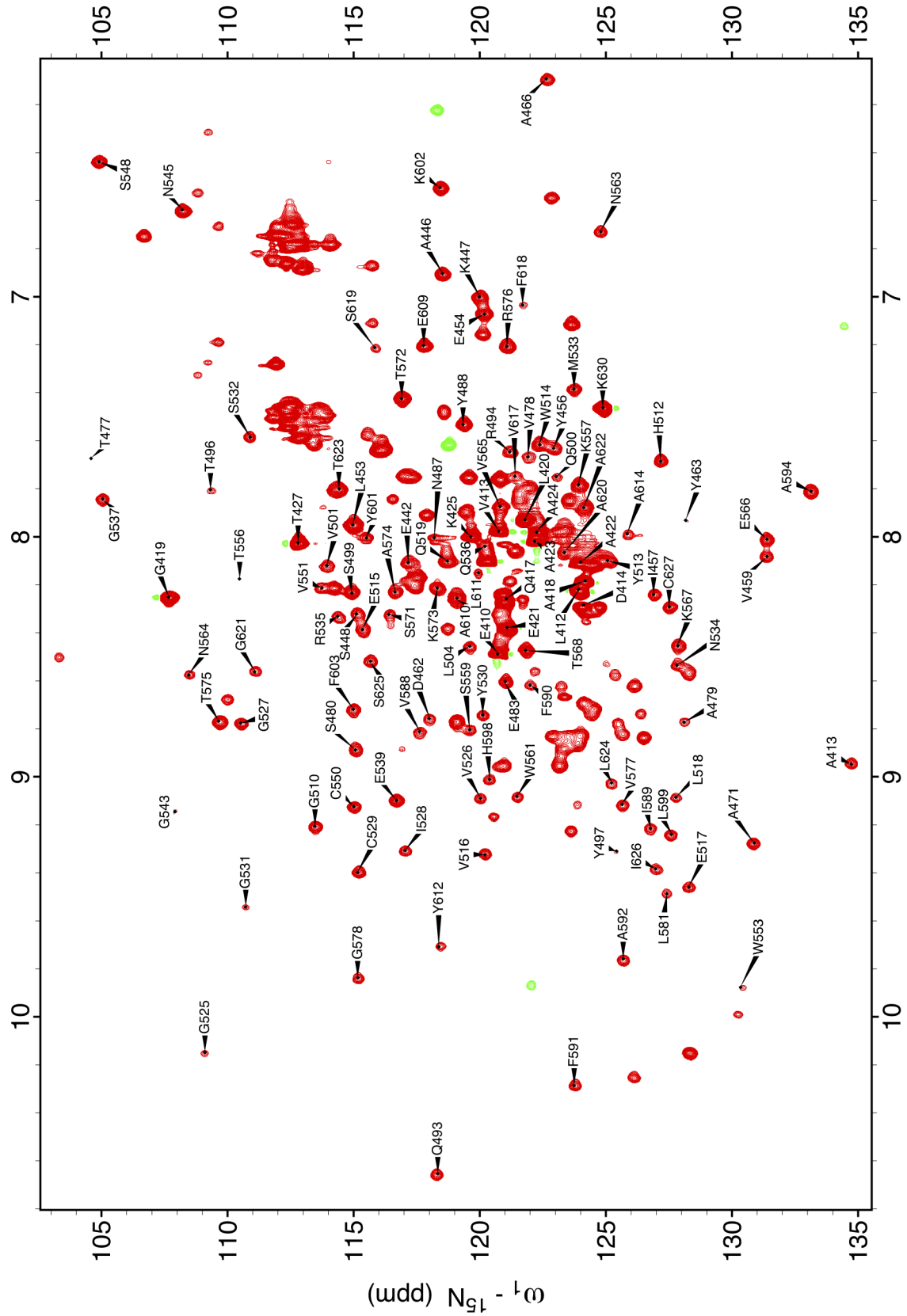

Figure A.5.: HSQC of TRIM25 407-630: 65 % of the backbone amids of the TRIM25 PRY/SPRY domain were assigned to the sequence by transfer from the assignment for 439-630 and analysis of an HNCACB.

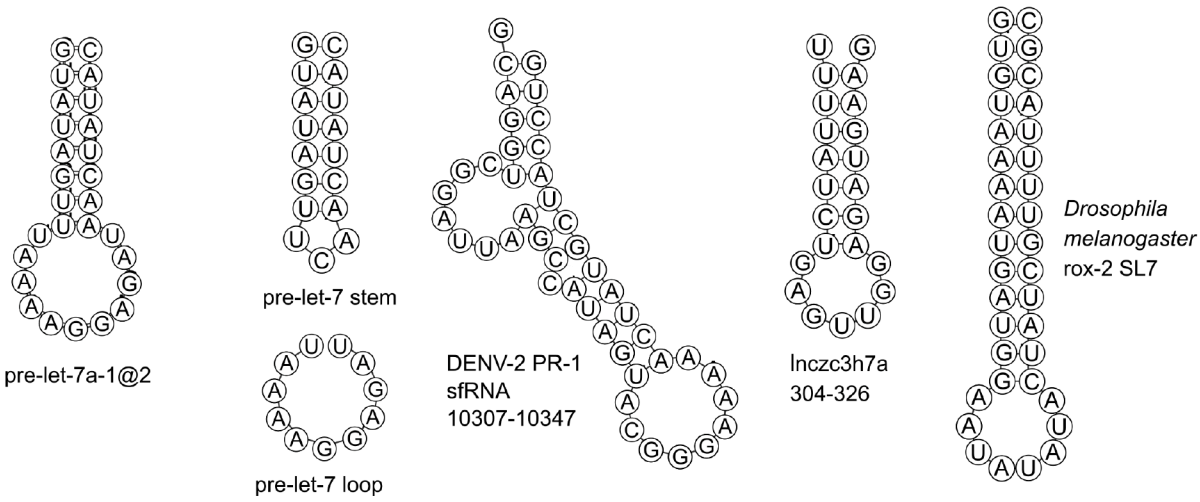

Figure A.6.: Structures of RNAs used in this thesis. Note the similarity of loop sizes in the stem-loop RNAs.

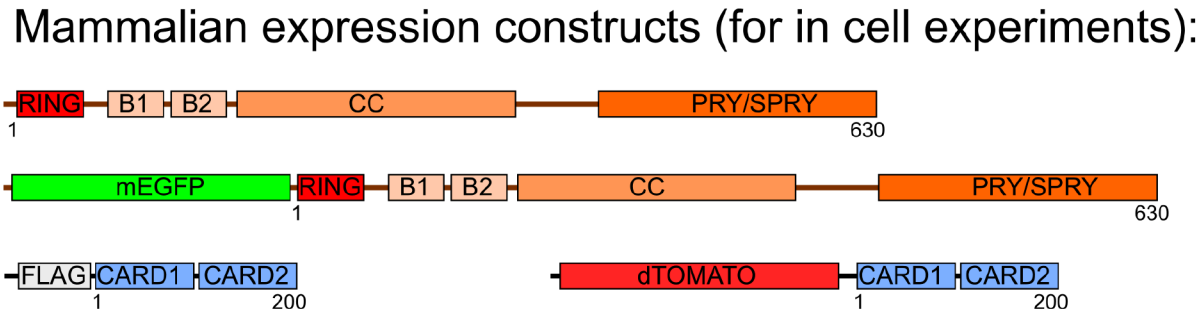

Figure A.7.: Overview of protein constructs used for in cell experiments. Full-length TRIM25 and FLAG-tagged RIG-I CARDs were used for in cell ubiquitination assays. GFP-fused TRIM25 and dTomato-fused RIG-I CARDs were used for live cell microscopy.

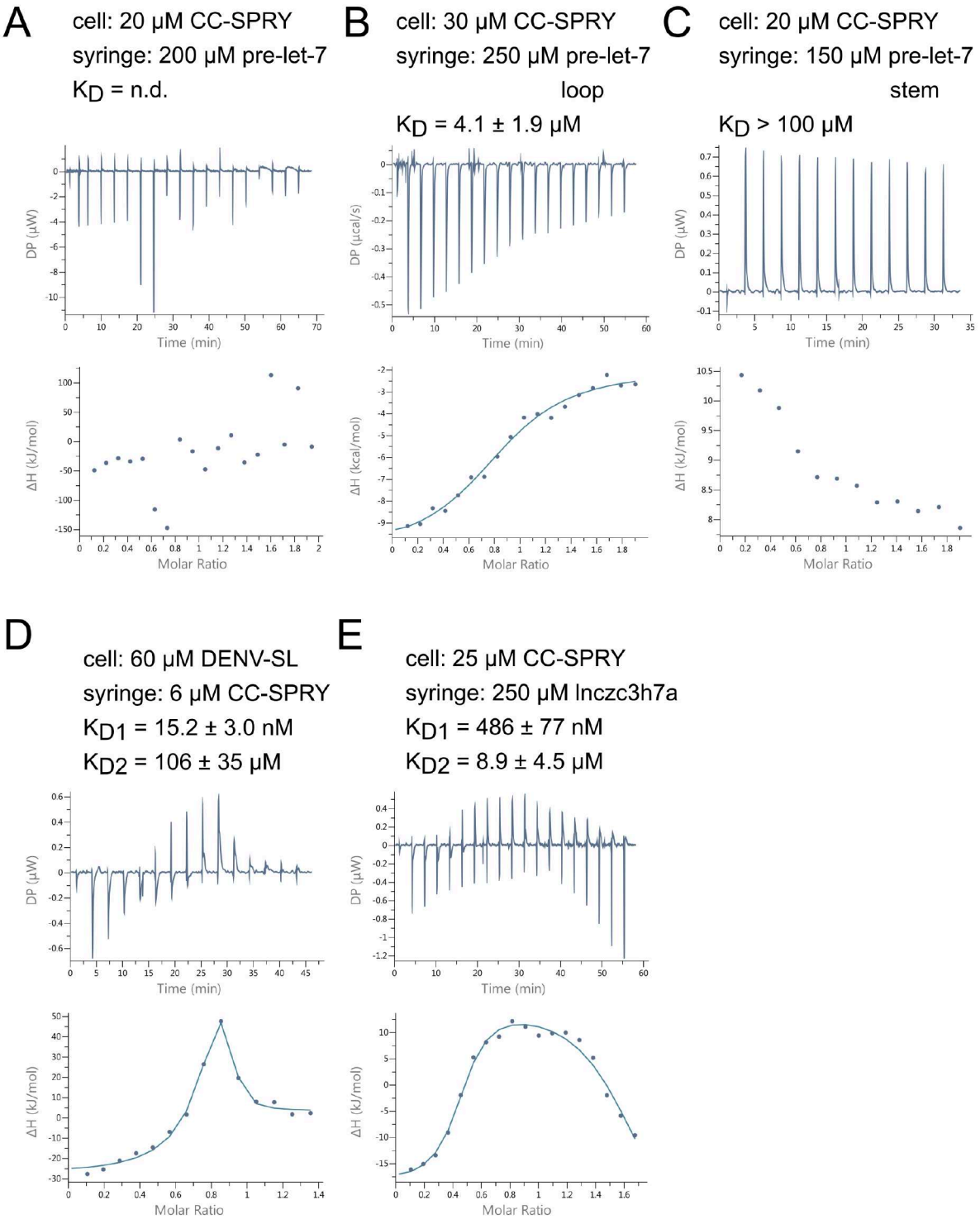

Figure A.8.: ITC curves of TRIM25 CC-PRY/SPRY WT titrated by various RNAs. Binding to short purely single or double-stranded RNAs **(B, C)** is weak, while longer stem-loop RNAs show binding with nanomolar affinity **(A, D, E)** and complex calorigrams that require models with at least two sequential binding events.

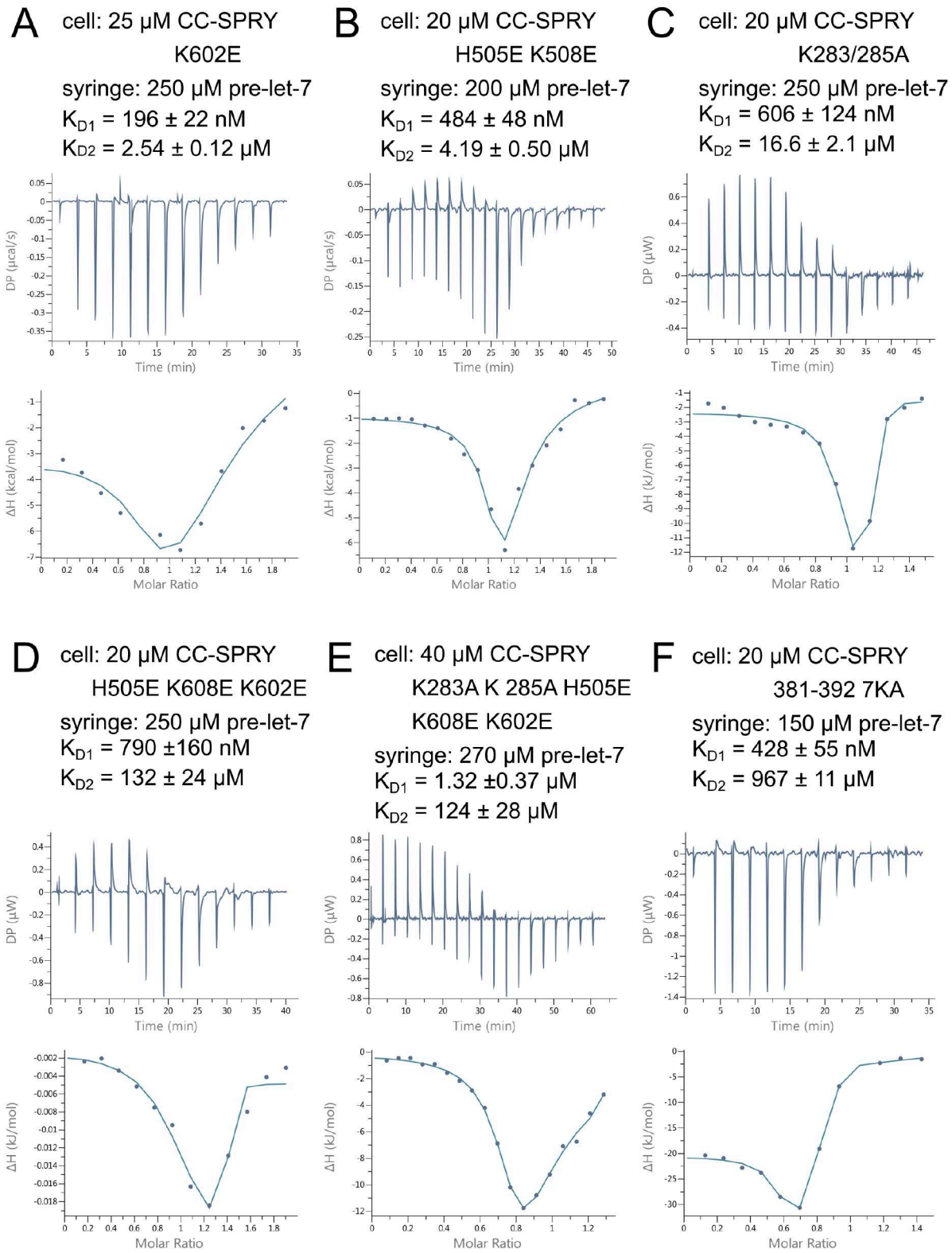
A
cell: 25 μM CC-SPRY K602E
syringe: 250 μM pre-let-7
K_{D1} = 196 ± 22 nM
K_{D2} = 2.54 ± 0.12 μM
B
cell: 20 μM CC-SPRY H505E K508E
syringe: 200 μM pre-let-7
K_{D1} = 484 ± 48 nM
K_{D2} = 4.19 ± 0.50 μM
C
cell: 20 μM CC-SPRY K283/285A
syringe: 250 μM pre-let-7
K_{D1} = 606 ± 124 nM
K_{D2} = 16.6 ± 2.1 μM
D
cell: 20 μM CC-SPRY H505E K608E K602E
syringe: 250 μM pre-let-7
K_{D1} = 790 ±160 nM
K_{D2} = 132 ± 24 μM
E
cell: 40 μM CC-SPRY K283A K 285A H505E K608E K602E
syringe: 270 μM pre-let-7
K_{D1} = 1.32 ±0.37 μM
K_{D2} = 124 ± 28 μM
F
cell: 20 μM CC-SPRY 381-392 7KA
syringe: 150 μM pre-let-7
K_{D1} = 428 ± 55 nM
K_{D2} = 967 ± 11 μM
DP (μcal/s)
DP (μW)
Time (min)
ΔH (kcal/mol)
ΔH (kJ/mol)
Molar Ratio

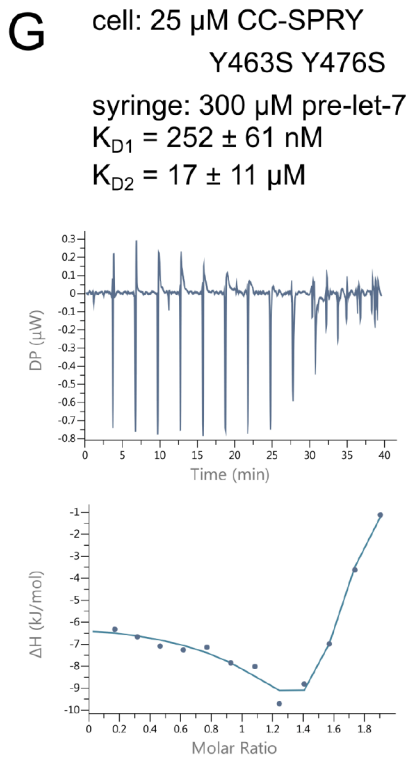

Figure A.9.: ITC curves of TRIM25 CC-PRY/SPRY mutants titrated by pre-let-7 (**previous and current page**). Mutants on the PRY/SPRY **(A, B, D)**, CC **(C)** and in the L2 linker **(F)** all affect RNA binding. The combination of the mutants on the CC and PRY/SPRY described in this thesis reduces binding of pre-let-7 about 20-fold **(E)**. In addition also the Y463S Y476S mutant, that affects the CC:PRY/SPRY mutant, reduces RNA binding **(G)**.

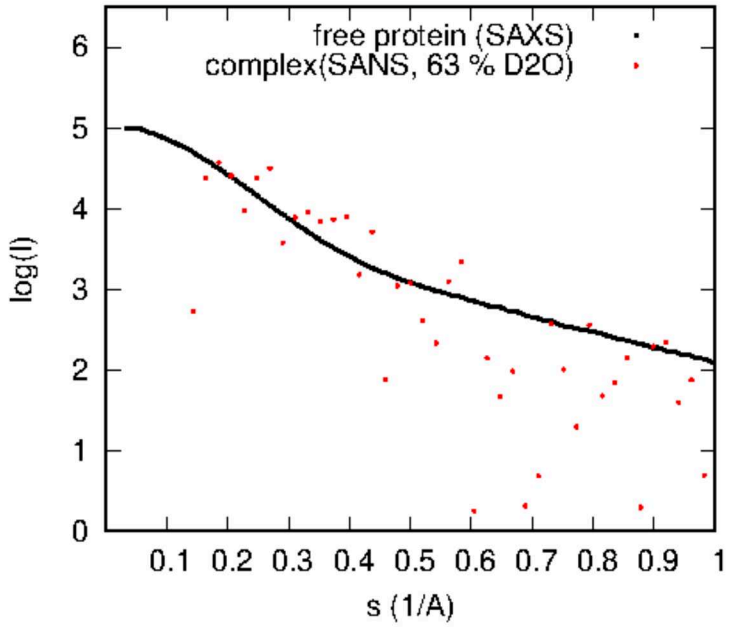

Figure A.10.: Comparison between SAXS of CC-PRY/SPRY (black) and SANS of CC-PRY/SPRY in complex with pre-let-7 at the RNA matching point (63 % D_2O, red). Despite the bad quality of data due to low solubility of the complex there is a significant change in the radius of gyration ($R_g = 6.83 \pm 0.05 nm$ for the free protein and $R_g = 4.26 \pm 0.42 nm$ for the complex.

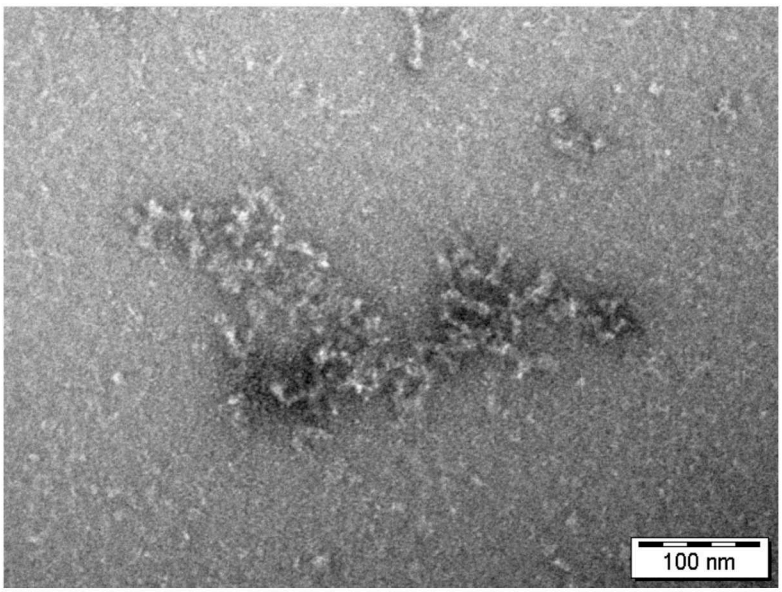

Figure A.11.: Negative stain electron microscopy of phase-separated droplets of TRIM25 CC-PRY/SPRY and DENV-SL shows the formation of large oligomeric filaments.

B. Supplementary tables

Table B.1.: Affinities of TRIM25 CC-PRY/SPRY to different RNAs estimated from filter binding assays.

protein	**RNA**	**K_D (M)**
CC-PRY/SPRY	pre-let-7-1a@2	$10.2 \pm 3.8nM$
	DENV-SL	$1.63 \pm 0.38nM$
	UNR SL6	$18.1 \pm 2.2nM$
	UNR SL67	$1.45 \pm 0.47nM$

Table B.2.: Summary of Small-angle X-ray scattering statistics. The sample marked with * was provided by Mathilde Lethier.

	TRIM25 CC-PRY/SPRY*	**TRIM25 CC-PRY/SPRY**	**TRIM25 CC-PRY/SPRY/pre-let-7**
(a) Sample Details			
Organism	*Homo sapiens*		
Source	*Trichoplusia ni* HiFive	*E. coli* BL21 (DE3)	*E. coli* BL21 (DE3)/in vitro transcription
Uniprot sequence ID	Q14258 189-630		
Description	TRIM25 189-630 (insect cell expressed)	TRIM25 189-630 (bacterially expressed)	TRIM25 189-630 in complex with the pre-let-7 stem-loop

	TRIM25 CC-PRY/SPRY*	**TRIM25 CC-PRY/SPRY**	**TRIM25 CC-PRY/SPRY/pre-let-7**
Molecular mass M from chemical composition (Da)	49,952 (monomer), 99,904 (dimer)	49,952 (monomer), 99,904 (dimer)	58,195 (monomer), 116390(dimer)
loading concentration (mg/ml)	1.0-20	0.37-6.0	n.d.
injection volume (μl)	30	30	100
concentration (μM)	8-400	7.4-120	n.d.
Solvent composition	20 mM Na_2HPO_4, pH 6.5, 150 mM NaCl	20 mM MES, pH 6.5, 75 mM NaCl and 0.5 mM TCEP	
(b) collection parameter			
Source and instrument	ESRF BM29 BioSAXS	Hamburg PETRA-III P12 with Dectris Pilatus 6M	
Wavelength (Å)	0.992	1.22	1.24
Sample-detector distance (m)	2.867	3.000	3.000
q-measurement range (Å)	0.0034-0.494	0.0226-7.405	0.0252-7.3176
Radiation damage monitoring	frame-by-frame comparison		
Exposure time (s)	1x10	0.05x20	0.195x40
Sample configuration	sample changer with flow through capillary measurement		
Sample temperature (°C)	20	20	25
(c) Software employed			
SAXS data processing	(q) vs. q using Bsx cube, solvent subtraction and curve merging using PRIMUSqt from ATSAS (Franke et al., 2017)		
Basic analyses:	Guinier, P(r), Vp PRIMUSqt from ATSAS 2.7.1 (Franke et al., 2017)		

	TRIM25 CC-PRY/SPRY*	**TRIM25 CC-PRY/SPRY**	**TRIM25 CC-PRY/SPRY/pre-let-7**
Atomic structure modelling	CRYSOL 2.8.2 from PRIMUSqt in ATSAS 2.8 (Svergun et al., 1995)		
(d) Structural parameters			
Guinier analysis			
I(0) (raw)	142.75 ± 0.36	51290 ± 160	34043 ± 42
R_g (Å)	69.8± 0.04	68.3±0.5	56.3 ± 0.1
qR_g max	1.28	1.50	1.40
Coefficient of correlation, R2	0.99	0.82	0.80
P(r) Analysis from AUTOGNOM			
I(0) (raw)	142.65	54320	35340
R_g (Å)	70.9	78.0	61.3
dmax (Å)	253	305.6	226.6
q range ($Å^{-1}$)	0.0058-0.122	0.202-3.06	0.148-2.50
χ^2 (total estimate from GNOM)	0.52	0.60	0.73
Porod volume ($Å^{-3}$) (ratio VP/calculated M)	222000	302540	182720

Table B.3.: Summary of X-ray crystallography statistics. No solution was obtained for TRIM25 CC-PRY/SPRY/pre-let-7. The solution for the PRY/SPRY domain was not completely refined, as no additional density corresponding to the RNA was found.

	TRIM25 CC-PRY/SPRY/pre-let-7	**TRIM25 PRY/SPRY [with pre-let-7]**
Data collection		
Space group	P 6 2 2	P1 2_1 1
Cell dimensions		
a, b, c (Å)	105.646, 105,646, 282.938	37.462, 103.820, 52.118

	TRIM25 CC-PRY/SPRY/pre-let-7	**TRIM25 PRY/SPRY [with pre-let-7]**
α, β, γ (°)	90.000, 90.000, 120.000	90.000, 98.702, 90.000
Number of reflections	6976 (383)	23778 (1013)
Number of unique reflections	2734 (811)	3665 (1023)
Resolution (Å)	65.67-5.21 (11.6-5.21)	(8.68-3.88)
R_{merge}	0.230 (0.531)	0.7109 (7.1088)
$CC_{1/2}$	0.985	0.000
$\langle I/\sigma I \rangle$	2.0 (0.7)	3.6 (1.9)
Completeness (%)	71.7 (60.6)	99.5 (98.9)
Redundancy	2.6(2.5)	6.5(6.2)
Refinement		
Resolution (Å)	n.a.	51.96-3.88
No. of reflections (test set)	n.a.	3665 (183)
R_{work}/R_{free}	n.a.	0.409/0.409
Number of atoms		
Protein	n.a.	1516
RNA	n.a.	0
Others	n.a.	0
Average B factors (Å^2)	n.a.	0.5
RMS deviation from ideality		
Bond length (Å)	n.a.	0.0051
Bond angles (°)	n.a.	1.833
Ramachandran statistics		
Favored regions (%)	n.a.	88.32
Allowed regions (%)	n.a.	8.97
Outliers regions (%)	n.a.	2.72

C. Sequence alignment of human TRIM-PRY/SPRY proteins

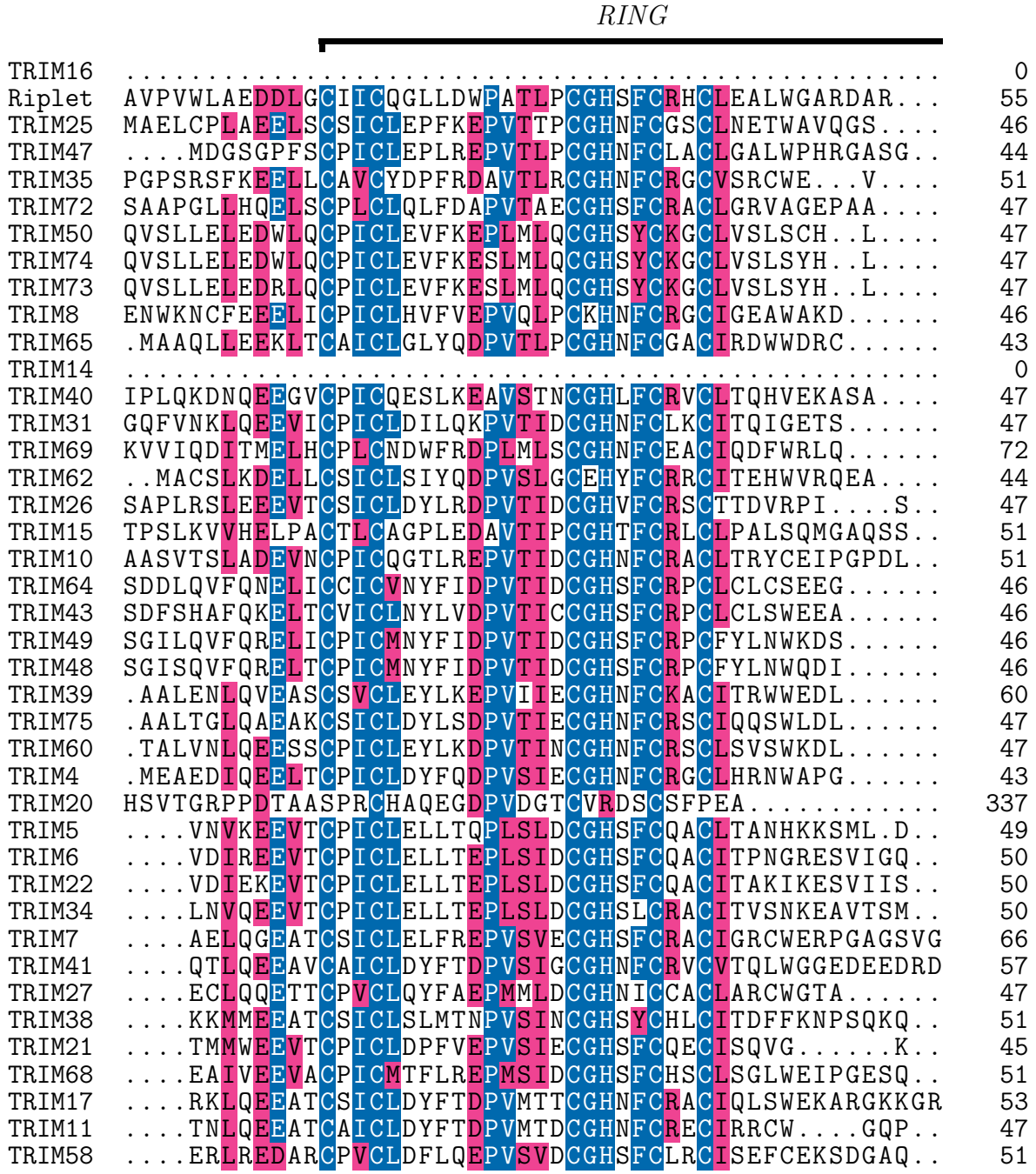

```
TRIM16  ..................................................   0
Riplet  ..................................................  55
TRIM25  ..................................................  46
TRIM47  ..................................................  44
TRIM35  ..................................................  51
TRIM72  ..................................................  47
TRIM50  ..................................................  47
TRIM74  ..................................................  47
TRIM73  ..................................................  47
TRIM8   ..................................................  46
TRIM65  ..................................................  43
TRIM14  ..................................................   0
TRIM40  ..................................................  47
TRIM31  ..................................................  47
TRIM69  ..................................................  72
TRIM62  ..................................................  44
TRIM26  ..................................................  47
TRIM15  ..................................................  51
TRIM10  ..................................................  51
TRIM64  ..................................................  46
TRIM43  ..................................................  46
TRIM49  ..................................................  46
TRIM48  ..................................................  46
TRIM39  ..................................................  60
TRIM75  ..................................................  47
TRIM60  ..................................................  47
TRIM4   ..................................................  43
TRIM20  ..................................................  337
TRIM5   ..................................................  49
TRIM6   ..................................................  50
TRIM22  ..................................................  50
TRIM34  ..................................................  50
TRIM7   ..................................................  66
TRIM41  ELDREEEEEDGEEEEVEAVGAGAGWDTPMRDEDYEGDMEEEVEEEEEGVF  107
TRIM27  ..................................................  47
TRIM38  ..................................................  51
TRIM21  ..................................................  45
TRIM68  ..................................................  51
TRIM17  ..................................................  53
TRIM11  ..................................................  47
TRIM58  ..................................................  51
```

TRIM16	. . . . .	0
Riplet	. . . . .	55
TRIM25	. . . . .	46
TRIM47	. . . . .	44
TRIM35	. . . . .	51
TRIM72	. . . . .	47
TRIM50	. . . . .	47
TRIM74	. . . . .	47
TRIM73	. . . . .	47
TRIM8	. . . . .	46
TRIM65	. . . . .	43
TRIM14	. . . . .	0
TRIM40	. . . . .	47
TRIM31	. . . . .	47
TRIM69	. . . . .	72
TRIM62	. . . . .	44
TRIM26	. . . . .	47
TRIM15	. . . . .	51
TRIM10	. . . . .	51
TRIM64	. . . . .	46
TRIM43	. . . . .	46
TRIM49	. . . . .	46
TRIM48	. . . . .	46
TRIM39	. . . . .	60
TRIM75	. . . . .	47
TRIM60	. . . . .	47
TRIM4	. . . . .	43
TRIM20	. . . . .	337
TRIM5	. . . . .	49
TRIM6	. . . . .	50
TRIM22	. . . . .	50
TRIM34	. . . . .	50
TRIM7	. . . . .	66
TRIM41	WTSGMSRSSWDNMDYVWEEEDEEEDLDYYLGDMEEEDLRGEDEEDEEEVL	157
TRIM27	. . . . .	47
TRIM38	. . . . .	51
TRIM21	. . . . .	45
TRIM68	. . . . .	51
TRIM17	. . . . .	53
TRIM11	. . . . .	47
TRIM58	. . . . .	51

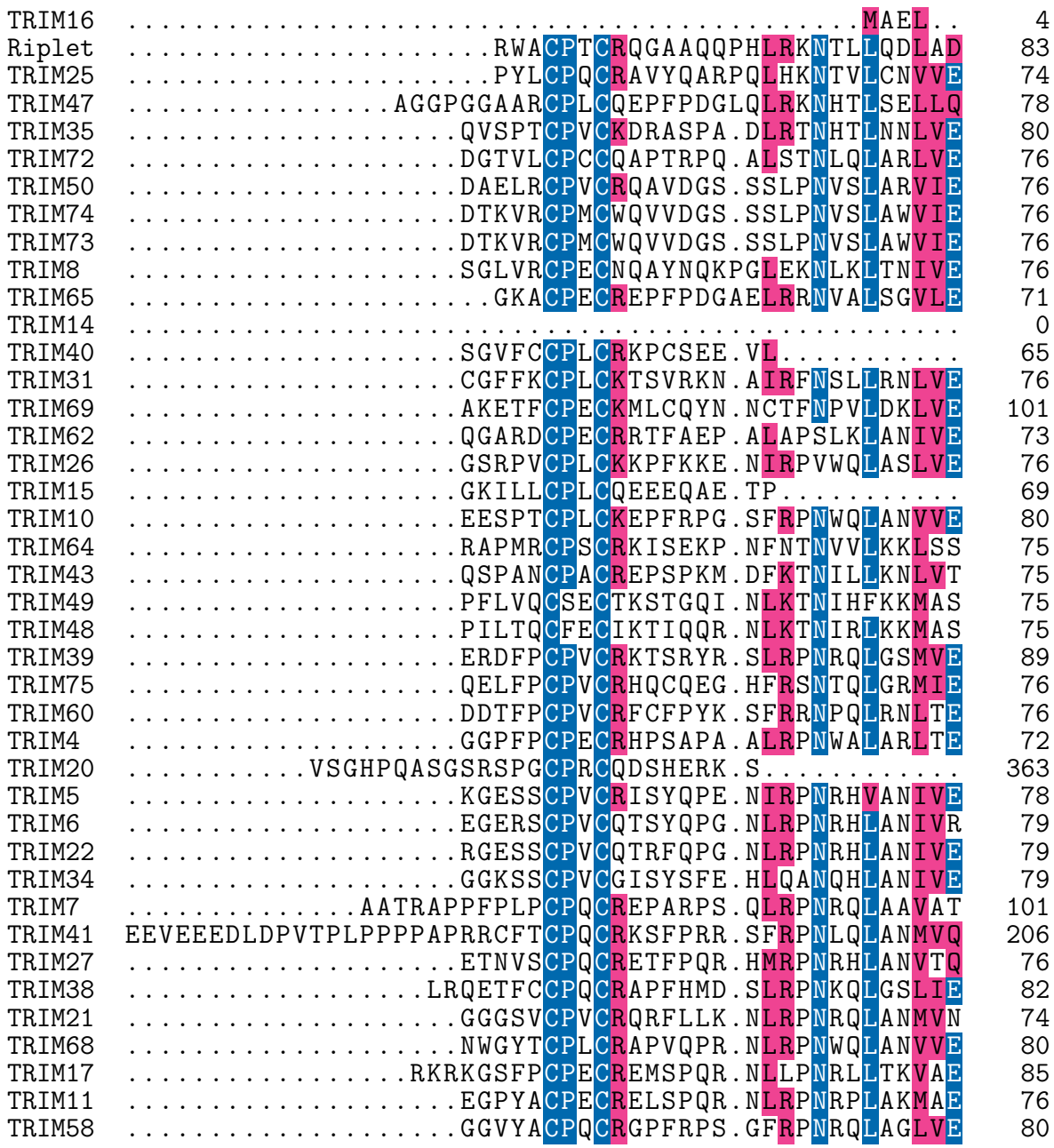
TRIM16 ..... MAEL.. 4
Riplet ..... RWACPTCRQGAAQQPHLRKNTLLQDLAD 83
TRIM25 ..... PYLCPQCRAVYQARPQLHKNTVLCNVVE 74
TRIM47 ..... AGGPGGAARCPLCQEPFPDGLQLRKNHTLSELLQ 78
TRIM35 ..... QVSPTCPVCKDRASPA.DLRTNHTLNNLVE 80
TRIM72 ..... DGTVLCPCCQAPTRPQ.ALSTNLQLARLVE 76
TRIM50 ..... DAELRCPVCRQAVDGS.SSLPNVSLARVIE 76
TRIM74 ..... DTKVRCPMCWQVVDGS.SSLPNVSLAWVIE 76
TRIM73 ..... DTKVRCPMCWQVVDGS.SSLPNVSLAWVIE 76
TRIM8 ..... SGLVRCPECNQAYNQKPGLEKNLKLTNIVE 76
TRIM65 ..... GKACPECREPFPDGAELRRNVALSGVLE 71
TRIM14 0
TRIM40 ..... SGVFCCPLCRKPCSEE.VL..... 65
TRIM31 ..... CGFFKCPLCKTSVRKN.AIRFNSLLRNLVE 76
TRIM69 ..... AKETFCPECKMLCQYN.NCTFNPVLDKLVE 101
TRIM62 ..... QGARDCPECRRTFAEP.ALAPSLKLANIVE 73
TRIM26 ..... GSRPVCPLCKKPFKKE.NIRPVWQLASLVE 76
TRIM15 ..... GKILLCPLCQEEEQAE.TP..... 69
TRIM10 ..... EESPTCPLCKEPFRPG.SFRPNWQLANVVE 80
TRIM64 ..... RAPMRCPSCRKISEKP.NFNTNVVLKKLSS 75
TRIM43 ..... QSPANCPACREPSPKM.DFKTNILLKNLVT 75
TRIM49 ..... PFLVQCSECTKSTGQI.NLKTNIHFKKMAS 75
TRIM48 ..... PILTQCFECIKTIQQR.NLKTNIRLKKMAS 75
TRIM39 ..... ERDFPCPVCRKTSRYR.SLRPNRQLGSMVE 89
TRIM75 ..... QELFPCPVCRHQCQEG.HFRSNTQLGRMIE 76
TRIM60 ..... DDTFPCPVCRFCFPYK.SFRRNPQLRNLTE 76
TRIM4 ..... GGPFPCPECRHPSAPA.ALRPNWALARLTE 72
TRIM20 ..... VSGHPQASGSRSPGCPRCQDSHERK.S..... 363
TRIM5 ..... KGESSCPVCRISYQPE.NIRPNRHVANIVE 78
TRIM6 ..... EGERSCPVCQTSYQPG.NLRPNRHLANIVR 79
TRIM22 ..... RGESSCPVCQTRFQPG.NLRPNRHLANIVE 79
TRIM34 ..... GGKSSCPVCGISYSFE.HLQANQHLANIVE 79
TRIM7 ..... AATRAPPFPLPCPQCREPARPS.QLRPNRQLAAVAT 101
TRIM41 EEVEEEDLDPVTPLPPPPAPRRCFTCPQCRKSFPRR.SFRPNLQLANMVQ 206
TRIM27 ..... ETNVSCPQCRETFPQR.HMRPNRHLANVTQ 76
TRIM38 ..... LRQETFCCPQCRAPFHMD.SLRPNKQLGSLIE 82
TRIM21 ..... GGGSVCPVCRQRFLLK.NLRPNRQLANMVN 74
TRIM68 ..... NWGYTCPLCRAPVQPR.NLRPNWQLANVVE 80
TRIM17 ..... RKRKGSFPCPECREMSPQR.NLLPNRLLTKVAE 85
TRIM11 ..... EGPYACPECRELSPQR.NLRPNRPLAKMAE 76
TRIM58 ..... GGVYACPQCRGPFRPS.GFRPNRQLAGLVE 80

RING

```
TRIM16  ......DLMAPGPLPRATAQPPAPLSPDSGSPSPDSGSASPVEEEDVGSS   48
Riplet  KYRRAAREIQAGSDPAHC........PCPGSSS.....LSS.........  111
TRIM25  QFLQADLAREP.PADVWT.............................  91
TRIM47  LRQGSGPGSGPGPAPALA........PEPSAPS.....ALPSVP......  109
TRIM35  KLLREEAEGAR.....................................  91
TRIM72  GLAQ............................................  80
TRIM50  ALRL............................................  80
TRIM74  ALRL............................................  80
TRIM73  ALRL............................................  80
TRIM8   KFNALHVEKPP.....................................  87
TRIM65  VVRAGPARDPG.....................................  82
TRIM14  .....MA..........................................   2
TRIM40  ................................................  65
TRIM31  KIQALQA.........................................  83
TRIM69  KIKKLPL.........................................  108
TRIM62  RYSSFPL.........................................  80
TRIM26  NIERLKV.........................................  83
TRIM15  .....MA..........................................  71
TRIM10  NIERLQL.........................................  87
TRIM64  LARQTRP.........................................  82
TRIM43  IARKASL.........................................  82
TRIM49  LARKVSL.........................................  82
TRIM48  LARKASL.........................................  82
TRIM39  IAKQLQA.........................................  96
TRIM75  IAKLLQS.........................................  83
TRIM60  IAKQLQI.........................................  83
TRIM4   KTQRRRL.........................................  79
TRIM20  ................................................  363
TRIM5   KLREVKL.........................................  85
TRIM6   RLREVVL.........................................  86
TRIM22  RVKEVKM.........................................  86
TRIM34  RLKEVKL.........................................  86
TRIM7   LLRRFSL.........................................  108
TRIM41  VIRQMHP.........................................  213
TRIM27  LVKQLRT.........................................  83
TRIM38  ALKET............................................  87
TRIM21  NLKEISQ.........................................  81
TRIM68  KVRLLRL.........................................  87
TRIM17  MAQQ..H.........................................  90
TRIM11  MARR..L.........................................  81
TRIM58  SVRR..L.........................................  85
```

B-Box1

```
TRIM16  EKLGRETEEQDSDSAEQGDPAGEGKEVLCDFCLDDTRRVKAVKSCLTCMV   98
Riplet  ..................................................   111
TRIM25  ............PPARASAPS.PNAQVACDHCLKEA.A...VKTCLVCMA   124
TRIM47  ........EPSAPCAPEPWPA.GEEPVRCDACPEGA.ALPAALSCLSCLA   149
TRIM35  ........................W.........T.S.............    94
TRIM72  ..................................................    80
TRIM50  ....................................P.G.............    82
TRIM74  ....................................P.G.............    82
TRIM73  ....................................P.G.............    82
TRIM8   ........................AALHCVFCRRGP.PLPAQKVCLRCEA   112
TRIM65  ........................PDP.....GPGP...............    89
TRIM14  ........................GA.....ATGS.RT.............    10
TRIM40  ..................................................    65
TRIM31  ........................SE.....VQSK.R.............    90
TRIM69  ........................LK.......................   110
TRIM62  ........................DA.....ILNA.R.............    87
TRIM26  ........................DK.....GRQP.G.............    90
TRIM15  ........................PV.....PLGP.L.............    78
TRIM10  ........................VS.....TLGL.G.............    94
TRIM64  ........................Q......NIN................    86
TRIM43  ........................WQ.....FLS................    87
TRIM49  ........................WL.....FLS................    87
TRIM48  ........................WL.....FLS................    87
TRIM39  ........................VK........R.K.............   100
TRIM75  ........................TK.....SNKR.K.............    90
TRIM60  ........................RR.....SKRK.R.............    90
TRIM4   ........................GP.......................    81
TRIM20  .........................P.....GSLS.P.............   369
TRIM5   ........................SP.....E.GQ.K.............    91
TRIM6   ........................GP.....GKQL.K.............    93
TRIM22  ........................SP.....QEGQ.K.............    93
TRIM34  ........................SP.....DNGK.K.............    93
TRIM7   ........................PA.....AAPG.EH............   116
TRIM41  ........................TP.....GRGS.R.............   220
TRIM27  ........................ER.....PSGP.G.............    90
TRIM38  ....................................D.Q.............    89
TRIM21  ........................EA.....REGT.Q.............    88
TRIM68  ........................HP.....GMGL.K.............    94
TRIM17  ............................PGLQ.K.................    95
TRIM11  ........................HP.....PSPV.P.............    88
TRIM58  ........................GL.....GAGP.G.............    92
```

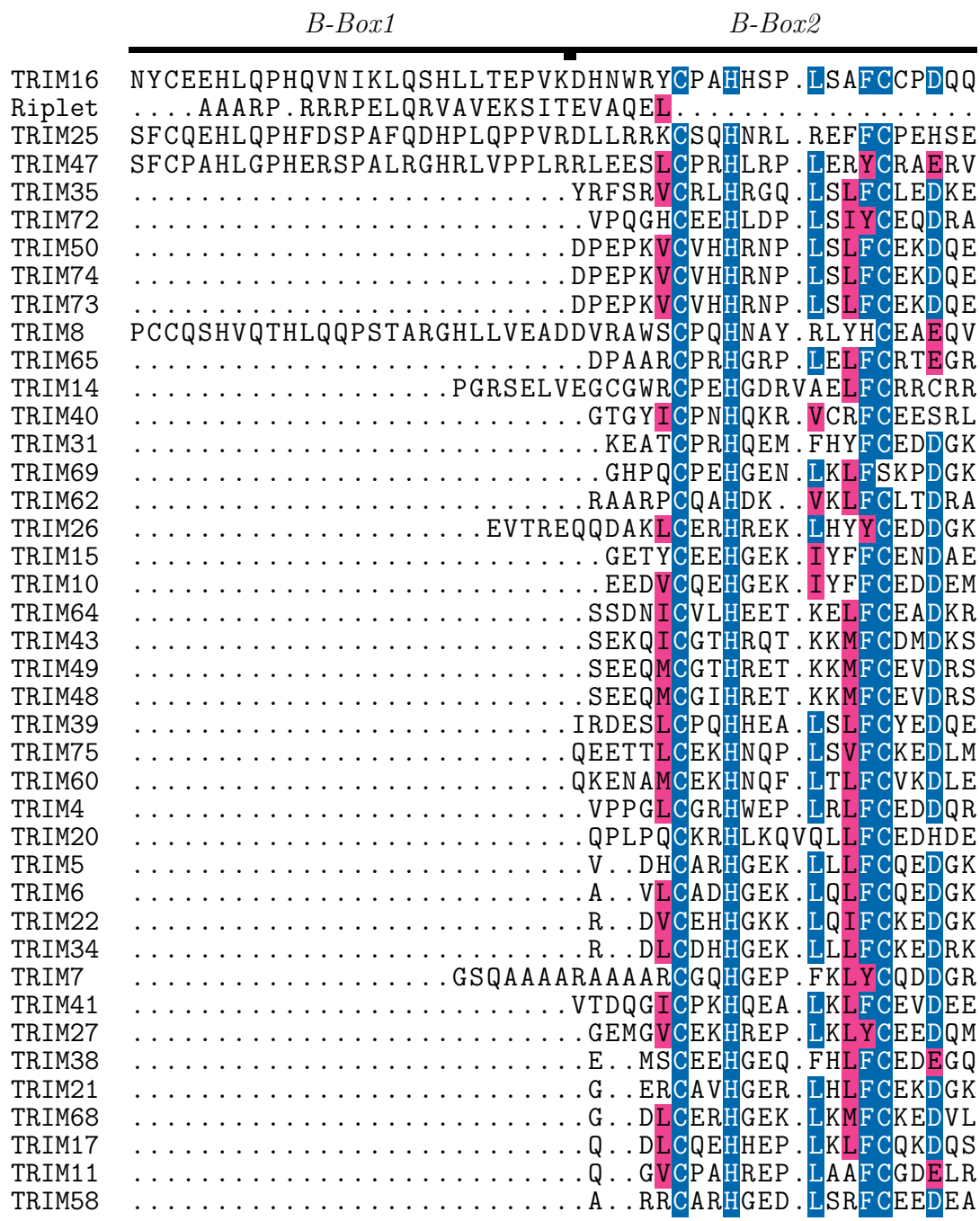
B-Box1
B-Box2
TRIM16 NYCEEHLQPHQVNIKLQSHLLTEPVKDHNWRYCPAHHSP.LSAFCCPDQQ 147
Riplet ....AAARP.RRRPELQRVAVEKSITEVAQEL.................. 138
TRIM25 SFCQEHLQPHFDSPAFQDHPLQPPVRDLLRRKCSQHNRL.REFFCPEHSE 173
TRIM47 SFCPAHLGPHERSPALRGHRLVPPLRRLEESLCPRHLRP.LERYCRAERV 198
TRIM35 ..........................YRFSRVCRLHRGQ.LSLFCLEDKE 117
TRIM72 ..........................VPQGHCEEHLDP.LSIYCEQDRA 102
TRIM50 ........................DPEPKVCVHHRNP.LSLFCEKDQE 105
TRIM74 ........................DPEPKVCVHHRNP.LSLFCEKDQE 105
TRIM73 ........................DPEPKVCVHHRNP.LSLFCEKDQE 105
TRIM8 PCCQSHVQTHLQQPSTARGHLLVEADDVRAWSCPQHNAY.RLYHCEAEQV 161
TRIM65 ..........................DPAARCPRHGRP.LELFCRTEGR 111
TRIM14 ....................PGRSELVEGCGWRCPEHGDRVAELFCRRCRR 41
TRIM40 ..........................GTGYICPNHQKR.VCRFCEESRL 87
TRIM31 ....KEATCPRHQEM.FHYFCEDDGK 111
TRIM69 ....GHPQCPEHGEN.LKLFSKPDGK 131
TRIM62 ....RAARPCQAHDK..VKLFCLTDRA 108
TRIM26 ......................EVTREQQDAKLCERHREK.LHYYCEDDGK 118
TRIM15 ....GETYCEEHGEK.IYFFCENDAE 99
TRIM10 ....EEDVCQEHGEK.IYFFCEDDEM 115
TRIM64 ..........................SSDNICVLHEET.KELFCEADKR 108
TRIM43 ..........................SEKQICGTHRQT.KKMFCDMDKS 109
TRIM49 ..........................SEEQMCGTHRET.KKMFCEVDRS 109
TRIM48 ..........................SEEQMCGIHRET.KKMFCEVDRS 109
TRIM39 ..........................IRDESLCPQHHEA.LSLFCYEDQE 123
TRIM75 ..........................QEETTLCEKHNQP.LSVFCKEDLM 113
TRIM60 ..........................QKENAMCEKHNQF.LTLFCVKDLE 113
TRIM4 ..........................VPPGLCGRHWEP.LRLFCEDDQR 103
TRIM20 ..........................QPLPQCKRHLKQVQLLFCEDHDE 392
TRIM5 ..........................V..DHCARHGEK.LLLFCQEDGK 111
TRIM6 ..........................A..VLCADHGEK.LQLFCQEDGK 113
TRIM22 ..........................R..DVCEHHGKK.LQIFCKEDGK 113
TRIM34 ..........................R..DLCDHHGEK.LLLFCKEDRK 113
TRIM7 ....................GSQAAAARAAAARCGQHGEP.FKLYCQDDGR 146
TRIM41 ..........................VTDQGICPKHQEA.LKLFCEVDEE 243
TRIM27 ..........................GEMGVCEKHREP.LKLYCEEDQM 112
TRIM38 ..........................E..MSCEEHGEQ.FHLFCEDEGQ 109
TRIM21 ..........................G..ERCAVHGER.LHLFCEKDGK 108
TRIM68 ..........................G..DLCERHGEK.LKMFCKEDVL 114
TRIM17 ..........................Q..DLCQEHHEP.LKLFCQKDQS 115
TRIM11 ..........................Q..GVCPAHREP.LAAFCGDELR 108
TRIM58 ..........................A..RRCARHGED.LSRFCEEDEA 112

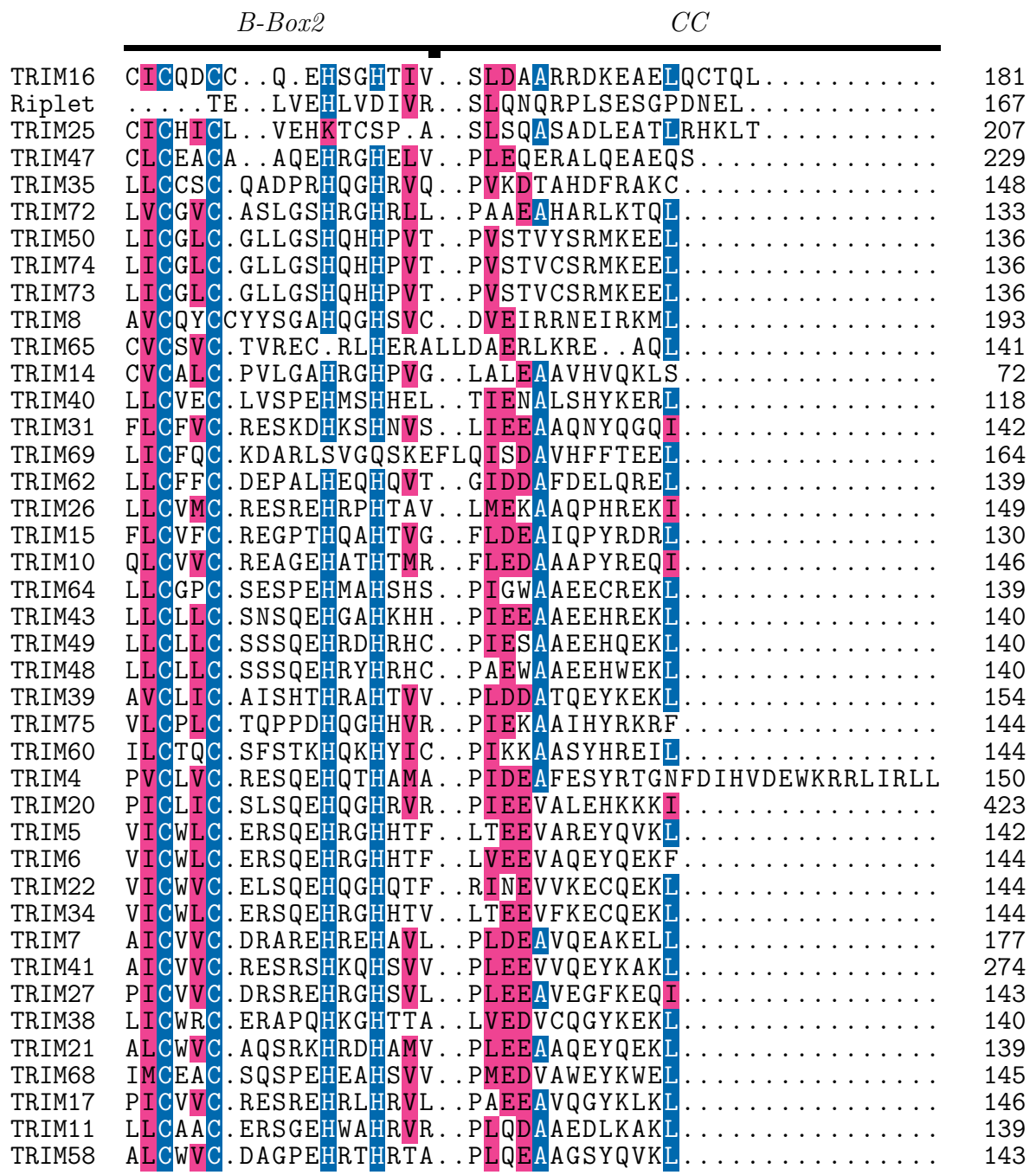
B-Box2
CC
TRIM16 CICQDCC..Q.EHSGHTIV..SLDAARRDKEAELQCTQL..... 181
Riplet .....TE..LVEHLVDIVR..SLQNQRPLSESGPDNEL..... 167
TRIM25 CICHICL..VEHKTCSP.A..SLSQASADLEATLRHKLT..... 207
TRIM47 CLCEACA..AQEHRGHELV..PLEQERALQEAEQS..... 229
TRIM35 LLCCSC.QADPRHQGHRVQ..PVKDTAHDFRAKC..... 148
TRIM72 LVCGVC.ASLGSHRGHRLL..PAAEAHARLKTQL..... 133
TRIM50 LICGLC.GLLGSHQHHPVT..PVSTVYSRMKEEL..... 136
TRIM74 LICGLC.GLLGSHQHHPVT..PVSTVCSRMKEEL..... 136
TRIM73 LICGLC.GLLGSHQHHPVT..PVSTVCSRMKEEL..... 136
TRIM8 AVCQYCCYYSGAHQGHSVC..DVEIRRNEIRKML..... 193
TRIM65 CVCSVC.TVREC.RLHERALLDAERLKRE..AQL..... 141
TRIM14 CVCALC.PVLGAHRGHPVG..LALEAAVHVQKLS..... 72
TRIM40 LLCVEC.LVSPEHMSHHEL..TIENALSHYKERL..... 118
TRIM31 FLCFVC.RESKDHKSHNVS..LIEEAAQNYQGQI..... 142
TRIM69 LICFQC.KDARLSVGQSKEFLQISDAVHFFTEEL..... 164
TRIM62 LLCFFC.DEPALHEQHQVT..GIDDAFDELQREL..... 139
TRIM26 LLCVMC.RESREHRPHTAV..LMEKAAQPHREKI..... 149
TRIM15 FLCVFC.REGPTHQAHTVG..FLDEAIQPYRDRL..... 130
TRIM10 QLCVVC.REAGEHATHTMR..FLEDAAAPYREQI..... 146
TRIM64 LLCGPC.SESPEHMAHSHS..PIGWAAEECREKL..... 139
TRIM43 LLCLLC.SNSQEHGAHKHH..PIEEAAEEHREKL..... 140
TRIM49 LLCLLC.SSSQEHRDHRHC..PIESAAEEHQEKL..... 140
TRIM48 LLCLLC.SSSQEHRYHRHC..PAEWAAEEHWEKL..... 140
TRIM39 AVCLIC.AISHTHRAHTVV..PLDDATQEYKEKL..... 154
TRIM75 VLCPLC.TQPPDHQGHHVR..PIEKAAIHYRKRF..... 144
TRIM60 ILCTQC.SFSTKHQKHYIC..PIKKAASYHREIL..... 144
TRIM4 PVCLVC.RESQEHQTHAMA..PIDEAFESYRTGNFDIHVDEWKRRLIRLL 150
TRIM20 PICLIC.SLSQEHQGHRVR..PIEEVALEHKKKI..... 423
TRIM5 VICWLC.ERSQEHRGHHTF..LTEEVAREYQVKL..... 142
TRIM6 VICWLC.ERSQEHRGHHTF..LVEEVAQEYQEKF..... 144
TRIM22 VICWVC.ELSQEHQGHQTF..RINEVVKECQEKL..... 144
TRIM34 VICWLC.ERSQEHRGHHTV..LTEEVFKECQEKL..... 144
TRIM7 AICVVC.DRAREHREHAVL..PLDEAVQEAKELL..... 177
TRIM41 AICVVC.RESRSHKQHSVV..PLEEVVQEYKAKL..... 274
TRIM27 PICVVC.DRSREHRGHSVL..PLEEAVEGFKEQI..... 143
TRIM38 LICWRC.ERAPQHKGHTTA..LVEDVCQGYKEKL..... 140
TRIM21 ALCWVC.AQSRKHRDHAMV..PLEEAAQEYQEKL..... 139
TRIM68 IMCEAC.SQSPEHEAHSVV..PMEDVAWEYKWEL..... 145
TRIM17 PICVVC.RESREHRLHRVL..PAEEAVQGYKLKL..... 146
TRIM11 LLCAAC.ERSGEHWAHRVR..PLQDAAEDLKAKL..... 139
TRIM58 ALCWVC.DAGPEHRTHRTA..PLQEAAGSYQVKL..... 143

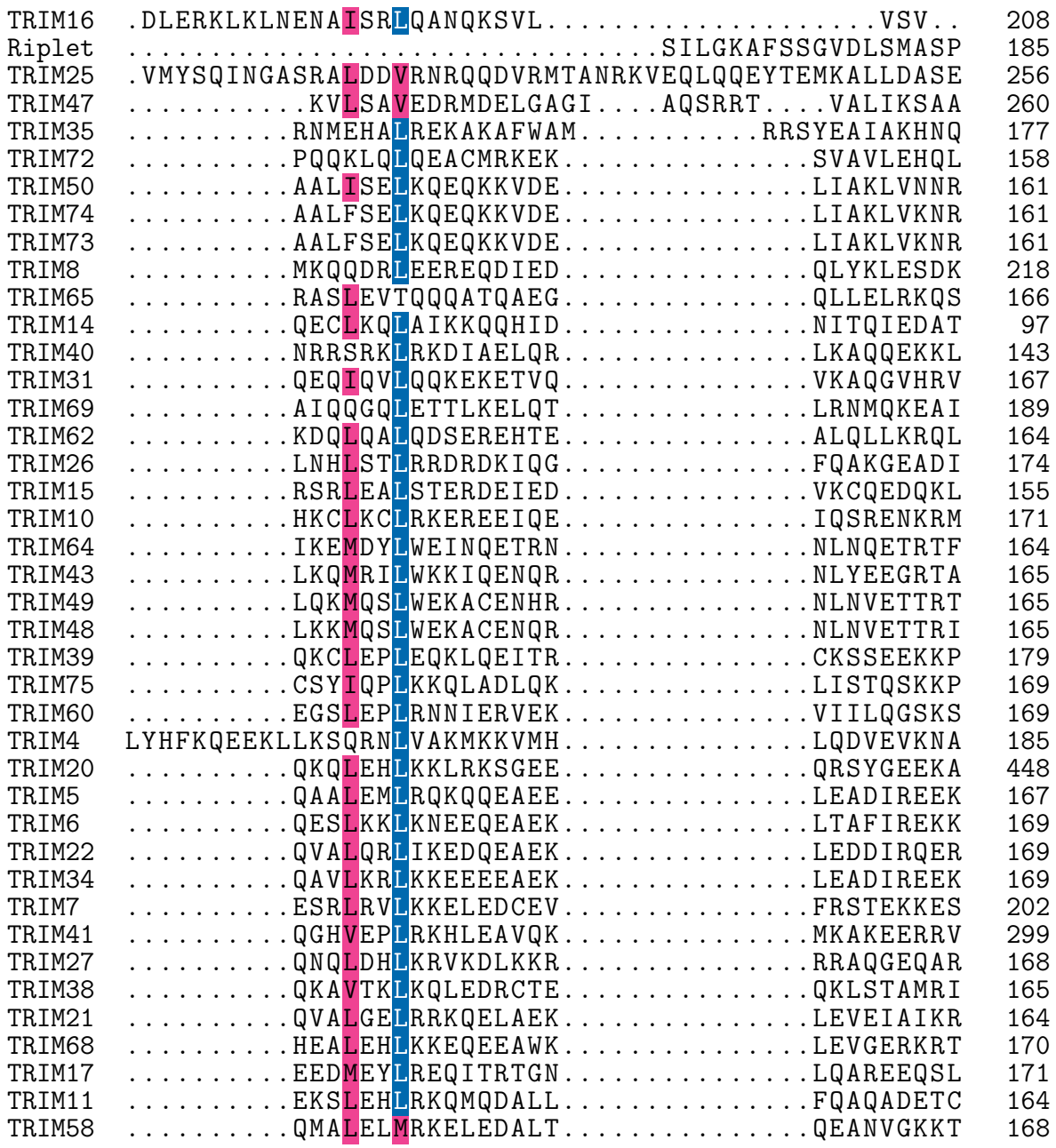
TRIM16 .DLERKLKLNENAISRLQANQKSVL.....VSV.. 208
Riplet .....SILGKAFSSGVDLSMASP 185
TRIM25 .VMYSQINGASRALDDVRNRQQDVRMTANRKVEQLQQEYTEMKALLDASE 256
TRIM47 .....KVLSAVEDRMDELGAGI....AQSRRT....VALIKSAA 260
TRIM35 .....RNMEHALREKAKAFWAM.....RRSYEAIAKHNQ 177
TRIM72 .....PQQKLQLQEACMRKEK.....SVAVLEHQL 158
TRIM50 .....AALISELKQEQKKVDE.....LIAKLVNNR 161
TRIM74 .....AALFSELKQEQKKVDE.....LIAKLVKNR 161
TRIM73 .....AALFSELKQEQKKVDE.....LIAKLVKNR 161
TRIM8 .....MKQQDRLEEREQDIED.....QLYKLESDK 218
TRIM65 .....RASLEVTQQQATQAEG.....QLLELRKQS 166
TRIM14 .....QECLKQLAIKKQQHID.....NITQIEDAT 97
TRIM40 .....NRRSRKLRKDIAELQR.....LKAQQEKKL 143
TRIM31 .....QEQIQVLQQKEKETVQ.....VKAQGVHRV 167
TRIM69 .....AIQQGQLETTLKELQT.....LRNMQKEAI 189
TRIM62 .....KDQLQALQDSEREHTE.....ALQLLKRQL 164
TRIM26 .....LNHLSTLRRDRDKIQG.....FQAKGEADI 174
TRIM15 .....RSRLEALSTERDEIED.....VKCQEDQKL 155
TRIM10 .....HKCLKCLRKEREEIQE.....IQSRENKRM 171
TRIM64 .....IKEMDYLWEINQETRN.....NLNQETRTF 164
TRIM43 .....LKQMRILWKKIQENQR.....NLYEEGRTA 165
TRIM49 .....LQKMQSLWEKACENHR.....NLNVETTRT 165
TRIM48 .....LKKMQSLWEKACENQR.....NLNVETTRI 165
TRIM39 .....QKCLEPLEQKLQEITR.....CKSSEEKKP 179
TRIM75 .....CSYIQPLKKQLADLQK.....LISTQSKKP 169
TRIM60 .....EGSLEPLRNNIERVEK.....VIILQGSKS 169
TRIM4 LYHFKQEEKLLKSQRNLVAKMKKVMH.....LQDVEVKNA 185
TRIM20 .....QKQLEHLKKLRKSGEE.....QRSYGEEKA 448
TRIM5 .....QAALEMLRQKQQEAEE.....LEADIREEK 167
TRIM6 .....QESLKKLKNEEQEAEK.....LTAFIREKK 169
TRIM22 .....QVALQRLIKEDQEAEK.....LEDDIRQER 169
TRIM34 .....QAVLKRLKKEEEEEAEK.....LEADIREEK 169
TRIM7 .....ESRLRVLKKELEDCEV.....FRSTEKKES 202
TRIM41 .....QGHVEPLRKHLEAVQK.....MKAKEERRV 299
TRIM27 .....QNQLDHLKRVKDLKKR.....RRAQGEQAR 168
TRIM38 .....QKAVTKLKQLEDRCTE.....QKLSTAMRI 165
TRIM21 .....QVALGELRRKQELAEK.....LEVEIAIKR 164
TRIM68 .....HEALEHLKKEQEEAWK.....LEVGERKRT 170
TRIM17 .....EEDMEYLREQITRTGN.....LQAREEQSL 171
TRIM11 .....EKSLEHLRKQMQDALL.....FQAQADETC 164
TRIM58 .....QMALELMRKELEDALT.....QEANVGKKT 168

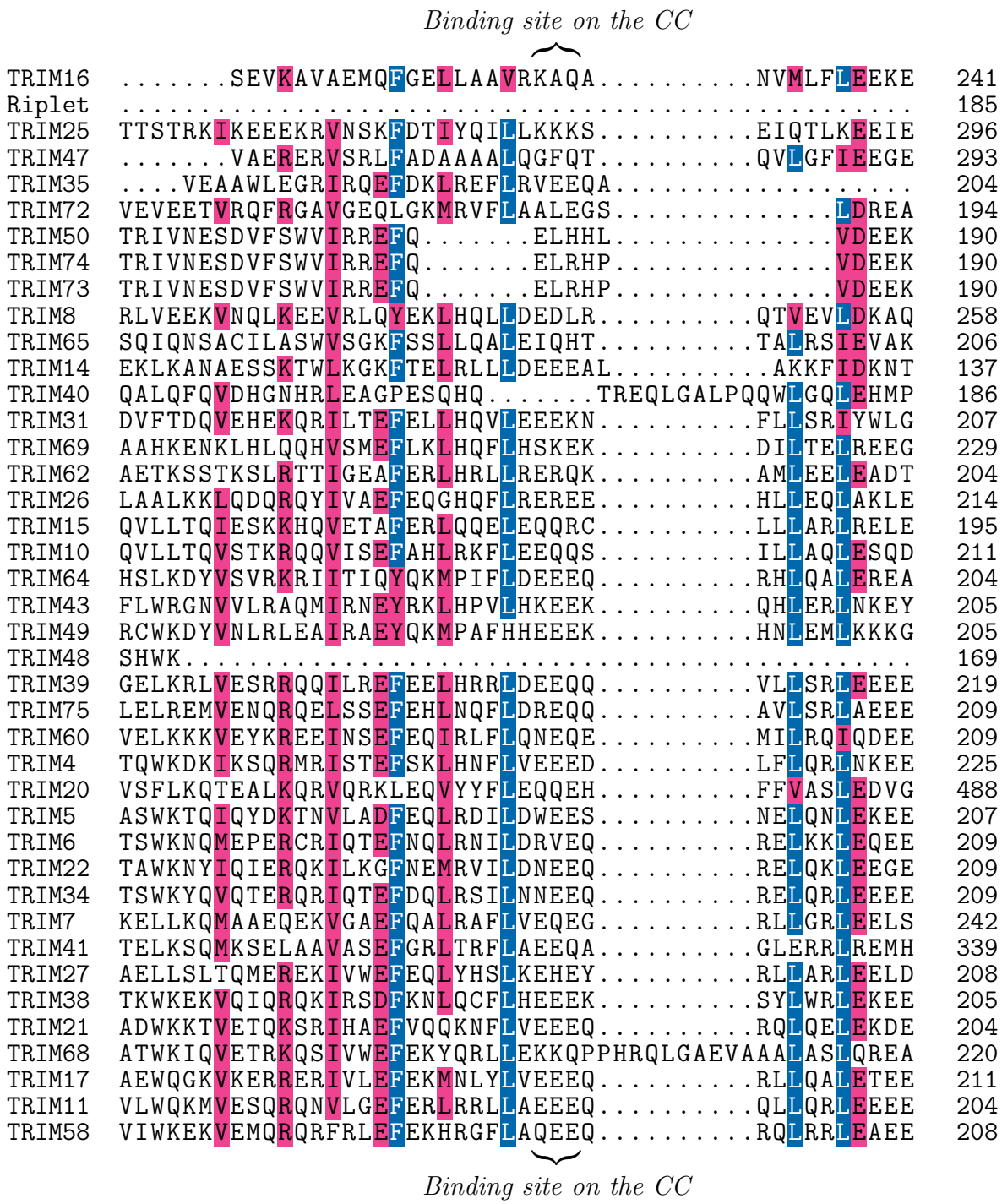
Binding site on the CC
TRIM16 .....SEVKAVAEMQFGELLAAVRKAQA.....NVMLFLEEKE 241
Riplet 185
TRIM25 TTSTRKIKEEEKRVNSKFDTIYQILLKKKS.....EIQTLKEEIE 296
TRIM47 .....VAERERVSRLFADAAAALQGFQT.....QVLGFIEEGE 293
TRIM35 ....VEAAWLEGRIRQEFDKLREFLRVEEQA..... 204
TRIM72 VEVEETVRQFRGAVGEQLGKMRVFLAALEGS.....LDREA 194
TRIM50 TRIVNESDVFSWVIRREFQ.....ELHHL.....VDEEK 190
TRIM74 TRIVNESDVFSWVIRREFQ.....ELRHP.....VDEEK 190
TRIM73 TRIVNESDVFSWVIRREFQ.....ELRHP.....VDEEK 190
TRIM8 RLVEEKVNQLKEEVRLQYEKLHQLLDEDLR.....QTVEVLDKAQ 258
TRIM65 SQIQNSACILASWVSGKFSSLLQALEIQHT.....TALRSIEVAK 206
TRIM14 EKLKANAESSKTWLKGKFTELRLLLDEEEAL.....AKKFIDKNT 137
TRIM40 QALQFQVDHGNHRLEAGPESQHQ.....TREQLGALPQQWLGQLEHMP 186
TRIM31 DVFTDQVEHEKQRILTEFELLHQVLEEEKN.....FLLSRIYWLG 207
TRIM69 AAHKENKLHLQQHVSMEFLKLHQFLHSKEK.....DILTELREEG 229
TRIM62 AETKSSTKSLRTTIGEAFERLHRLLRERQK.....AMLEELEADT 204
TRIM26 LAALKKLQDQRQYIVAEFEQGHQFLREREE.....HLLEQLAKLE 214
TRIM15 QVLLTQIESKKHQVETAFERLQQELEQQRC.....LLLARLRELE 195
TRIM10 QVLLTQVSTKRQQVISEFAHLRKFLEEQQS.....ILLAQLESQD 211
TRIM64 HSLKDYVSVRKRIITIQYQKMPIFLDEEEQ.....RHLQALEREA 204
TRIM43 FLWRGNVVLRAQMIRNEYRKLHPVLHKEEK.....QHLERLNKEY 205
TRIM49 RCWKDYVNLRLEAIRAEYQKMPAFHHEEEK.....HNLEMLKKKG 205
TRIM48 SHWK..... 169
TRIM39 GELKRLVESRRQQILREFEELHRRLDEEQQ.....VLLSRLEEEE 219
TRIM75 LELREMVENQRQELSSEFEHLNQFLDREQQ.....AVLSRLAEEE 209
TRIM60 VELKKKVEYKREEINSEFEQIRLFLQNEQE.....MILRQIQDEE 209
TRIM4 TQWKDKIKSQRMRISTEFSKLHNFLVEEED.....LFLQRLNKEE 225
TRIM20 VSFLKQTEALKQRVQRKLEQVYYFLEQQEH.....FFVASLEDVG 488
TRIM5 ASWKTQIQYDKTNVLADFEQLRDILDWEES.....NELQNLEKEE 207
TRIM6 TSWKNQMEPERCRIQTEFNQLRNILDRVEQ.....RELKKLEQEE 209
TRIM22 TAWKNYIQIERQKILKGFNEMRVILDNEEQ.....RELQKLEEGE 209
TRIM34 TSWKYQVQTERQRIQTEFDQLRSILNNEEQ.....RELQRLEEEE 209
TRIM7 KELLKQMAAEQEKVGAEFQALRAFLVEQEG.....RLLGRLEELS 242
TRIM41 TELKSQMKSELAAVASEFGRLTRFLAEEQA.....GLERRLREMH 339
TRIM27 AELLSLTQMEREKIVWEFEQLYHSLKEHEY.....RLLARLEELD 208
TRIM38 TKWKEKVQIQRQKIRSDFKNLQCFLHEEEK.....SYLWRLEKEE 205
TRIM21 ADWKKTVETQKSRIHAEFVQQKNFLVEEEQ.....RQLQELEKDE 204
TRIM68 ATWKIQVETRKQSIVWEFEKYQRLLEKKQPPHRQLGAEVAAALASLQREA 220
TRIM17 AEWQGKVKERRERIVLEFEKMNLYLVEEEQ.....RLLQALETEE 211
TRIM11 VLWQKMVESQRQNVLGEFERLRRLLAEEEQ.....QLLQRLEEEE 204
TRIM58 VIWKEKVEMQRQRFRLEFEKHRGFLAQEEQ.....RQLRRLEAEE 208
Binding site on the CC

```
TRIM16  QAALSQANGIK..........AHLEYRSAEMEKSKQELERM.AAISNTV  279
Riplet  .........KL..........VTSDTAAGKIR................  198
TRIM25  QSLTKRDEFEF..........L...EKASKLRGISTKPVYI.PEVELNH  331
TRIM47  AAMLGRSQGDL..........RRQEEQRSRLSRARQNLSQV.PEADSVS  331
TRIM35  ..ILDAMAEETRQKQLLADEKMKQLTEETEVLAHEIERLQME.MKED.DV  250
TRIM72  ERVRGEAGVALRR.......ELGSLNSYLEQLRQMEKVLEEV.ADKP.QT  235
TRIM50  ARCLEGIGGHTRGLVASLDMQLEQAQGTRERLAQAECVLEQF.GNED.HH  238
TRIM74  ARCLEGIGGHTRGLVASLDMQLEQAQGTRERLAQAECVLEQF.GNED.HH  238
TRIM73  ARCLEGIGGHTRGLVASLDMQLEQAQGTRERLAQAECVLEQF.GNED.HH  238
TRIM8   AKFCSENAAQA..........LHLGERMQEAKKLLGSLQLL.FDKTEDV  296
TRIM65  TQALAQARDEEQRLR....VHLEAVARHGCRIRELLEQVDEQTFLQE..S  250
TRIM14  QLTLQVYREQA..........DSCREQLDIMNDLSNRVWSI.SQEPDPV  175
TRIM40  AEAAR.....I..........LDISRAVTQLRSLVIDLERT.AKEL.DT  218
TRIM31  HEGTEAGKHYV..........ASTEPQLNDLKKLVDSLKTK.QNMP.PR  244
TRIM69  KALNEEMELNL..........SQLQEQCLLAKDMLVSIQAKTEQQN.SF  267
TRIM62  ARTLTDIEQKV..........QRYSQQLRKVQE.......G.......A  229
TRIM26  QELTEGREKFK..........SRGVGELARLALVISELEGK.AQQP.AA  251
TRIM15  QQIWKERDEYI..........TKVSEEVTRLGAQVKELEEK.CQQP.AS  232
TRIM10  GDILRQRDEFD..........LLVAGEICRFSALIEELEEK.NERP.AR  248
TRIM64  EELFQQLQDSQ..........VRMTQHLERMKDMYRELWET.CHVP.DV  241
TRIM43  QEIFQQLQRSW..........VKMDQKSKHLKEMYQELMEM.CHKP.DV  242
TRIM49  KDIFHRLHLSK..........AKMAHRREILRGMYEELNEM.CHKP.DV  242
TRIM48  ....................................................  169
TRIM39  QDILQRLRENA..........AHLGDKRRDLAHLAAEVEGK.CLQS.GF  256
TRIM75  KDNQQKLSANI..........TAFSNYSATLKSQLSKVVEL.SELS.EL  246
TRIM60  MNILAKLNENL..........VELSDYVSTLKHLLREVEGK.SVQS.NL  246
TRIM4   EETKKKLNENT..........LKLNQTIASLKKLILEVGEK.SQAP.TL  262
TRIM20  QMVGQIRKAYD..........TRVSQDIALLDALIGELEAK.ECQS.EW  525
TRIM5   EDILKSLTNSE..........TEMVQQTQSLRELISDLEHR.LQGS.VM  244
TRIM6   KKGLRIIEEAE..........NDLVHQTQSLRELISDLERR.CQGS.TM  246
TRIM22  VNVLDNLAAAT..........DQLVQQRQDASTLISDLQRR.LRGS.SV  246
TRIM34  KKTLDKFAEAE..........DELVQQKQLVRELISDVECR.SQWS.TM  246
TRIM7   REVAQKQNENL..........AQLGVEITQLSKLSSQIQET.AQKP.DL  279
TRIM41  EAQLGRAGAAA..........SRLAEQAAQLSRLLAEAQER.SQQG.GL  376
TRIM27  LAIYNSINGAI..........TQFSCNISHLSSLIAQLEEK.QQQP.TR  245
TRIM38  QQTLSRLRDYE..........AGLGLKSNELKSHILELEEK.CQGS.AQ  242
TRIM21  REQLRILGEKE..........AKLAQQSQALQELISELDRR.CHSS.AL  241
TRIM68  AETMQKLELNH..........SELIQQSQVLWRMIAELKER.SQRP.VR  257
TRIM17  EETASRLRESV..........ACLDRQGHSLELLLLQLEER.STQG.PL  248
TRIM11  LEVLPRLREGA..........AHLGQQSAHLAELIAELEGR.CQLP.AL  241
TRIM58  RATLQRLRESK..........SRLVQQSKALKELADELQER.CQRP.AL  245
```

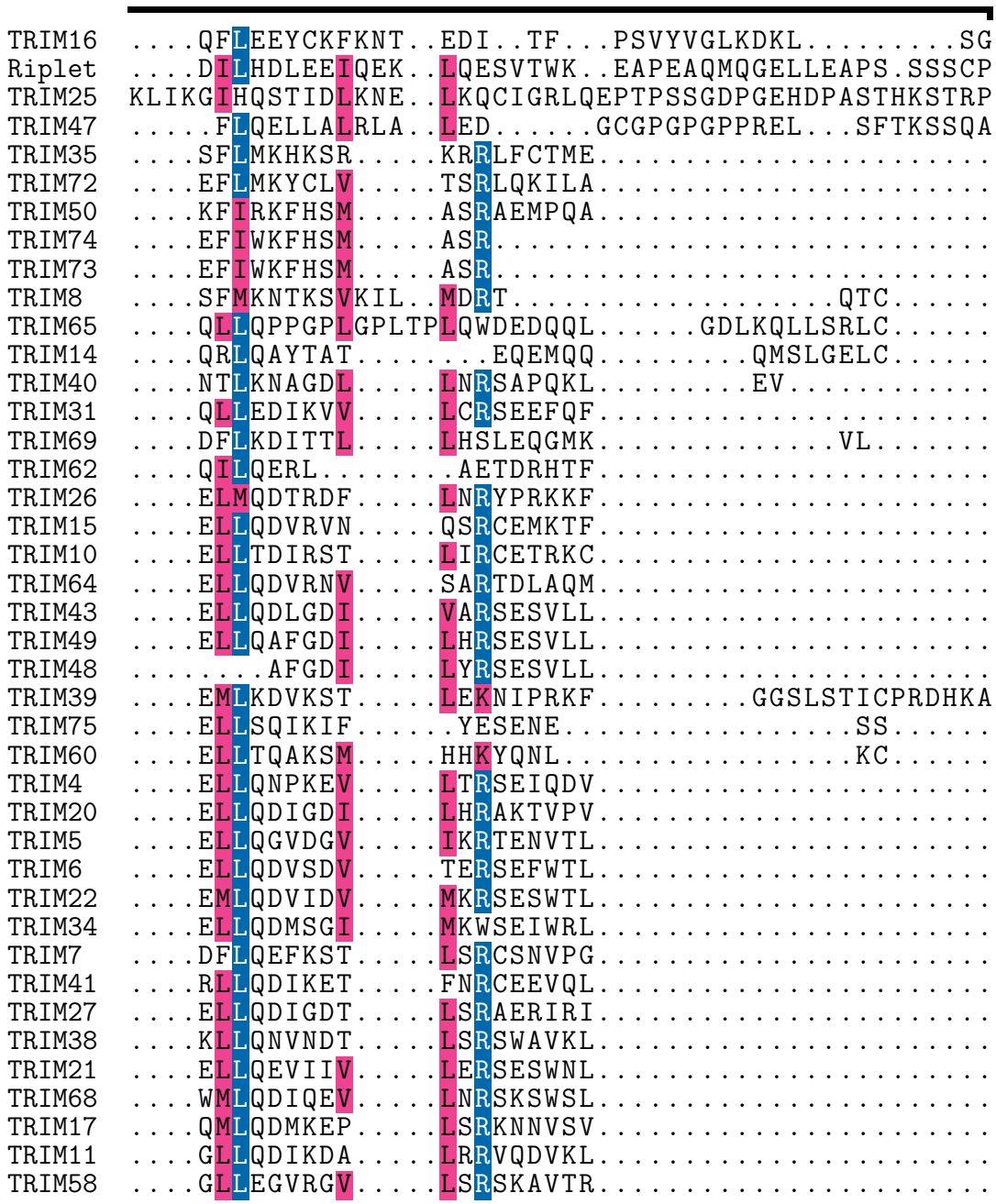
TRIM16 ....QFLEEYCKFKNT..EDI..TF...PSVYVGLKDKL.....SG 309
Riplet ....DILHDLEEIQEK..LQESVTWK..EAPEAQMQGELLEAPS.SSSCP 239
TRIM25 KLIKGIHQSTIDLKNE..LKQCIGRLQEPTPSSGDPGEHDPASTHKSTRP 379
TRIM47 .....FLQELLALRLA..LED......GCGPGPGPPREL...SFTKSSQA 365
TRIM35 ....SFLMKHKSR.....KRRLFCTME..... 268
TRIM72 ....EFLMKYCLV.....TSRLQKILA..... 253
TRIM50 ....KFIRKFHSM.....ASRAEMPQA..... 256
TRIM74 ....EFIWKFHSM.....ASR..... 250
TRIM73 ....EFIWKFHSM.....ASR..... 250
TRIM8 ....SFMKNTKSVKIL..MDRT.....QTC..... 315
TRIM65 ....QLLQPPGPLGPLTPLQWDEDQQL.....GDLKQLLSRLC..... 284
TRIM14 ....QRLQAYTAT.....EQEMQQ.....QMSLGELC..... 198
TRIM40 ....NTLKNAGDL.....LNRSAPQKL.....EV..... 238
TRIM31 ....QLLEDIKVV.....LCRSEEFQF..... 262
TRIM69 ....DFLKDITTL.....LHSLEQGMK.....VL..... 287
TRIM62 ....QILQERL.....AETDRHTF..... 244
TRIM26 ....ELMQDTRDF.....LNRYPRKKF..... 269
TRIM15 ....ELLQDVRVN.....QSRCEMKTF..... 250
TRIM10 ....ELLTDIRST.....LIRCETRKC..... 266
TRIM64 ....ELLQDVRNV.....SARTDLAQM..... 259
TRIM43 ....ELLQDLGDI.....VARSESVLL..... 260
TRIM49 ....ELLQAFGDI.....LHRSESVLL..... 260
TRIM48 .....AFGDI.....LYRSESVLL..... 183
TRIM39 ....EMLKDVKST.....LEKNIPRKF.....GGSLSTICPRDHKA 288
TRIM75 ....ELLSQIKIF.....YESENE.....SS..... 263
TRIM60 ....ELLTQAKSM.....HHKYQNL.....KC..... 264
TRIM4 ....ELLQNPKEV.....LTRSEIQDV..... 280
TRIM20 ....ELLQDIGDI.....LHRAKTVPV..... 543
TRIM5 ....ELLQGVDGV.....IKRTENVTL..... 262
TRIM6 ....ELLQDVSDV.....TERSEFWTL..... 264
TRIM22 ....EMLQDVIDV.....MKRSESWTL..... 264
TRIM34 ....ELLQDMSGI.....MKWSEIWRL..... 264
TRIM7 ....DFLQEFKST.....LSRCSNVPG..... 297
TRIM41 ....RLLQDIKET.....FNRCEEVQL..... 394
TRIM27 ....ELLQDIGDT.....LSRAERIRI..... 263
TRIM38 ....KLLQNVNDT.....LSRSWAVKL..... 260
TRIM21 ....ELLQEVIIV.....LERSESWNL..... 259
TRIM68 ....WMLQDIQEV.....LNRSKSWSL..... 275
TRIM17 ....QMLQDMKEP.....LSRKNNVSV..... 266
TRIM11 ....GLLQDIKDA.....LRRVQDVKL..... 259
TRIM58 ....GLLEGVRGV.....LSRSKAVTR..... 263

Lysine-rich region in L2

```
TRIM16   IRKVITESTV.....HLIQLLENYKK.K..LQEFSKE.....EEYD...   342
Riplet   ......................LPDQ...S..HPAL..............   248
TRIM25   VKKVSKEEKKS.....KKPPPVPALPS.K..LPTFGAP.....EQLV...   413
TRIM47   VRAVRDM.........................L.AVACV.....NQWE...   382
TRIM35   ............PEPVQP..GMLIDVCKY.....................   283
TRIM72   ............ESP..PPARLDIQLPII.....................   268
TRIM50   ............RPLEGAFSPISFKPGLH.....................   273
TRIM74   ...................................................   250
TRIM73   ...................................................   250
TRIM8    ................TSSSLSPTKIGHLNSKLFLNEV...........   337
TRIM65   ..GLLLEEGS.....HPGAPAK.....P.VDLAPV..............   306
TRIM14   ................HPVPLSFEPVKS.FFKGLVEAVESTLQTPLDIR  230
TRIM40   ......................IYPQLEKG.VSELLL.......QPPQ...   256
TRIM31   ................LNPTPVPLELEKK.LSEAKS............R  282
TRIM69   ................ATRELISRKL.........N..............   298
TRIM62   LAGVAS..............LS.ERLKG.KIHETN.......LTYEDFP   270
TRIM26   ................WVGKPIARVVK.K.KTGEFS.......DKLL...   291
TRIM15   ................VSPEAISPDLV.K.KIRDFH.......RKIL...   272
TRIM10   ................RKPVAVSPELG.Q.RIRDFP.......QQAL...   288
TRIM64   ................QKPQPVNPELT...SWCITG..............   276
TRIM43   ................HMPQPVNPELT...AGPITG..............   277
TRIM49   ................HMPQPLNPELS...AGPITG..............   277
TRIM48   ................HMPQPLNLALR...AGPITG..............   200
TRIM39   LLGLVKEINRCEKVKTMEVTSVSIELEKN.FSNFPR..............   323
TRIM75   ....................PSIFSIHLKRD.GCSFPP..............   280
TRIM60   ....................PELFSFRLTKY.GFSLPP..............   281
TRIM4    ................NYS..LEAVKVKT.VCQIPL..............   297
TRIM20   ................PEKWTTP.QEIKQ.KIQLLH.......QKSE...   565
TRIM5    ................KKPETFP.KNQRR.VFRAPD.......L.......   281
TRIM6    ................RKPEALP.TKLRS.MFRAPD.......L.......   283
TRIM22   ................KKPKSVS.KKLKS.VFRVPD.......L.......   283
TRIM34   ................KKPKMVS.KKLKT.VFHAPD.......L.......   283
TRIM7    ................PKPTTVS.SEMKN.KVWNVS.......LKTF...   319
TRIM41   ................QPPEVWSPDPCQP.HSHDFL..............   413
TRIM27   ................PEPWITP.PDLQE.KIHIFA.......QKCL...   285
TRIM38   ................ETSEAVS.LELHT.MCNVSK.......L.YF...   281
TRIM21   ................KDLDITS.PELRS.VCHVPG..............   277
TRIM68   ................QQPEPIS.LELKT.DCRVLG..............   293
TRIM17   ................QCPEVAPPTRPRT.VCRVPG..............   285
TRIM11   ................QPPEVVP.MELRT.VCRVPG..............   277
TRIM58   ................LEAENIP.MELKT.ACCIPG..............   281
```

Lysine-rich region in L2

```
                                                                PRY
TRIM16  ....................IRTQ........VSAVVQRKYWTSKPEPS   363
Riplet  ...................................................R   249
TRIM25  .......DLKQAG........LEAAAKATSSHPNSTSLKAK.VLETFLAK   447
TRIM47  .......QLRGPGGNEDGPQKLDSEADAEPQDLESTN.....LLESE..A   418
TRIM35  ................LGSL......Q.............Y...RVWKK   294
TRIM72  ................SDDF......K.............F...QVWRK   279
TRIM50  ................QADI......K.............L...TVWKR   284
TRIM74  ...................................................   250
TRIM73  ...................................................   250
TRIM8   ...................................A.......KKEKQ   343
TRIM65  ..............EAPGPL......APVP..............STVCP   321
TRIM14  LKESINCQLSDPSSTKPGTL......LKTS................PSP   257
TRIM40  ..............KL.....................................   258
TRIM31  ............HDSITGSL......KKFKDQLQADRKKDEN...RFFKS   311
TRIM69  ............LGQYKGPI......QYM................VWRE   313
TRIM62  ............TSKYTGPL......QYTI................WKS   285
TRIM26  ..............SLQRGL......REFQGK.................   303
TRIM15  ..............TLPEMM......RMFSEN.................   284
TRIM10  ..............PLQREM......KMFLEK.................   300
TRIM64  ...................................................   276
TRIM43  ...................................................   277
TRIM49  ...................................................   277
TRIM48  ...................................................   200
TRIM39  ........................QYFA.....................   327
TRIM75  ........................QYSA.....................   284
TRIM60  ........................QYSG.....................   285
TRIM4   ...................................................   297
TRIM20  ..............FVEKST......KYFSETLRSEME.......MFNVP   588
TRIM5   ................KGML......EVFR.....................   289
TRIM6   ................KRML......RVCR.....................   291
TRIM22  ................SGML......QVLK.....................   291
TRIM34  ................SRML......QMFR.....................   291
TRIM7   ..............VLKGML......KKFKEDLRGE..............   335
TRIM41  ................TDAI................V.......R..KM   421
TRIM27  ..............FLTESL......KQFTEKMQSDME.......K..IQ   306
TRIM38  ..............D.....................................   282
TRIM21  ...................................................   277
TRIM68  ...................................................   293
TRIM17  ...................................................   285
TRIM11  ...................................................   277
TRIM58  ...................................................   281
```

```
TRIM16   TREQFLQ.........YAYDITFDPDTAHKYLRLQEENRKVTNTTP..WE   402
Riplet   RASRFAQ.........WAIHPTFNLKSLSCSLEVSKDSRTV.TVSH..RP   287
TRIM25   SRPELLE.........YYIKVILDYNTAHNKVALSECYTVA.SVAE..MP   485
TRIM47   PRDYFLK.........FAYIVDLDSDTADKFLQLFGTKG.V.KRVL..CP   455
TRIM35   MLASVES..........VPFSFDPNTAAGWLSVSDDLTSVTNH....GY   329
TRIM72   MFRALMP.........ALEELTFDPSSAHPSLVVSSSGRRVECSEQ..KA   318
TRIM50   LFRKVLP.........APEPLKLDPATAHPLLELSKGNTVVQCGLL..A.   322
TRIM74   ..................................................   250
TRIM73   ..................................................   250
TRIM8    LRKMLEGP.........FSTPV.........PF................   358
TRIM65   LRRKLWQ.........NYRNLTFDPVSANRHFYLSRQDQQVKHCRQ....   358
TRIM14   ERSLLLK.........YARTPTLDPDTMHARLRLSADRLTVRCGLL....   294
TRIM40   ..................................................   258
TRIM31   MNKNDMKSWGLLQKNNHKMNKTSEPGSSSAG......GR.TTSGPP..NH   352
TRIM69   MQDTLCP.........GLSPLTLDPKTAHPNLVLSKSQTSVWHGD...IK   351
TRIM62   LFQDIHP.........VPAALTLDPGTAHQRLILSDDCTIVAYGNL..HP   324
TRIM26   LLRDLEY.........KTVSVTLDPQSASGYLQLSEDWKCVTYTS...LY   341
TRIM15   LAHHLEI.........DSGVITLDPQTASRSLVLSEDRKSVRYTR...QK   322
TRIM10   LCFELDY.........EPAHISLDPQTSHPKLLLSEDHQRAQFSY...KW   338
TRIM64   VLDMLNN.........FRVDSALSTEMIPCYISLSEDVRYVIFGDD...H   314
TRIM43   LVYRLNR.........FRVEISFHFEVTNHNIRLFEDVRSWMFR......   312
TRIM49   LRDRLNQ.........FRVHITLHHEEANSDIFLCEILRSMCIGCD...H   315
TRIM48   LRDRLNQ.........F..............................   208
TRIM39   LRKILKQ.........LIADVTLDPETAHPNLVLSEDRKSVKFVET..RL   366
TRIM75   LQRIIKK.........FKVEIILDPETAHPNLIVSEDKKRVRFTK...RK   322
TRIM60   LDRIIKP.........FQVDVILDLNTAHPQLLVSEDRKAVRYER...KK   323
TRIM4    MKEMLKR.........FQVAVNLAEDTAHPKLVFSQEGRYVKNTASASSW   338
TRIM20   ELIGAQA.........HAVNVILDAETAYPNLIFSDDLKSVRLG.N..KW   626
TRIM5    ELTDVRR.........YWVDVTVAPNNISCA.VISEDKRQVSSP.K..PQ   326
TRIM6    ELTDVQS.........YWVDVTLNPHTANLNLVLAKNRRQVRFV.G..AK   329
TRIM22   ELTDVQY.........YWVDVMLNPGSATSNVAISVDQRQVKTV.R..TC   329
TRIM34   ELTAVRC.........YWVDVTLNSVNLNLNLVLSEDQRQVISV.P..IW   329
TRIM7    ...LEKE.........EKVELTLDPDTANPRLILSLDLKGVRLG.E..RA   370
TRIM41   SRMFCQA.........ARVDLTLDPDTAHPALMLSPDRRGVRLA.E..RR   459
TRIM27   ELREAQL.........YSVDVTLDPDTAYPSLILSDNLRQVRYS.Y..LQ   344
TRIM38   VKKMLRS.........HQVSVTLDPDTAHHELILSEDRRQVTRG.Y..TQ   320
TRIM21   LKKMLRT.........CAVHITLDPDTANPWLILSEDRRQVRLG.D..TQ   315
TRIM68   LREILKT.........YAADVRLDPDTAYSRLIVSEDRKRVHYG.D..TN   331
TRIM17   QIEVLRG.........FLEDVVPDATSAYPYLLLYESRQRRYLGSS..PE   324
TRIM11   LVETLRR.........FRGDVTLDPDTANPELILSEDRRSVQRG.D..LR   315
TRIM58   RRELLRK.........FQVDVKLDPATAHPSLLLTADLRSVQDG.E..PW   319
```

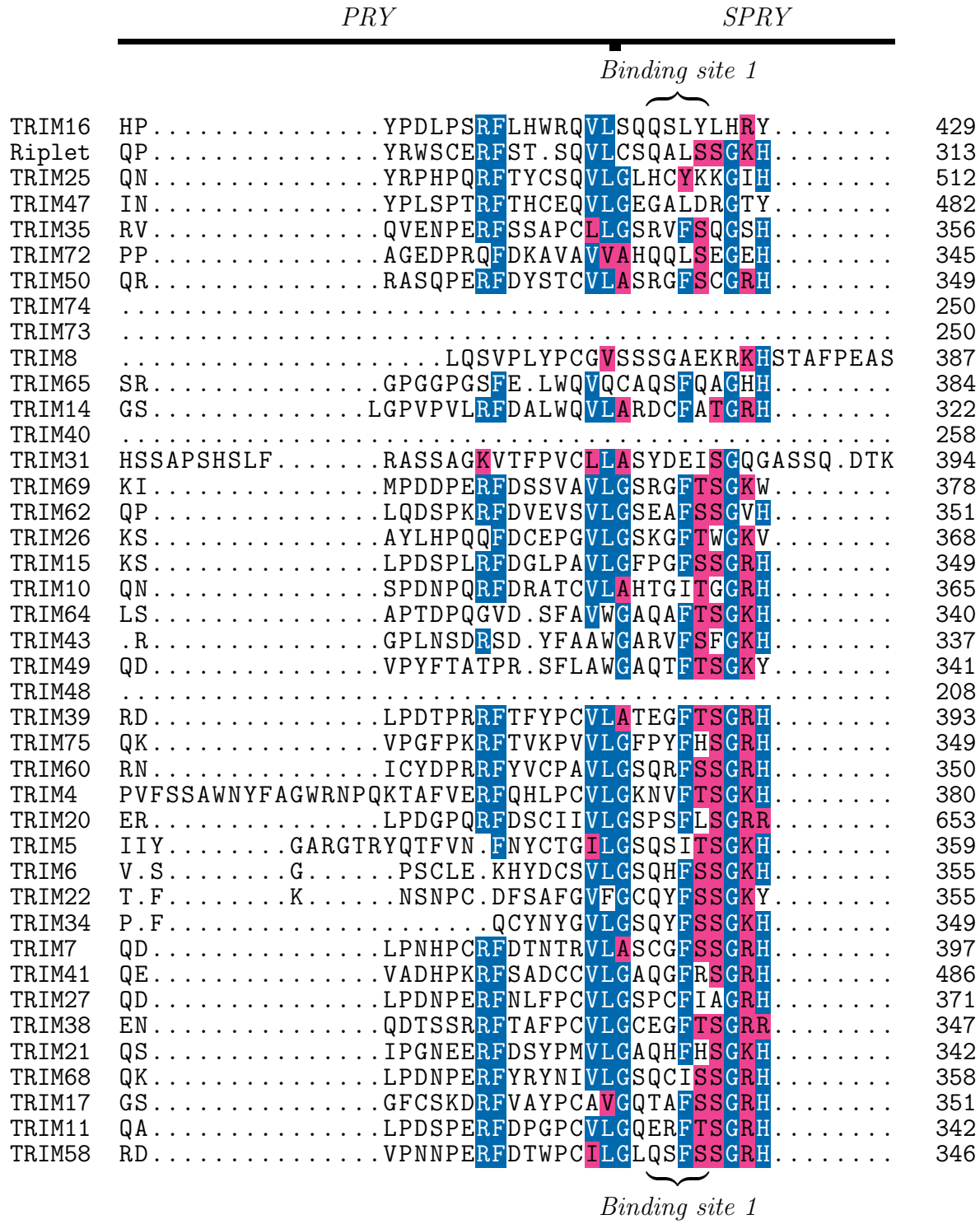
PRY
SPRY
Binding site 1
TRIM16 HP.....YPDLPSRFLHWRQVLSQQSLYLHRY..... 429
Riplet QP.....YRWSCERFST.SQVLCSQALSSGKH..... 313
TRIM25 QN.....YRPHPQRFTYCSQVLGLHCYKKGIH..... 512
TRIM47 IN.....YPLSPTRFTHCEQVLGEGALDRGTY..... 482
TRIM35 RV.....QVENPERFSSAPCLLGSRVFSQGSH..... 356
TRIM72 PP.....AGEDPRQFDKAVAVVAHQQLSEGEH..... 345
TRIM50 QR.....RASQPERFDYSTCVLASRGFSCGRH..... 349
TRIM74 250
TRIM73 250
TRIM8 .....LQSVPLYPCGVSSSGAEKRKHSTAFPEAS 387
TRIM65 SR.....GPGGPGSFE.LWQVQCAQSFQAGHH..... 384
TRIM14 GS.....LGPVPVLRFDALWQVLARDCFATGRH..... 322
TRIM40 258
TRIM31 HSSAPSHSLF.....RASSAGKVTFPVCLLASYDEISGQQGASSQ.DTK 394
TRIM69 KI.....MPDDPERFDSSVAVLGSRGFTSGKW..... 378
TRIM62 QP.....LQDSPKRFDVEVSVLGSEAFSSGVH..... 351
TRIM26 KS.....AYLHPQQFDCEPGVLGSKGFTWGKV..... 368
TRIM15 KS.....LPDSPLRFDGLPAVLGFPGFSSGRH..... 349
TRIM10 QN.....SPDNPQRFDRATCVLAHTGITGGRH..... 365
TRIM64 LS.....APTDPQGVD.SFAVWGAQAFTSGKH..... 340
TRIM43 .R.....GPLNSDRSD.YFAAWGARVFSFGKH..... 337
TRIM49 QD.....VPYFTATPR.SFLAWGAQTFTSGKY..... 341
TRIM48 208
TRIM39 RD.....LPDTPRRFTFYPCVLATEGFTSGRH..... 393
TRIM75 QK.....VPGFPKRFTVKPVVLGFPYFHSGRH..... 349
TRIM60 RN.....ICYDPRRFYVCPAVLGSQRFSSGRH..... 350
TRIM4 PVFSSAWNYFAGWRNPQKTAFVERFQHLPCVLGKNVFTSGKH..... 380
TRIM20 ER.....LPDGPQRFDSCIIVLGSPSFLSGRR..... 653
TRIM5 IIY.....GARGTRYQTFVN.FNYCTGILGSQSITSGKH..... 359
TRIM6 V.S.....G.....PSCLE.KHYDCSVLGSQHFSSGKH..... 355
TRIM22 T.F.....K.....NSNPC.DFSAFGVFGCQYFSSGKY..... 355
TRIM34 P.F.....QCYNYGVLGSQYFSSGKH..... 349
TRIM7 QD.....LPNHPCRFDTNTRVLASCGFSSGRH..... 397
TRIM41 QE.....VADHPKRFSADCCVLGAQGFRSGRH..... 486
TRIM27 QD.....LPDNPERFNLFPCVLGSPCFIAGRH..... 371
TRIM38 EN.....QDTSSRRFTAFPCVLGCEGFTSGRR..... 347
TRIM21 QS.....IPGNEERFDSYPMVLGAQHFHSGKH..... 342
TRIM68 QK.....LPDNPERFYRYNIVLGSQCISSGRH..... 358
TRIM17 GS.....GFCSKDRFVAYPCAVGQTAFSSGRH..... 351
TRIM11 QA.....LPDSPERFDPGPCVLGQERFTSGRH..... 342
TRIM58 RD.....VPNNPERFDTWPCILGLQSFSSGRH..... 346
Binding site 1

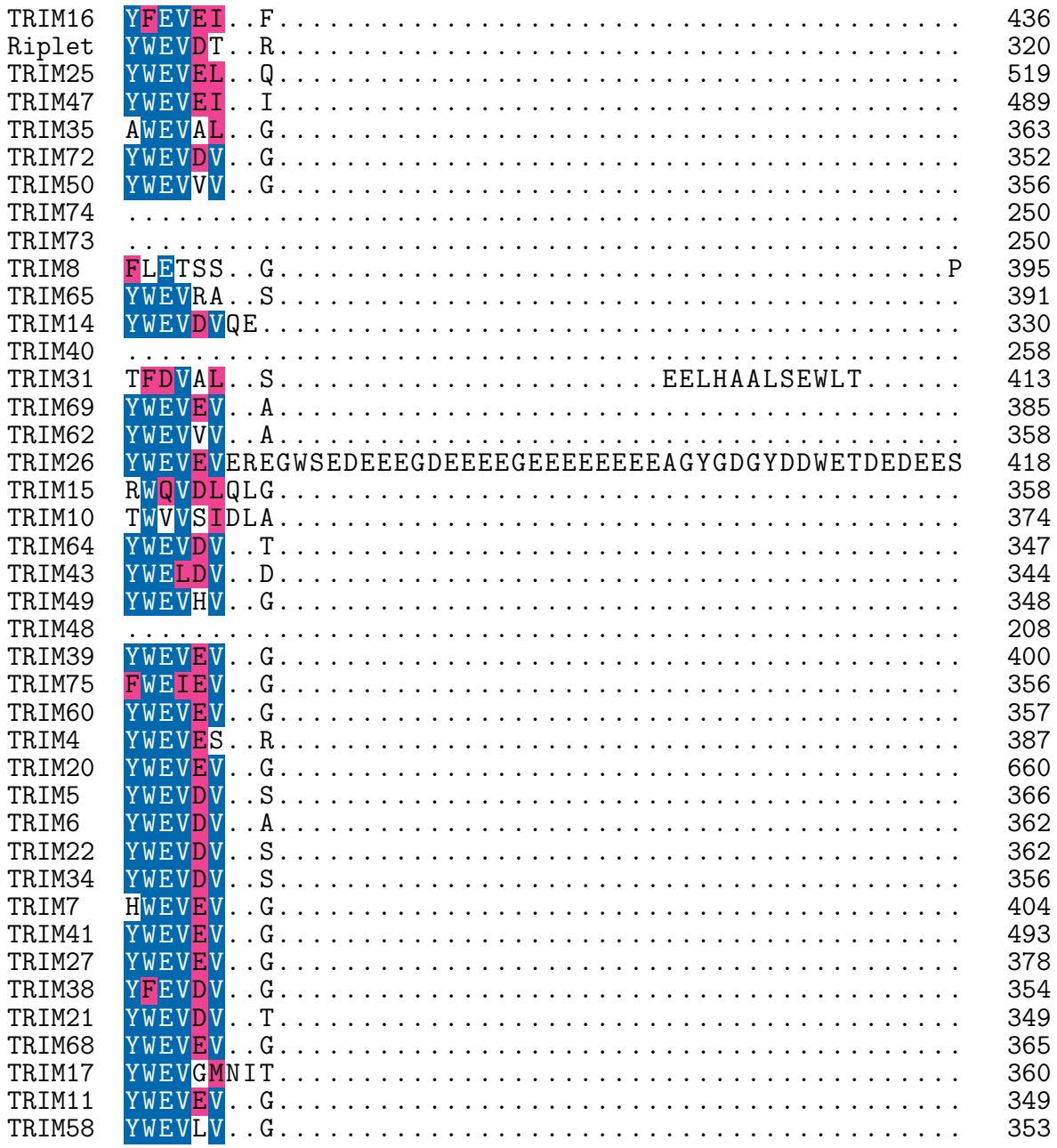
TRIM16 YFEVEI..F 436
Riplet YWEVDT..R 320
TRIM25 YWEVEL..Q 519
TRIM47 YWEVEI..I 489
TRIM35 AWEVAL..G 363
TRIM72 YWEVDV..G 352
TRIM50 YWEVVV..G 356
TRIM74 250
TRIM73 250
TRIM8 FLETSS..G P 395
TRIM65 YWEVRA..S 391
TRIM14 YWEVDVQE 330
TRIM40 258
TRIM31 TFDVAL..S EELHAALSEWLT 413
TRIM69 YWEVEV..A 385
TRIM62 YWEVVV..A 358
TRIM26 YWEVEVEREGWSEDEEEGDEEEEGEEEEEEEEAGYGDGYDDWETDEDEES 418
TRIM15 RWQVDLQLG 358
TRIM10 TWVVSIDLA 374
TRIM64 YWEVDV..T 347
TRIM43 YWELDV..D 344
TRIM49 YWEVHV..G 348
TRIM48 208
TRIM39 YWEVEV..G 400
TRIM75 FWEIEV..G 356
TRIM60 YWEVEV..G 357
TRIM4 YWEVES..R 387
TRIM20 YWEVEV..G 660
TRIM5 YWEVDV..S 366
TRIM6 YWEVDV..A 362
TRIM22 YWEVDV..S 362
TRIM34 YWEVDV..S 356
TRIM7 HWEVEV..G 404
TRIM41 YWEVEV..G 493
TRIM27 YWEVEV..G 378
TRIM38 YFEVDV..G 354
TRIM21 YWEVDV..T 349
TRIM68 YWEVEV..G 365
TRIM17 YWEVGMNIT 360
TRIM11 YWEVEV..G 349
TRIM58 YWEVLV..G 353

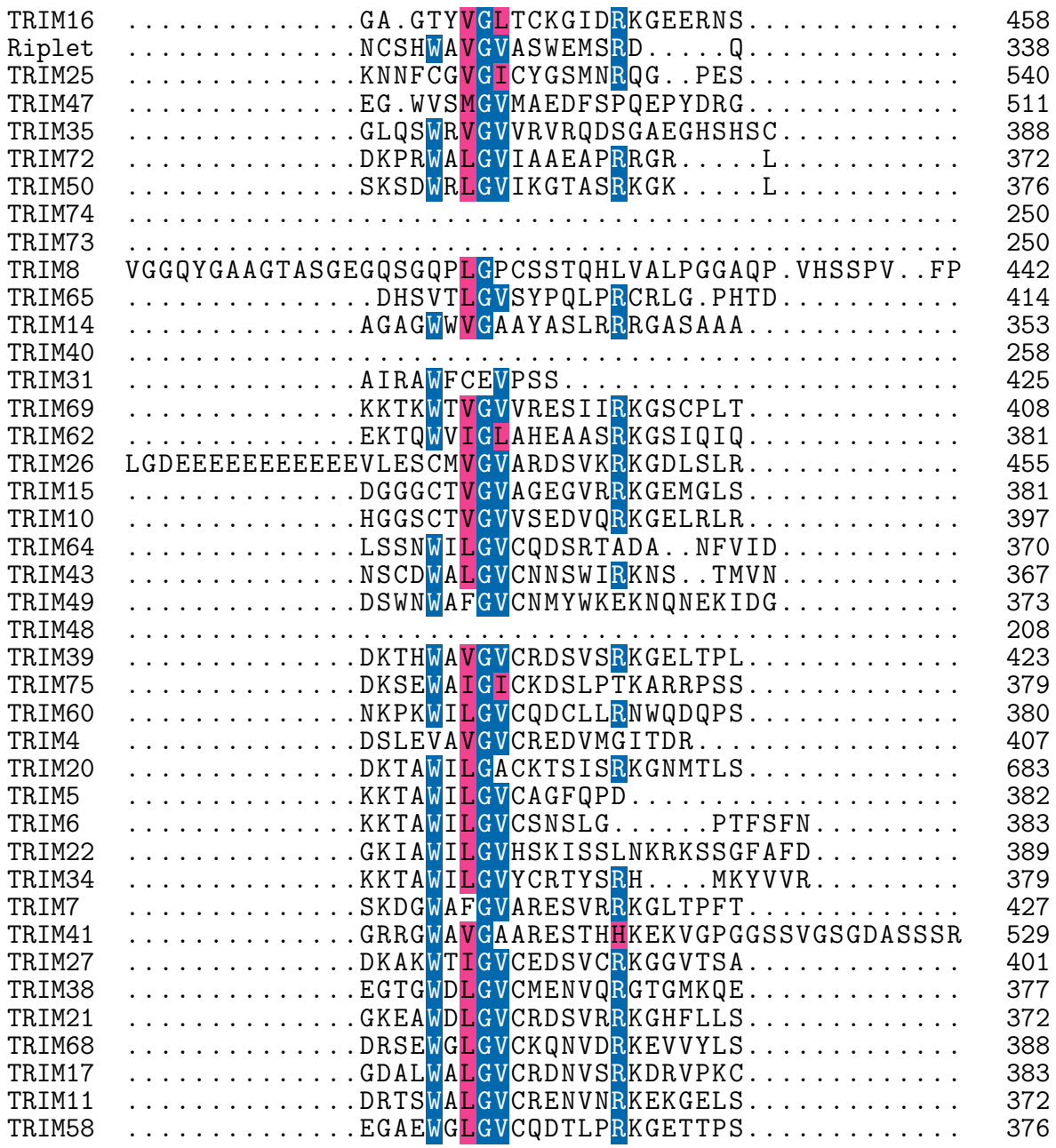
TRIM16 ..............GA.GTYVGLTCKGIDRKGEERNS..... 458
Riplet ..............NCSHWAVGVASWEMSRD.....Q..... 338
TRIM25 ..............KNNFCGVGICYGSMNRQG..PES..... 540
TRIM47 ..............EG.WVSMGVMAEDFSPQEPYDRG..... 511
TRIM35 ..............GLQSWRVGVVRVRQDSGAEGHSHSC..... 388
TRIM72 ..............DKPRWALGVIAAEAPRRGR.....L..... 372
TRIM50 ..............SKSDWRLGVIKGTASRKGK.....L..... 376
TRIM74 250
TRIM73 250
TRIM8 VGGQYGAAGTASGEGQSGQPLGPCSSTQHLVALPGGAQP.VHSSPV..FP 442
TRIM65 ..............DHSVTLGVSYPQLPRCRLG.PHTD..... 414
TRIM14 ..............AGAGWWVGAAYASLRRRGASAAA..... 353
TRIM40 258
TRIM31 ..............AIRAWFCEVPSS..... 425
TRIM69 ..............KKTKWTVGVVRESIIRKGSCPLT..... 408
TRIM62 ..............EKTQWVIGLAHEAASRKGSIQIQ..... 381
TRIM26 LGDEEEEEEEEEEEVLESCMVGVARDSVKRKGDLSLR..... 455
TRIM15 ..............DGGGCTVGVAGEGVRRKGEMGLS..... 381
TRIM10 ..............HGGSCTVGVVSEDVQRKGELRLR..... 397
TRIM64 ..............LSSNWILGVCQDSRTADA..NFVID..... 370
TRIM43 ..............NSCDWALGVCNNSWIRKNS..TMVN..... 367
TRIM49 ..............DSWNWAFGVCNMYWKEKNQNEKIDG..... 373
TRIM48 208
TRIM39 ..............DKTHWAVGVCRDSVSRKGELTPL..... 423
TRIM75 ..............DKSEWAIGICKDSLPTKARRPSS..... 379
TRIM60 ..............NKPKWILGVCQDCLLRNWQDQPS..... 380
TRIM4 ..............DSLEVAVGVCREDVMGITDR..... 407
TRIM20 ..............DKTAWILGACKTSISRKGNMTLS..... 683
TRIM5 ..............KKTAWILGVCAGFQPD..... 382
TRIM6 ..............KKTAWILGVCSNSLG......PTFSFN..... 383
TRIM22 ..............GKIAWILGVHSKISSLNKRKSSGFAFD..... 389
TRIM34 ..............KKTAWILGVYCRTYSRH....MKYVVR..... 379
TRIM7 ..............SKDGWAFGVARESVRRKGLTPFT..... 427
TRIM41 ..............GRRGWAVGAARESTHHKEKVGPGGSSVGSGDASSSR 529
TRIM27 ..............DKAKWTIGVCEDSVCRKGGVTSA..... 401
TRIM38 ..............EGTGWDLGVCMENVQRGTGMKQE..... 377
TRIM21 ..............GKEAWDLGVCRDSVRRKGHFLLS..... 372
TRIM68 ..............DRSEWGLGVCKQNVDRKEVVYLS..... 388
TRIM17 ..............GDALWALGVCRDNVSRKDRVPKC..... 383
TRIM11 ..............DRTSWALGVCRENVNRKEKGELS..... 372
TRIM58 ..............EGAEWGLGVCQDTLPRKGETTPS..... 376

```
TRIM16  ............CISGNNFS..........WSLQW..........NGK   474
Riplet  ............VLGRTMDS..........CCVEW..........KGT   354
TRIM25  ............RLGRNSAS..........WCVEW..........FNT   556
TRIM47  ............RLGRNAHS..........CCLQW..........NGR   527
TRIM35  ............YHDTRSGF..........WYVCR..........TQG   404
TRIM72  ............HAVPSQGL..........WLLGL..........REG   388
TRIM50  ............NRSPEHGV..........WLIGL..........KEG   392
TRIM74  ..................................................   250
TRIM73  ..................................................   250
TRIM8   PSQYPNGSAAQQPMLPQYGGRKILVCSVDNCYCSSVANHGGHQPYPRSGH   492
TRIM65  ............NIGRGPCS..........WGLCV..........QED   430
TRIM14  ............RLGCNRQS..........WCLKR..........YDL   369
TRIM40  ..................................................   258
TRIM31  ..................................................   425
TRIM69  ..............PEQGF..........WLLRL..........RNQ   421
TRIM62  ..............PSRGF..........YCIVM..........HDG   394
TRIM26  ..............PEDGV..........WALRL..........SSS   468
TRIM15  ..............AEDGV..........WAVII..........SHQ   394
TRIM10  ..............PEEGV..........WAVRL..........AWG   410
TRIM64  ..............SDERF..........FLISS..........KRS   383
TRIM43  ..............SEDIF..........LLLCL..........KVD   380
TRIM49  ..............EDGLF..........LLGCV..........KND   386
TRIM48  ..................................................   208
TRIM39  ..............PETGY..........WRVRL..........WNG   436
TRIM75  ..............AQQEC..........WRIE...........LQD   391
TRIM60  ..............VLGGF..........WAIGR..........YMK   393
TRIM4   ............SKMSPDVGI..........WAIYW..........SAA   424
TRIM20  ..............PENGY..........WVVIM..........MKE   696
TRIM5   ..AM.CNIEKNENYQPKYGY..........WVIGL..........EEG   407
TRIM6   ..HFAQNHSAYSRYQPQSGY..........WVIGL..........QHN   409
TRIM22  ..PSVNYSKVYSRYRPQYGY..........WVIGL..........QNT   415
TRIM34  ..RCANRQNLYTKYRPLFGY..........WVIGL..........QNK   405
TRIM7   ..............PEEGV..........WALQL..........NGG   440
TRIM41  HHHRRRRLHLPQQPLLQREV..........WCVGT..........NGK   557
TRIM27  ..............PQNGF..........WAVSL..........WYG   414
TRIM38  ..............PQSGF..........WTLRL..........CKK   390
TRIM21  ..............SKSGF..........WTIWL..........WNK   385
TRIM68  ..............PHYGF..........WVIRL..........RKG   401
TRIM17  ..............PENGF..........WVVQL..........SKG   396
TRIM11  ..............AGNGF..........WILVF..........LGS   385
TRIM58  ..............PENGV..........WALWL..........LKG   389
```

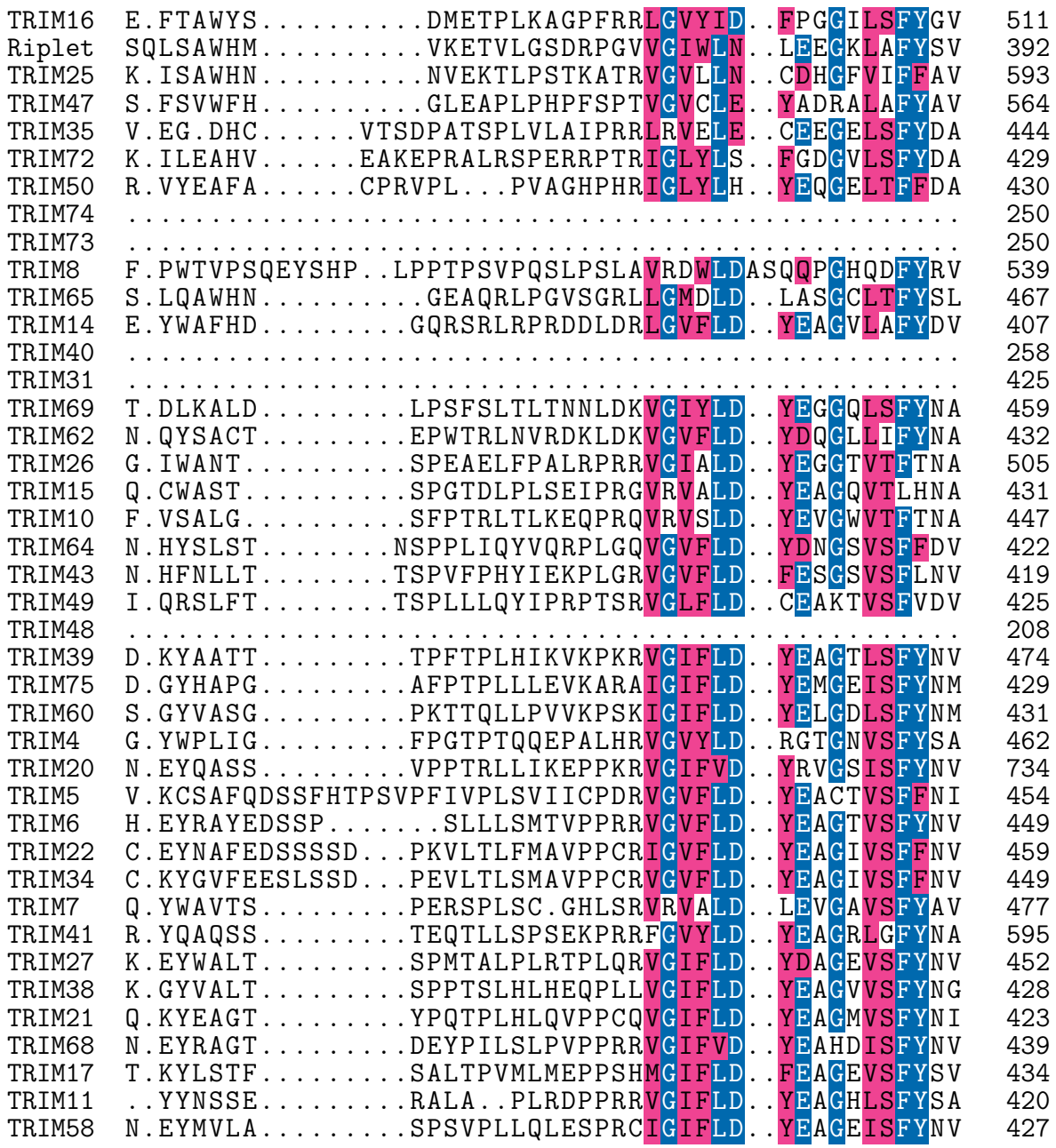
TRIM16 E.FTAWYS.....DMETPLKAGPFRRLGVYID..FPGGILSFYGV 511
Riplet SQLSAWHM.....VKETVLGSDRPGVVGIWLN..LEEGKLAFYSV 392
TRIM25 K.ISAWHN.....NVEKTLPSTKATRVGVLLN..CDHGFVIFFAV 593
TRIM47 S.FSVWFH.....GLEAPLPHPFSPTVGVCLE..YADRALAFYAV 564
TRIM35 V.EG.DHC.....VTSDPATSPLVLAIPRRLRVELE..CEEGELSFYDA 444
TRIM72 K.ILEAHV.....EAKEPRALRSPERRPTRIGLYLS..FGDGVLSFYDA 429
TRIM50 R.VYEAFA.....CPRVPL...PVAGHPHRIGLYLH..YEQGELTFFDA 430
TRIM74 250
TRIM73 250
TRIM8 F.PWTVPSQEYSHP..LPPTPSVPQSLPSLAVRDWLDASQQPGHQDFYRV 539
TRIM65 S.LQAWHN.....GEAQRLPGVSGRLLGMDLD..LASGCLTFYSL 467
TRIM14 E.YWAFHD.....GQRSRLRPRDDLDRLGVFLD..YEAGVLAFYDV 407
TRIM40 258
TRIM31 425
TRIM69 T.DLKALD.....LPSFSLTLTNNLDKVGIYLD..YEGGQLSFYNA 459
TRIM62 N.QYSACT.....EPWTRLNVRDKLDKVGVFLD..YDQGLLIFYNA 432
TRIM26 G.IWANT.....SPEAELFPALRPRRVGIALD..YEGGTVTFTNA 505
TRIM15 Q.CWAST.....SPGTDLPLSEIPRGVRVALD..YEAGQVTLHNA 431
TRIM10 F.VSALG.....SFPTRLTLKEQPRQVRVSLD..YEVGWVTFTNA 447
TRIM64 N.HYSLST.....NSPPLIQYVQRPLGQVGVFLD..YDNGSVSFFDV 422
TRIM43 N.HFNLLT.....TSPVFPHYIEKPLGRVGVFLD..FESGSVSFLNV 419
TRIM49 I.QRSLFT.....TSPLLLQYIPRPTSRVGLFLD..CEAKTVSFVDV 425
TRIM48 208
TRIM39 D.KYAATT.....TPFTPLHIKVKPKRVGIFLD..YEAGTLSFYNV 474
TRIM75 D.GYHAPG.....AFPTPLLLEVKARAIGIFLD..YEMGEISFYNM 429
TRIM60 S.GYVASG.....PKTTQLLPVVKPSKIGIFLD..YELGDLSFYNM 431
TRIM4 G.YWPLIG.....FPGTPTQQEPALHRVGVYLD..RGTGNVSFYSA 462
TRIM20 N.EYQASS.....VPPTRLLIKEPPKRVGIFVD..YRVGSISFYNV 734
TRIM5 V.KCSAFQDSSFHTPSVPFIVPLSVIICPDRVGVFLD..YEACTVSFFNI 454
TRIM6 H.EYRAYEDSSP.....SLLLSMTVPPRRVGVFLD..YEAGTVSFYNV 449
TRIM22 C.EYNAFEDSSSSD...PKVLTLFMAVPPCRIGVFLD..YEAGIVSFFNV 459
TRIM34 C.KYGVFEESLSSD...PEVLTLSMAVPPCRVGVFLD..YEAGIVSFFNV 449
TRIM7 Q.YWAVTS.....PERSPLSC.GHLSRVRVALD..LEVGAVSFYAV 477
TRIM41 R.YQAQSS.....TEQTLLSPSEKPRRFGVYLD..YEAGRLGFYNA 595
TRIM27 K.EYWALT.....SPMTALPLRTPLQRVGIFLD..YDAGEVSFYNV 452
TRIM38 K.GYVALT.....SPPTSLHLHEQPLLVGIFLD..YEAGVVSFYNG 428
TRIM21 Q.KYEAGT.....YPQTPLHLQVPPCQVGIFLD..YEAGMVSFYNI 423
TRIM68 N.EYRAGT.....DEYPILSLPVPPRRVGIFVD..YEAHDISFYNV 439
TRIM17 T.KYLSTF.....SALTPVMLMEPPSHMGIFLD..FEAGEVSFYSV 434
TRIM11 ..YYNSSE.....RALA..PLRDPPRRVGIFLD..YEAGHLSFYSA 420
TRIM58 N.EYMVLA.....SPSVPLLQLESPRCIGIFLD..YEAGEISFYNV 427

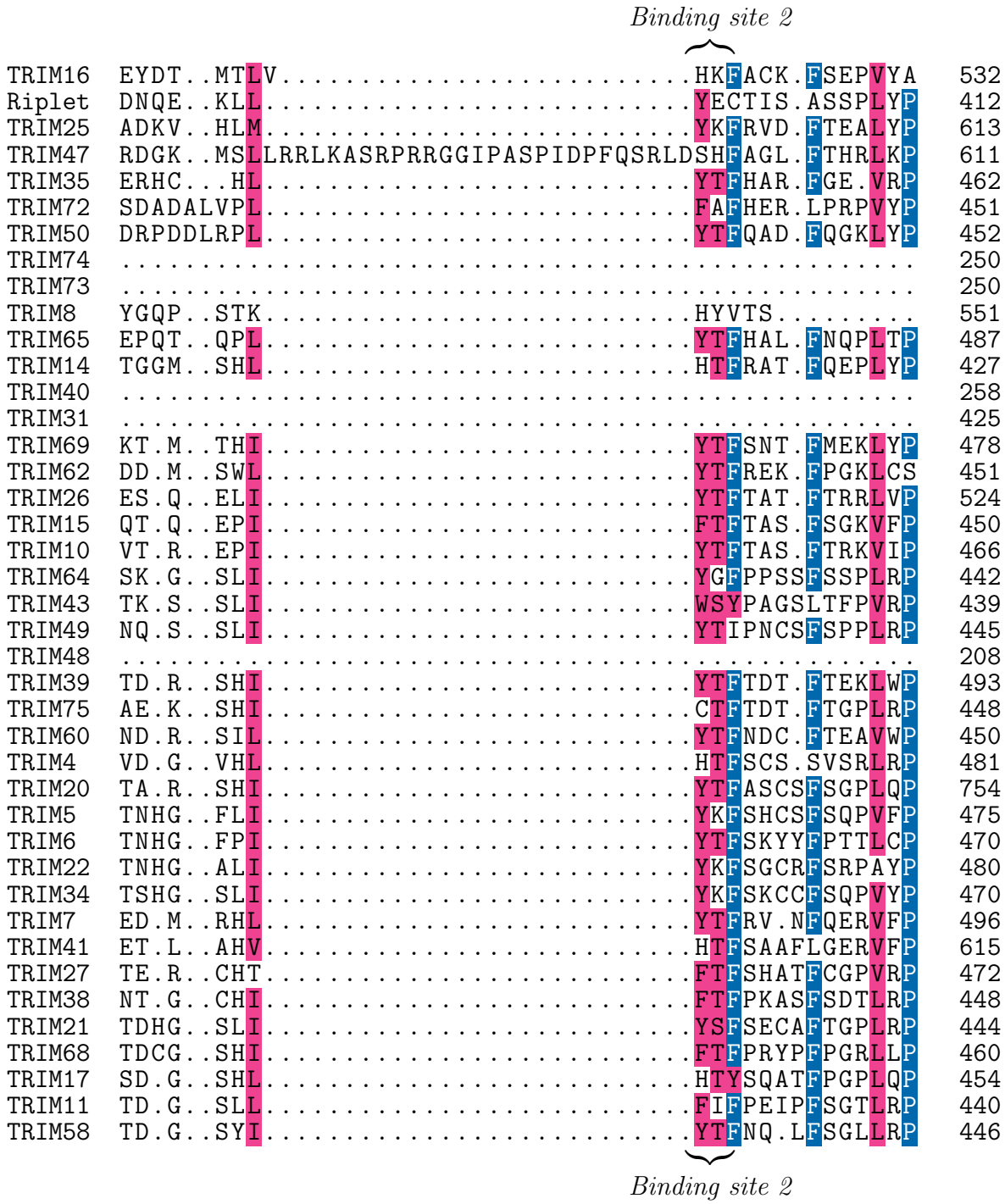
Binding site 2
TRIM16 EYDT..MTLV.....HKFACK.FSEPVYA 532
Riplet DNQE..KLL.....YECTIS.ASSPLYP 412
TRIM25 ADKV..HLM.....YKFRVD.FTEALYP 613
TRIM47 RDGK..MSLLRRLKASRPRRGGIPASPIDPFQSRLDSHFAGL.FTHRLKP 611
TRIM35 ERHC...HL.....YTFHAR.FGE.VRP 462
TRIM72 SDADALVPL.....FAFHER.LPRPVYP 451
TRIM50 DRPDDLRPL.....YTFQAD.FQGKLYP 452
TRIM74 250
TRIM73 250
TRIM8 YGQP..STK.....HYVTS..... 551
TRIM65 EPQT..QPL.....YTFHAL.FNQPLTP 487
TRIM14 TGGM..SHL.....HTFRAT.FQEPLYP 427
TRIM40 258
TRIM31 425
TRIM69 KT.M..THI.....YTFSNT.FMEKLYP 478
TRIM62 DD.M..SWL.....YTFREK.FPGKLCS 451
TRIM26 ES.Q..ELI.....YTFTAT.FTRRLVP 524
TRIM15 QT.Q..EPI.....FTFTAS.FSGKVFP 450
TRIM10 VT.R..EPI.....YTFTAS.FTRKVIP 466
TRIM64 SK.G..SLI.....YGFPPSSFSSPLRP 442
TRIM43 TK.S..SLI.....WSYPAGSLTFPVRP 439
TRIM49 NQ.S..SLI.....YTIPNCSFSPPLRP 445
TRIM48 208
TRIM39 TD.R..SHI.....YTFTDT.FTEKLWP 493
TRIM75 AE.K..SHI.....CTFTDT.FTGPLRP 448
TRIM60 ND.R..SIL.....YTFNDC.FTEAVWP 450
TRIM4 VD.G..VHL.....HTFSCS.SVSRLRP 481
TRIM20 TA.R..SHI.....YTFASCSFSGPLQP 754
TRIM5 TNHG..FLI.....YKFSHCSFSQPVFP 475
TRIM6 TNHG..FPI.....YTFSKYYFPTTLCP 470
TRIM22 TNHG..ALI.....YKFSGCRFSRPAYP 480
TRIM34 TSHG..SLI.....YKFSKCCFSQPVYP 470
TRIM7 ED.M..RHL.....YTFRV.NFQERVFP 496
TRIM41 ET.L..AHV.....HTFSAAFLGERVFP 615
TRIM27 TE.R..CHT.....FTFSHATFCGPVRP 472
TRIM38 NT.G..CHI.....FTFPKASFSDTLRP 448
TRIM21 TDHG..SLI.....YSFSECAFTGPLRP 444
TRIM68 TDCG..SHI.....FTFPRYPFPGRLLP 460
TRIM17 SD.G..SHL.....HTYSQATFPGPLQP 454
TRIM11 TD.G..SLL.....FIFPEIPFSGTLRP 440
TRIM58 TD.G..SYI.....YTFNQ.LFSGLLRP 446
Binding site 2

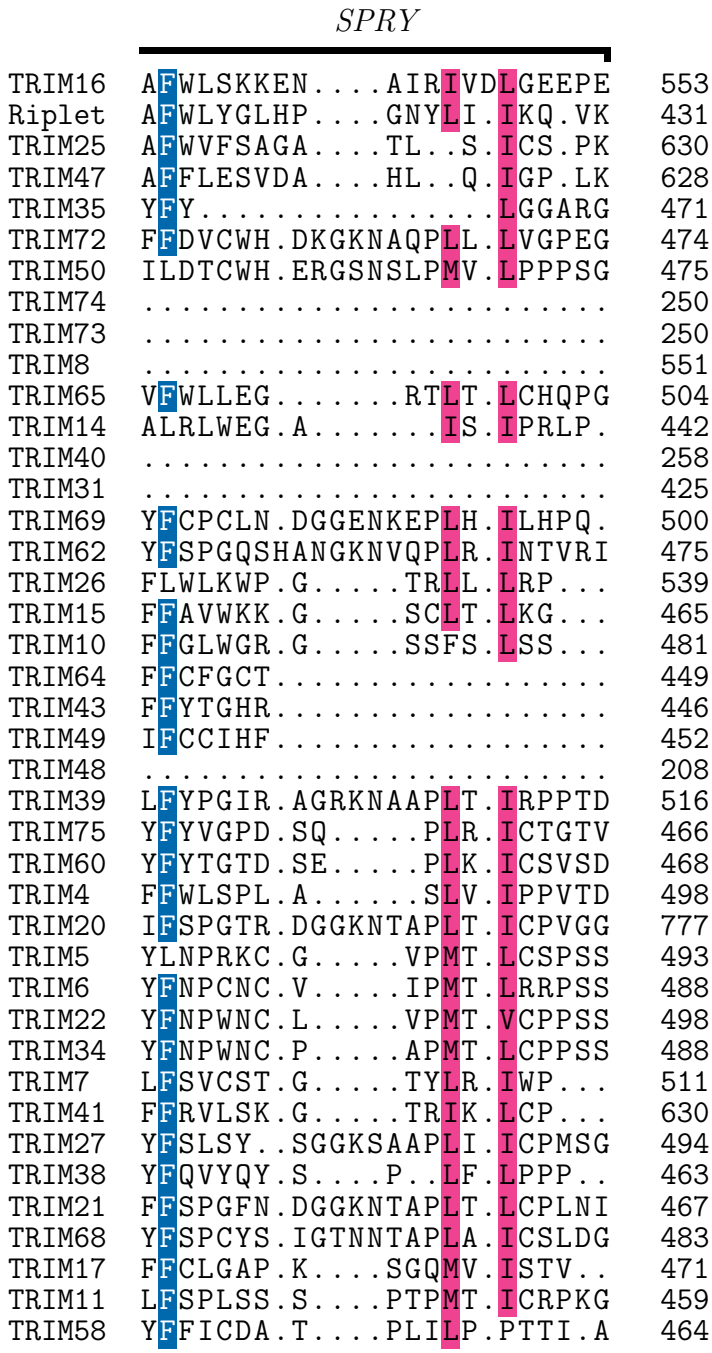

Figure C.1.: Sequence alignment of all human TRIM-PRY/SPRY proteins and Riplet (RN135)

Acknowledgements

First and foremost I would like to thank Janosch Hennig for given me the opportunity to work on this exciting project, for giving me the freedom to develop it in the directions I found most fascinating and for trusting that a chemist could do biology.

I thank the members of my thesis advisor committee Prof. Carsten Sachse, Prof. Hans-Georg Kräusslich and Stephen Cusack for their time, effort and thoughtful advice. Carsten Sachse I want to thank additionally for reviewing this thesis and joining my defence committee. Stephen Cusack I also thank for the opportunity to collaborate on the CC:PRY/SPRY and TRIM25/RIG-I interactions.

I would like to especially thank Prof. Dr. Irmgard Sinning for kindly agreeing to review my thesis and join my defense committee on very short notice! I thank the members of my defence committee Prof. Bernd Bukau and Sebastian Eustermann for taking the time and effort to read my thesis and join for the defence.

I would like to thank Sandra Augsten for support on many levels of this project. Especially the in cell assays presented in this work were only possible with her help and experience. Apart from that I also want to thank her for all her work to keep the lab running, her advice and friendship. Bernd Simon I thank for his continuous support since my master thesis. It is to a huge extent thanks to his supervision, training and enthusiasm that I endeavoured into another NMR/SAXS project for my PhD. In this project he supported me through help with the molecular modelling and of course through NMR trouble shooting. Pawel Masiewicz I thank for all his help on the RNA side of the project. He trained me in RNA production, established the HPLC purification of RNA and provided help with filter-binding assays. I would like to thank my interns Delaram Pouyabahar and Panos Spatharas for their hard work and support in early stages of this projects. It was great fun working with them and I learned at least as much as they did during this time. I would also like to thank all the other members of the Hennig group for their friendship and support. Especially, I am thankful for Jakub's efforts to keep my work/life balance in check, Felix and Cecilia for sharing the burden of working on TRIM proteins with me and Nele for never actually taking me to insect cell room .

I thank Kathryn Perez for the training in the use of ITC, troubleshooting, discussion of results and company during long experiments in the biophysics lab. Vladimir Rybin and Robert Opitz I thank for their support with biophysical experiments during early stages of the project. I thank Brice Murciano for setting up 277 crystallisation plates for me

without complain as well as advice and support. I thank Mathilde Lethier for the fruitful collaboration and providing samples. Abul Tarafder introduced me to negative stain sample preparation. Martin Schorb, Felix Weis and Stefan Terjung provided training and support on the electron and confocal microscopes. Julia Rossmanith provided training and advice on insect cell expression. Nikolay Dobrev has been an invaluable source of advice since the days of my master thesis and a source of chocolate and encouragement during synchrotron trips. Magdalena Büscher provided plasmids, cells and I am looking forward to bringing our ongoing collaboration on the p62/vaultRNA interaction to an successful end.

I would like to thank Prof. Katrin Rittinger and her team for the great collaboration on the CC:PRY/SPRY interaction, free exchange of plasmids and protocols and thoughtful discussions of many aspects of my project. Frank Gabel patiently supported my SANS measurements on samples of too often homeopathic concentrations and offered helpful advice on the theory and practice of SAS experiments and the interpretation of results. This work relied heavily on the use of large scale facilities such as synchrotrons and neutron sources and I want to acknowledge the beamline scientists that supported my measurements there: Gabriele Giachin, Gordon Leonard, Christoph Müller-Dieckmann at ESRF, Isabel Bento, Gleb Bourenkov, Saravanan Panneerselvam at EMBL-DESY, Anne Martel at ILL and Marie-Sousai Appavou at MLZ. Throughout my PhD beamtime was available plentifully due to the efforts in writing BAG proposals and organising synchrotron trips of Klemens Wild and Orsolya Barabas.

The last four years wouldn't have been the same without the friends I made at EMBL and beyond. Their silliness and their sincerity made the hardships of a PhD much easier to bear. I want to especially thank (in order of appearance) my fellow travellers Kuba, Sanjana, Diana, Filipe, Ashna, Felix, Lara and Areeb. This list would not be complete without expressing my gratitude to my oldest friend Markus Hellenbrand for his support and friendship since our school days.

Last but not least, I thank my parents for their unconditional love and support.

Bibliography

[4] S. Hatakeyama, "TRIM family proteins: Roles in autophagy, immunity, and carcinogenesis," *Trends Biochem. Sci.*, vol. 42, pp. 297–311, Apr 2017.

[5] C. Langevin, J.-P. Levraud, and P. Boudinot, "Fish antiviral tripartite motif (TRIM) proteins," *Fish Shellfish Immunol.*, vol. 86, pp. 724 – 733, 2019.

[6] A. Reymond, G. Meroni, A. Fantozzi, G. Merla, S. Cairo, L. Luzi, D. Riganelli, E. Zanaria, S. Messali, S. Cainarca, A. Guffanti, S. Minucci, P. G. Pelicci, and A. Ballabio, "The tripartite motif family identifies cell compartments," *EMBO J.*, vol. 20, pp. 2140–2151, 05 2001.

[7] Y. Chu and X. Yang, "SUMO E3 ligase activity of TRIM proteins," *Oncogene*, vol. 30, p. 1108, 10 2010.

[8] Q. Liang, H. Deng, X. Li, X. Wu, Q. Tang, T.-H. Chang, H. Peng, r. Rauscher, Frank J, K. Ozato, and F. Zhu, "Tripartite motif-containing protein 28 is a small ubiquitin-related modifier E3 ligase and negative regulator of IFN regulatory factor 7," *J. Immunol.*, vol. 187, pp. 4754–4763, 11 2011.

[9] M. Martin-Vicente, L. M. Medrano, S. Resino, A. Garcia-Sastre, and I. Martinez, "TRIM25 in the regulation of the antiviral innate immunity," *Front. Immunol.*, vol. 8, p. 1187, 2017.

[10] M. G. Koliopoulos, M. Lethier, A. G. van der Veen, K. Haubrich, J. Hennig, E. Kowalinski, R. V. Stevens, S. R. Martin, C. Reis e Sousa, S. Cusack, and K. Rittinger, "Molecular mechanism of influenza A NS1-mediated TRIM25 recognition and inhibition," *Nat. Commun.*, vol. 9, no. 1, p. 1820, 2018.

[11] M. Lim, J. A. Newman, H. L. Williams, L. Masino, H. Aitkenhead, A. E. Gravard, O. Gileadi, and J. Q. Svejstrup, "A ubiquitin-binding domain that binds a structural fold distinct from that of ubiquitin.," *Structure*, vol. 27, pp. 1316–1325, Aug 2019.

[12] F. Diaz-Griffero, X. Li, H. Javanbakht, B. Song, S. Welikala, M. Stremlau, and J. Sodroski, "Rapid turnover and polyubiquitylation of the retroviral restriction factor TRIM5," *Virology*, vol. 349, pp. 300–315, Jun 2006.

[13] X. Li and J. Sodroski, "The TRIM5alpha B-box 2 domain promotes cooperative binding to the retroviral capsid by mediating higher-order self-association," *J. Virol.*, vol. 82, pp. 11495–11502, Dec 2008.

[14] C. Dickson, A. J. Fletcher, M. Vaysburd, J.-C. Yang, D. L. Mallery, J. Zeng, C. M. Johnson, S. H. McLaughlin, M. Skehel, S. Maslen, J. Cruickshank, N. Huguenin-Dezot, J. W. Chin, D. Neuhaus, and L. C. James, "Intracellular antibody signalling is regulated by phosphorylation of the Fc receptor TRIM21," *eLife*, vol. 7, p. e32660, 04 2018.

[15] M. Sardiello, S. Cairo, B. Fontanella, A. Ballabio, and G. Meroni, "Genomic analysis of the TRIM family reveals two groups of genes with distinct evolutionary properties," *BMC Evol. Biol.*, vol. 8, no. 1, p. 225, 2008.

[16] J. Hennig, A. Bresell, M. Sandberg, K. D. M. Hennig, M. Wahren-Herlenius, B. Persson, and M. Sunnerhagen, "The fellowship of the RING: the RING-B-box linker region interacts with the RING in TRIM21/ro52, contains a native autoantigenic epitope in sjogren syndrome, and is an integral and conserved region in TRIM proteins," *J. Mol. Biol.*, vol. 377, pp. 431–449, Mar 2008.

[17] F. P. Williams, K. Haubrich, C. Perez-Borrajero, and J. Hennig, "Emerging RNA-binding roles in the TRIM family of ubiquitin ligases.," *Biol Chem*, vol. 400, pp. 1443–1464, Oct 2019.

[18] K. M. Short and T. C. Cox, "Subclassification of the RBCC/TRIM superfamily reveals a novel motif necessary for microtubule binding," *J. Biol. Chem.*, vol. 281, pp. 8970–8980, Mar 2006.

[19] K. Ozato, D.-M. Shin, T.-H. Chang, and r. Morse, Herbert C, "TRIM family proteins and their emerging roles in innate immunity," *Nat. Rev. Immunol.*, vol. 8, pp. 849–860, 11 2008.

[20] I. Marín, "Origin and diversification of TRIM ubiquitin ligases," *PLoS ONE*, vol. 7, p. e50030, 11 2012.

[21] M. U. Gack, Y. C. Shin, C.-H. Joo, T. Urano, C. Liang, L. Sun, O. Takeuchi, S. Akira, Z. Chen, S. Inoue, and J. U. Jung, "TRIM25 RING-finger E3 ubiquitin

ligase is essential for RIG-I-mediated antiviral activity," *Nature*, vol. 446, p. 916, 03 2007.

[22] N. Biris, A. Tomashevski, A. Bhattacharya, F. Diaz-Griffero, and D. N. Ivanov, "Rhesus monkey TRIM5alpha SPRY domain recognizes multiple epitopes that span several capsid monomers on the surface of the HIV-1 mature viral core," *J. Mol. Biol.*, vol. 425, pp. 5032–5044, Dec 2013.

[23] J. Zhang, C. Zhang, J. Cui, J. Ou, J. Han, Y. Qin, F. Zhi, and R.-F. Wang, "TRIM45 functions as a tumor suppressor in the brain via its E3 ligase activity by stabilizing p53 through K63-linked ubiquitination," *Cell Death Dis.*, vol. 8, p. e2831, May 2017.

[24] A. Rybak, H. Fuchs, K. Hadian, L. Smirnova, E. A. Wulczyn, G. Michel, R. Nitsch, D. Krappmann, and F. G. Wulczyn, "The let-7 target gene mouse lin-41 is a stem cell specific E3 ubiquitin ligase for the miRNA pathway protein Ago2," *Nat. Cell Biol.*, vol. 11, pp. 1411–1420, Dec 2009.

[25] Y. Zou, H. Chiu, A. Zinovyeva, V. Ambros, C.-F. Chuang, and C. Chang, "Developmental decline in neuronal regeneration by the progressive change of two intrinsic timers," *Science*, vol. 340, pp. 372–376, Apr 2013.

[26] R. V. Stevens, D. Esposito, and K. Rittinger, "Characterisation of class VI TRIM RING domains: linking RING activity to C-terminal domain identity," *Life Science Alliance*, vol. 2, no. 3, 2019.

[27] M. Akutsu, I. Dikic, and A. Bremm, "Ubiquitin chain diversity at a glance," *J. Cell Sci.*, vol. 129, p. 875, 03 2016.

[28] P. Grumati and I. Dikic, "Ubiquitin signaling and autophagy," *Journal of Biological Chemistry*, vol. 293, pp. 5404–5413, 04 2018.

[29] J. F. Linares, A. Duran, T. Yajima, M. Pasparakis, J. Moscat, and M. T. Diaz-Meco, "K63 polyubiquitination and activation of mtor by the p62-TRAF6 complex in nutrient-activated cells," *Molecular Cell*, vol. 51, no. 3, pp. 283 – 296, 2013.

[30] D. Komander and M. Rape, "The ubiquitin code," *Annual Review of Biochemistry*, vol. 81, pp. 203–229, 2020/01/23 2012.

[31] J. Jin, X. Li, S. P. Gygi, and J. W. Harper, "Dual E1 activation systems for ubiquitin differentially regulate E2 enzyme charging," *Nature*, vol. 447, pp. 1135 EP –, 06 2007.

[32] Y. Ye and M. Rape, "Building ubiquitin chains: E2 enzymes at work," *Nature reviews. Molecular cell biology*, vol. 10, pp. 755–764, 11 2009.

[33] W. Li, M. H. Bengtson, A. Ulbrich, A. Matsuda, V. A. Reddy, A. Orth, S. K. Chanda, S. Batalov, and C. A. P. Joazeiro, "Genome-wide and functional annotation of human E3 ubiquitin ligases identifies MULAN, a mitochondrial E3 that regulates the organelle's dynamics and signaling.," *PLoS One*, vol. 3, p. e1487, Jan 2008.

[34] L. Buetow and D. T. Huang, "Structural insights into the catalysis and regulation of E3 ubiquitin ligases," *Nat. Rev. Mol. Cell Biol.*, vol. 17, pp. 626–642, Oct 2016.

[35] F. Cano, D. Miranda-Saavedra, and P. J. Lehner, "RNA-binding E3 ubiquitin ligases: novel players in nucleic acid regulation.," *Biochem Soc Trans*, vol. 38, pp. 1621–1626, Dec 2010.

[36] F. Cano, H. Bye, L. M. Duncan, K. Buchet-Poyau, M. Billaud, M. R. Wills, and P. J. Lehner, "The RNA-binding E3 ubiquitin ligase MEX-3C links ubiquitination with MHC-I mRNA degradation," *EMBO J.*, vol. 31, pp. 3596–3606, 08 2012.

[37] Q. Zhang, L. Fan, F. Hou, A. Dong, Y.-X. Wang, and Y. Tong, "New insights into the RNA-binding and E3 ubiquitin ligase activities of Roquins," *Sci. Rep.*, vol. 5, p. 15660, 10 2015.

[38] S. C. Kwon, H. Yi, K. Eichelbaum, S. Föhr, B. Fischer, K. T. You, A. Castello, J. Krijgsveld, M. W. Hentze, and V. N. Kim, "The RNA-binding protein repertoire of embryonic stem cells," *Nat. Struct. Mol. Biol.*, vol. 20, p. 1122, 08 2013.

[39] R. A. Fridell, L. S. Harding, H. P. Bogerd, and B. R. Cullen, "Identification of a novel human zinc finger protein that specifically interacts with the activation domain of lentiviral Tat proteins," *Virology*, vol. 209, pp. 347–357, Jun 1995.

[40] F. J. Slack, M. Basson, Z. Liu, V. Ambros, H. R. Horvitz, and G. Ruvkun, "The lin-41 RBCC gene acts in the c. elegans heterochronic pathway between the let-7 regulatory RNA and the LIN-29 transcription factor," *Mol. Cell*, vol. 5, pp. 659–669, Apr 2000.

[41] J. Sonoda and R. P. Wharton, "Drosophila Brain Tumor is a translational repressor," *Genes Dev.*, vol. 15, pp. 762–773, Mar 2001.

[42] A. G. Baltz, M. Munschauer, B. Schwanhäusser, A. Vasile, Y. Murakawa, M. Schueler, N. Youngs, D. Penfold-Brown, K. Drew, M. Milek, E. Wyler, R. Bon-

neau, M. Selbach, C. Dieterich, and M. Landthaler, "The mRNA-bound proteome and its global occupancy profile on protein-coding transcripts," *Mol. Cell*, vol. 46, no. 5, pp. 674 – 690, 2012.

[43] A. Castello, B. Fischer, K. Eichelbaum, R. Horos, B. M. Beckmann, C. Strein, N. E. Davey, D. T. Humphreys, T. Preiss, L. M. Steinmetz, J. Krijgsveld, and M. W. Hentze, "Insights into RNA biology from an atlas of mammalian mRNA-binding proteins," *Cell*, vol. 149, no. 6, pp. 1393 – 1406, 2012.

[44] J. Trendel, T. Schwarzl, R. Horos, A. Prakash, A. Bateman, M. W. Hentze, and J. Krijgsveld, "The human RNA-binding proteome and its dynamics during translational arrest," *Cell*, vol. 176, no. 1, pp. 391–403.e19, 2019.

[45] S. Li, L. Wang, B. Fu, and M. E. Dorf, "TRIM65: A cofactor for regulation of the microRNA pathway," *RNA Biol.*, vol. 11, no. 9, pp. 1113–1121, 2014.

[46] T. Treiber, N. Treiber, U. Plessmann, S. Harlander, J.-L. Daiß, N. Eichner, G. Lehmann, K. Schall, H. Urlaub, and G. Meister, "A compendium of RNA-binding proteins that regulate microRNA biogenesis," *Mol. Cell*, vol. 66, no. 2, pp. 270–284.e13, 2017.

[47] I. Loedige, D. Gaidatzis, R. Sack, G. Meister, and W. Filipowicz, "The mammalian TRIM-NHL protein TRIM71/LIN-41 is a repressor of mRNA function," *Nucleic Acids Res.*, vol. 41, pp. 518–532, 01 2013.

[48] I. Loedige, M. Stotz, S. Qamar, K. Kramer, J. Hennig, T. Schubert, P. Loffler, G. Langst, R. Merkl, H. Urlaub, and G. Meister, "The NHL domain of BRAT is an RNA-binding domain that directly contacts the hunchback mRNA for regulation," *Genes Dev.*, vol. 28, pp. 749–764, Apr 2014.

[49] R. A. Neumuller, J. Betschinger, A. Fischer, N. Bushati, I. Poernbacher, K. Mechtler, S. M. Cohen, and J. A. Knoblich, "Mei-P26 regulates microRNAs and cell growth in the Drosophila ovarian stem cell lineage," *Nature*, vol. 454, pp. 241–245, Jul 2008.

[50] C. M. Hammell, I. Lubin, P. R. Boag, T. K. Blackwell, and V. Ambros, "nhl-2 modulates microRNA activity in Caenorhabditis elegans," *Cell*, vol. 136, pp. 926–938, Mar 2009.

[51] F. Aeschimann, P. Kumari, H. Bartake, D. Gaidatzis, L. Xu, R. Ciosk, and H. Grosshans, "LIN41 post-transcriptionally silences mRNAs by two distinct and

position-dependent mechanisms," *Mol. Cell*, vol. 65, pp. 476–489, Feb 2017.

[52] J. C. Schwamborn, E. Berezikov, and J. A. Knoblich, "The TRIM-NHL protein TRIM32 activates microRNAs and prevents self-renewal in mouse neural progenitors," *Cell*, vol. 136, pp. 913–925, Mar 2009.

[53] B. Liu, N. L. Li, Y. Shen, X. Bao, T. Fabrizio, H. Elbahesh, R. J. Webby, and K. Li, "The C-terminal tail of TRIM56 dictates antiviral restriction of influenza a and b viruses by impeding viral RNA synthesis," *J. Virol.*, vol. 90, pp. 4369–4382, May 2016.

[54] J. D. Laver, X. Li, D. Ray, K. B. Cook, N. A. Hahn, S. Nabeel-Shah, M. Kekis, H. Luo, A. J. Marsolais, K. Y. Fung, T. R. Hughes, J. T. Westwood, S. S. Sidhu, Q. Morris, H. D. Lipshitz, and C. A. Smibert, "Brain tumor is a sequence-specific RNA-binding protein that directs maternal mRNA clearance during the Drosophila maternal-to-zygotic transition," *Genome Biol.*, vol. 16, p. 94, May 2015.

[55] I. Loedige, L. Jakob, T. Treiber, D. Ray, M. Stotz, N. Treiber, J. Hennig, K. B. Cook, Q. Morris, T. R. Hughes, J. C. Engelmann, M. P. Krahn, and G. Meister, "The crystal structure of the NHL domain in complex with RNA reveals the molecular basis of Drosophila brain-tumor-mediated gene regulation," *Cell Rep.*, vol. 13, pp. 1206–1220, Nov 2015.

[56] P. Kumari, F. Aeschimann, D. Gaidatzis, J. J. Keusch, P. Ghosh, A. Neagu, K. Pachulska-Wieczorek, J. M. Bujnicki, H. Gut, H. Grosshans, and R. Ciosk, "Evolutionary plasticity of the NHL domain underlies distinct solutions to RNA recognition," *Nat. Commun.*, vol. 9, p. 1549, Apr 2018.

[57] L. Du Pasquier, "Fish 'n' TRIMs," *J. Biol.*, vol. 8, no. 5, p. 50, 2009.

[58] S. Nisole, J. P. Stoye, and A. Saib, "TRIM family proteins: retroviral restriction and antiviral defence," *Nat. Rev. Microbiol.*, vol. 3, pp. 799–808, Oct 2005.

[59] B. K. Ganser-Pornillos, V. Chandrasekaran, O. Pornillos, J. G. Sodroski, W. I. Sundquist, and M. Yeager, "Hexagonal assembly of a restricting TRIM5alpha protein," *Proc. Natl. Acad. Sci. U.S.A.*, vol. 108, p. 534, 01 2011.

[60] M. Vaysburd, R. E. Watkinson, H. Cooper, M. Reed, K. O'Connell, J. Smith, J. Cruickshanks, and L. C. James, "Intracellular antibody receptor TRIM21 prevents fatal viral infection," *Proc. Natl. Acad. Sci. U.S.A.*, vol. 110, no. 30, pp. 12397–12401, 2013.

[61] D. Clift, C. So, W. A. McEwan, L. C. James, and M. Schuh, "Acute and rapid degradation of endogenous proteins by trim-away," *Nature Protocols*, vol. 13, no. 10, pp. 2149–2175, 2018.

[62] M. F. Caratozzolo, F. Marzano, F. Mastropasqua, E. Sbisà, and A. Tullo, "TRIM8: Making the right decision between the oncogene and tumour suppressor role," *Genes*, vol. 8, p. 354, 11 2017.

[63] L. A. Walsh, M. J. Alvarez, E. Y. Sabio, M. Reyngold, V. Makarov, S. Mukherjee, K.-W. Lee, A. Desrichard, Ş. Turcan, M. G. Dalin, V. K. Rajasekhar, S. Chen, L. T. Vahdat, A. Califano, and T. A. Chan, "An Integrated Systems Biology Approach Identifies TRIM25 as a Key Determinant of Breast Cancer Metastasis," *Cell Rep.*, vol. 20, pp. 1623–1640, 2018/01/04 2017.

[64] S. Li, L. Wang, B. Fu, M. A. Berman, A. Diallo, and M. E. Dorf, "Trim65 regulates microrna activity by ubiquitination of tnrc6," *Proceedings of the National Academy of Sciences*, vol. 111, no. 19, pp. 6970–6975, 2014.

[65] A. A. D'Cruz, N. J. Kershaw, J. J. Chiang, M. K. Wang, N. A. Nicola, J. J. Babon, M. U. Gack, and S. E. Nicholson, "Crystal structure of the TRIM25 B30.2 (pryspry) domain: a key component of antiviral signalling," *Biochemical Journal*, vol. 456, p. 231, 12 2013.

[66] J.-S. Woo, H.-Y. Suh, S.-Y. Park, and B.-H. Oh, "Structural basis for protein recognition by B30.2/SPRY domains," *Mol. Cell*, vol. 24, pp. 967–976, Dec 2006.

[67] A. H. Keeble, Z. Khan, A. Forster, and L. C. James, "TRIM21 is an IgG receptor that is structurally, thermodynamically, and kinetically conserved," *Proc. Natl. Acad. Sci. U.S.A.*, vol. 105, pp. 6045–6050, 04 2008.

[68] N. Biris, Y. Yang, A. B. Taylor, A. Tomashevski, M. Guo, P. J. Hart, F. Diaz-Griffero, and D. N. Ivanov, "Structure of the rhesus monkey TRIM5alpha PRYSPRY domain, the HIV capsid recognition module," *Proc. Natl. Acad. Sci. U.S.A.*, vol. 109, no. 33, pp. 13278–13283, 2012.

[69] S. Inoue, A. Orimo, T. Hosoi, S. Kondo, H. Toyoshima, T. Kondo, A. Ikegami, Y. Ouchi, H. Orimo, and M. Muramatsu, "Genomic binding-site cloning reveals an estrogen-responsive gene that encodes a ring finger protein," *Proceedings of the National Academy of Sciences*, vol. 90, pp. 11117–11121, 12 1993.

[70] K. Ikeda, A. Orimo, Y. Higashi, M. Muramatsu, and S. Inoue, "Efp as a primary

estrogen-responsive gene in human breast cancer," *FEBS Lett.*, vol. 472, no. 1, pp. 9–13, 2000.

[71] S. D. Thomson, S. Ali, L. Pickles, J. Taylor, P. E. Pace, M. Lymboura, S. Shousha, and R. C. Coombes, "Analysis of estrogen-responsive finger protein expression in benign and malignant human breast.," *Int J Cancer*, vol. 91, pp. 152–158, Jan 2001.

[72] T. Suzuki, T. Urano, T. Tsukui, K. Horie-Inoue, T. Moriya, T. Ishida, M. Muramatsu, Y. Ouchi, H. Sasano, and S. Inoue, "Estrogen-responsive finger protein as a new potential biomarker for breast cancer.," *Clin Cancer Res*, vol. 11, pp. 6148–6154, Sep 2005.

[73] A. Orimo, S. Inoue, O. Minowa, N. Tominaga, Y. Tomioka, M. Sato, J. Kuno, H. Hiroi, Y. Shimizu, M. Suzuki, T. Noda, and M. Muramatsu, "Underdeveloped uterus and reduced estrogen responsiveness in mice with disruption of the estrogen-responsive finger protein gene, which is a direct target of estrogen receptor alpha," *Proc. Natl. Acad. Sci. U.S.A.*, vol. 96, pp. 12027–12032, 10 1999.

[74] T. Urano, T. Saito, T. Tsukui, M. Fujita, T. Hosoi, M. Muramatsu, Y. Ouchi, and S. Inoue, "Efp targets 14-3-3 sigma for proteolysis and promotes breast tumour growth.," *Nature*, vol. 417, pp. 871–875, Jun 2002.

[75] X.-Y. Dong, X. Fu, S. Fan, P. Guo, D. Su, X. Sun, and J.-T. Dong, "Estrogen causes ATBF1 protein degradation through the estrogen-responsive E3 ubiquitin ligase EFP," *The Biochemical journal*, vol. 444, pp. 581–590, 06 2012.

[76] S. Wang, R. K. Kollipara, C. G. Humphries, S.-H. Ma, R. Hutchinson, R. Li, J. Siddiqui, S. A. Tomlins, G. V. Raj, and R. Kittler, "The ubiquitin ligase trim25 targets erg for degradation in prostate cancer," *Oncotarget*, vol. 7, pp. 64921–64931, 10 2016.

[77] K. Horie, T. Urano, K. Ikeda, and S. Inoue, "Estrogen-responsive RING finger protein controls breast cancer growth," *The Journal of steroid biochemistry and molecular biology*, vol. 85, pp. 101—104, June 2003.

[78] H. Mao, Y. Du, Z. Zhang, B. Cao, J. Zhao, H. Zhou, and X. Mao, "Nitroxoline shows antimyeloma activity by targeting the TRIM25/p53 axle.," *Anticancer Drugs*, vol. 28, pp. 376–383, Apr 2017.

[79] M. Okamoto, T. Kouwaki, Y. Fukushima, and H. Oshiumi, "Regulation of RIG-

I activation by K63-linked polyubiquitination," *Frontiers in immunology*, vol. 8, pp. 1942–1942, 01 2018.

[80] D. Kolakofsky, E. Kowalinski, and S. Cusack, "A structure-based model of RIG-I activation," *RNA*, vol. 18, pp. 2118–2127, Dec 2012.

[81] A. Peisley, B. Wu, H. Xu, Z. J. Chen, and S. Hur, "Structural basis for ubiquitin-mediated antiviral signal activation by RIG-I," *Nature*, vol. 509, pp. 110–114, 05 2014.

[82] F. Hou, L. Sun, H. Zheng, B. Skaug, Q.-X. Jiang, and Z. J. Chen, "MAVS forms functional prion-like aggregates to activate and propagate antiviral innate immune response," *Cell*, vol. 146, pp. 448–461, Aug 2011.

[83] C. Castanier, N. Zemirli, A. Portier, D. Garcin, N. Bidere, A. Vazquez, and D. Arnoult, "MAVS ubiquitination by the E3 ligase TRIM25 and degradation by the proteasome is involved in type I interferon production after activation of the antiviral RIG-I-like receptors," *BMC Biol.*, vol. 10, p. 44, May 2012.

[84] W. Zeng, L. Sun, X. Jiang, X. Chen, F. Hou, A. Adhikari, M. Xu, and Z. J. Chen, "Reconstitution of the RIG-I pathway reveals a signaling role of unanchored polyubiquitin chains in innate immunity," *Cell*, vol. 141, pp. 315–330, 04 2010.

[85] H. Oshiumi, M. Matsumoto, S. Hatakeyama, and T. Seya, "Riplet/RNF135, a RING finger protein, ubiquitinates RIG-I to promote interferon-beta induction during the early phase of viral infection," *Journal of Biological Chemistry*, vol. 284, pp. 807–817, 01 2009.

[86] K. Kuniyoshi, O. Takeuchi, S. Pandey, T. Satoh, H. Iwasaki, S. Akira, and T. Kawai, "Pivotal role of RNA-binding E3 ubiquitin ligase MEX3C in RIG-I-mediated antiviral innate immunity," *Proceedings of the National Academy of Sciences*, vol. 111, p. 5646, 04 2014.

[87] J. Yan, Q. Li, A.-P. Mao, M.-M. Hu, and H.-B. Shu, "TRIM4 modulates type I interferon induction and cellular antiviral response by targeting RIG-I for K63-linked ubiquitination," *Journal of Molecular Cell Biology*, vol. 6, pp. 154–163, 04 2014.

[88] T. J. Hayman, A. C. Hsu, T. B. Kolesnik, L. F. Dagley, J. Willemsen, M. D. Tate, P. J. Baker, N. J. Kershaw, L. Kedzierski, A. I. Webb, P. A. Wark, K. Kedzierska, S. L. Masters, G. T. Belz, M. Binder, P. M. Hansbro, N. A. Nicola, and

S. E. Nicholson, "RIPLET, and not TRIM25, is required for endogenous RIG-I-dependent antiviral responses.," *Immunol Cell Biol*, vol. 97, pp. 840–852, Oct 2019.

[89] M. U. Gack, R. A. Albrecht, T. Urano, K.-S. Inn, I.-C. Huang, E. Carnero, M. Farzan, S. Inoue, J. U. Jung, and A. García-Sastre, "Influenza A virus NS1 targets the ubiquitin ligase TRIM25 to evade recognition by RIG-I," *Cell host & microbe*, vol. 5, pp. 439–449, 05 2009.

[90] G. Manokaran, E. Finol, C. Wang, J. Gunaratne, J. Bahl, E. Z. Ong, H. C. Tan, O. M. Sessions, A. M. Ward, D. J. Gubler, E. Harris, M. A. Garcia-Blanco, and E. E. Ooi, "Dengue subgenomic RNA binds TRIM25 to inhibit interferon expression for epidemiological fitness," *Science*, vol. 350, pp. 217–221, 10 2015.

[91] Y. Hu, W. Li, T. Gao, Y. Cui, Y. Jin, P. Li, Q. Ma, X. Liu, and C. Cao, "The Severe Acute Respiratory Syndrome Coronavirus nucleocapsid inhibits type I interferon production by interfering with TRIM25-mediated RIG-I ubiquitination.," *J Virol*, vol. 91, Apr 2017.

[92] S. Gupta, P. Yla-Anttila, S. Callegari, M.-H. Tsai, H.-J. Delecluse, and M. G. Masucci, "Herpesvirus deconjugases inhibit the IFN response by promoting TRIM25 autoubiquitination and functional inactivation of the RIG-I signalosome.," *PLoS Pathog*, vol. 14, p. e1006852, Jan 2018.

[93] M. T. Sanchez-Aparicio, L. J. Feinman, A. Garcia-Sastre, and M. L. Shaw, "Paramyxovirus V proteins interact with the RIG-I/TRIM25 regulatory complex and inhibit RIG-I signaling.," *J Virol*, Jan 2018.

[94] Y. Qin, H. Cui, and H. Zhang, "Overexpression of TRIM25 in lung cancer regulates tumor cell progression.," *Technol Cancer Res Treat*, vol. 15, pp. 707–715, Oct 2016.

[95] K.-I. Takayama, T. Suzuki, T. Tanaka, T. Fujimura, S. Takahashi, T. Urano, K. Ikeda, and S. Inoue, "TRIM25 enhances cell growth and cell survival by modulating p53 signals via interaction with G3BP2 in prostate cancer," *Oncogene*, vol. 37, pp. 2165–2180, Apr 2018.

[96] F. Cao, D.-P. Li, L. Wang, M. Li, H. Zhang, and M. Tao, "TRIM25 promotes oncogenic activities through regulation of ZEB1 in breast cancer," *International Journal of Clinical and Experimental Pathology*, vol. 9, pp. 9751–9760, 01 2016.

[97] N.-R. Lee, J.-Y. Choi, I.-H. Yoon, J. K. Lee, and K.-S. Inn, "Positive regula-

tory role of c-Src-mediated TRIM25 tyrosine phosphorylation on RIG-I ubiquitination and RIG-I-mediated antiviral signaling pathway," *Cell. Immunol.*, vol. 332, pp. 94—100, October 2018.

[98] W. Zou and D.-E. Zhang, "The interferon-inducible ubiquitin-protein isopeptide ligase (E3) EFP also functions as an ISG15 E3 ligase.," *J Biol Chem*, vol. 281, pp. 3989–3994, Feb 2006.

[99] N. Sun, Y. Xue, T. Dai, X. Li, and N. Zheng, "Tripartite motif containing 25 promotes proliferation and invasion of colorectal cancer cells through TGF-beta signaling," *Bioscience reports*, vol. 37, p. BSR20170805, 07 2017.

[100] N. R. Choudhury, J. S. Nowak, J. Zuo, J. Rappsilber, S. H. Spoel, and G. Michlewski, "TRIM25 Is an RNA-Specific Activator of Lin28a/TuT4-Mediated Uridylation," *Cell Rep.*, vol. 9, pp. 1265–1272, 11 2014.

[101] M. U. Gack, A. Kirchhofer, Y. C. Shin, K.-S. Inn, C. Liang, S. Cui, S. Myong, T. Ha, K.-P. Hopfner, and J. U. Jung, "Roles of RIG-I N-terminal tandem CARD and splice variant in TRIM25-mediated antiviral signal transduction," *Proceedings of the National Academy of Sciences*, vol. 105, p. 16743, 10 2008.

[102] J. G. Sanchez, K. M. J. Sparrer, C. Chiang, R. A. Reis, J. J. Chiang, M. A. Zurenski, Y. Wan, M. U. Gack, and O. Pornillos, "TRIM25 binds RNA to modulate cellular anti-viral defense," *J. Mol. Biol.*, vol. 430, pp. 5280–5293, 2018.

[103] X. Zheng, X. Wang, F. Tu, Q. Wang, Z. Fan, and G. Gao, "TRIM25 is required for the antiviral activity of zinc finger antiviral protein.," *J Virol*, vol. 91, May 2017.

[104] M. M. H. Li, Z. Lau, P. Cheung, E. G. Aguilar, W. M. Schneider, L. Bozzacco, H. Molina, E. Buehler, A. Takaoka, C. M. Rice, D. P. Felsenfeld, and M. R. MacDonald, "TRIM25 enhances the antiviral action of Zinc-Finger Antiviral Protein (ZAP)," *PLoS Pathog.*, vol. 13, p. e1006145, Jan 2017.

[105] N. R. Choudhury, G. Heikel, M. Trubitsyna, P. Kubik, J. S. Nowak, S. Webb, S. Granneman, C. Spanos, J. Rappsilber, A. Castello, and G. Michlewski, "RNA-binding activity of TRIM25 is mediated by its PRY/SPRY domain and is required for ubiquitination," *BMC Biol.*, vol. 15, p. 105, 2017.

[106] N. R. Meyerson, L. Zhou, Y. R. Guo, C. Zhao, Y. J. Tao, R. M. Krug, and S. L. Sawyer, "Nuclear TRIM25 specifically targets influenza virus ribonucleoproteins to

block the onset of RNA chain elongation," *Cell Host Microbe*, vol. 22, pp. 627–638, Nov 2017.

[107] M. T. Sánchez-Aparicio, J. Ayllón, A. Leo-Macias, T. Wolff, A. García-Sastre, and M. S. Diamond, "Subcellular localizations of rig-i, trim25, and mavs complexes," *Journal of Virology*, vol. 91, pp. e01155–16, 01 2017.

[108] W. Zou, J. Wang, and D.-E. Zhang, "Negative regulation of isg15 e3 ligase efp through its autoisgylation.," *Biochem Biophys Res Commun*, vol. 354, pp. 321–327, Mar 2007.

[109] F. El-Asmi, F. P. McManus, C. E. B. de Carvalho, J. C. Valle-Casuso, P. Thibault, and M. K. Chelbi-Alix, "Cross-talk between SUMOylation and ISGylation in response to interferon," *Cytokine*, vol. 129, p. 155025, 2020.

[110] A. A. D'Cruz, N. J. Kershaw, T. J. Hayman, E. M. Linossi, J. J. Chiang, M. K. Wang, L. F. Dagley, T. B. Kolesnik, J.-G. Zhang, S. L. Masters, M. D. Griffin, M. U. Gack, J. M. Murphy, N. A. Nicola, J. J. Babon, and S. E. Nicholson, "Identification of a second binding site on the TRIM25 B30.2 domain," *Biochemical Journal*, 12 2017.

[111] A. Castello, B. Fischer, C. K. Frese, R. Horos, A.-M. Alleaume, S. Foehr, T. Curk, J. Krijgsveld, and M. W. Hentze, "Comprehensive identification of RNA-binding domains in human cells," *Mol. Cell*, vol. 63, pp. 696–710, Aug 2016.

[112] A. A. Hyman, C. A. Weber, and F. Julicher, "Liquid-liquid phase separation in biology.," *Annu Rev Cell Dev Biol*, vol. 30, pp. 39–58, 2014.

[113] M. G. Koliopoulos, D. Esposito, E. Christodoulou, I. A. Taylor, and K. Rittinger, "Functional role of TRIM E3 ligase oligomerization and regulation of catalytic activity," *EMBO J.*, vol. 35, pp. 1204–1218, Jun 2016.

[114] P. Wang, S. Benhenda, H. Wu, V. Lallemand-Breitenbach, T. Zhen, F. Jollivet, L. Peres, Y. Li, S.-J. Chen, Z. Chen, H. de Thé, and G. Meng, "RING tetramerization is required for nuclear body biogenesis and PML sumoylation," *Nat. Commun.*, vol. 9, no. 1, p. 1277, 2018.

[115] J. W. Gibbs, "On the equilibrium of heterogeneous substances," *American Journal of Science*, vol. Series 3 Vol. 16, pp. 441–458, 12 1878.

[116] A. C. Dumetz, A. M. Chockla, E. W. Kaler, and A. M. Lenhoff, "Protein phase behavior in aqueous solutions: crystallization, liquid-liquid phase separation, gels,

and aggregates," *Biophys. J.*, vol. 94, pp. 570–583, Jan 2008.

[117] P. Li, S. Banjade, H.-C. Cheng, S. Kim, B. Chen, L. Guo, M. Llaguno, J. V. Hollingsworth, D. S. King, S. F. Banani, P. S. Russo, Q.-X. Jiang, B. T. Nixon, and M. K. Rosen, "Phase transitions in the assembly of multivalent signalling proteins," *Nature*, vol. 483, pp. 336–340, 03 2012.

[118] K. E. Handwerger, J. A. Cordero, and J. G. Gall, "Cajal bodies, nucleoli, and speckles in the xenopus oocyte nucleus have a low-density, sponge-like structure.," *Mol Biol Cell*, vol. 16, pp. 202–211, Jan 2005.

[119] Y.-C. M. Chen, C. Kappel, J. Beaudouin, R. Eils, and D. L. Spector, "Live cell dynamics of promyelocytic leukemia nuclear bodies upon entry into and exit from mitosis.," *Mol Biol Cell*, vol. 19, pp. 3147–3162, Jul 2008.

[120] C. P. Brangwynne, C. R. Eckmann, D. S. Courson, A. Rybarska, C. Hoege, J. Gharakhani, F. Julicher, and A. A. Hyman, "Germline p granules are liquid droplets that localize by controlled dissolution/condensation.," *Science*, vol. 324, pp. 1729–1732, Jun 2009.

[121] C. P. Brangwynne, T. J. Mitchison, and A. A. Hyman, "Active liquid-like behavior of nucleoli determines their size and shape in *Xenopus laevis* oocytes," *Proceedings of the National Academy of Sciences of the United States of America*, vol. 108, pp. 4334–4339, 03 2011.

[122] S. Kroschwald, S. Maharana, D. Mateju, L. Malinovska, E. Nüske, I. Poser, D. Richter, and S. Alberti, "Promiscuous interactions and protein disaggregases determine the material state of stress-inducible rnp granules," *eLife*, vol. 4, pp. e06807–e06807, 08 2015.

[123] S. F. Banani, H. O. Lee, A. A. Hyman, and M. K. Rosen, "Biomolecular condensates: organizers of cellular biochemistry," *Nat. Rev. Mol. Cell Biol.*, vol. 18, pp. 285–298, May 2017.

[124] J. A. Dyck, G. G. Maul, W. H. J. Miller, J. D. Chen, A. Kakizuka, and R. M. Evans, "A novel macromolecular structure is a target of the promyelocyte-retinoic acid receptor oncoprotein," *Cell*, vol. 76, pp. 333–343, Jan 1994.

[125] F. van den Ent and J. Lowe, "Rf cloning: a restriction-free method for inserting target genes into plasmids.," *J Biochem Biophys Methods*, vol. 67, pp. 67–74, Apr 2006.

[126] A. de Marco, E. Deuerling, A. Mogk, T. Tomoyasu, and B. Bukau, "Chaperone-based procedure to increase yields of soluble recombinant proteins produced in e. coli," *BMC biotechnology*, vol. 7, pp. 32–32, 06 2007.

[127] U. K. Laemmli, "Cleavage of structural proteins during the assembly of the head of bacteriophage T4," *Nature*, vol. 227, no. 5259, pp. 680–685, 1970.

[128] W. Abdulrahman, L. Radu, F. Garzoni, O. Kolesnikova, K. Gupta, J. Osz-Papai, I. Berger, and A. Poterszman, *The Production of Multiprotein Complexes in Insect Cells Using the Baculovirus Expression System*, pp. 91–114. New York, NY: Springer New York, 2015.

[129] L. Freiburger, M. Sonntag, J. Hennig, J. Li, P. Zou, and M. Sattler, "Efficient segmental isotope labeling of multi-domain proteins using Sortase A," *Journal of biomolecular NMR*, vol. 63, pp. 1—8, September 2015.

[130] A. F. Carvalho, M. P. Pinto, C. P. Grou, R. Vitorino, P. Domingues, F. Yamao, C. Sá-Miranda, and J. E. Azevedo, "High-yield expression in *Escherichia coli* and purification of mouse ubiquitin-activating enzyme E1," *Molecular Biotechnology*, vol. 51, no. 3, pp. 254–261, 2012.

[131] M. R. Wilkins, E. Gasteiger, A. Bairoch, J. C. Sanchez, K. L. Williams, R. D. Appel, and D. F. Hochstrasser, "Protein identification and analysis tools in the ExPASy server.," *Methods Mol Biol*, vol. 112, pp. 531–552, 1999.

[132] F. Delaglio, S. Grzesiek, G. W. Vuister, G. Zhu, J. Pfeifer, and A. Bax, "NMRPipe: A multidimensional spectral processing system based on UNIX pipes," *Journal of Biomolecular NMR*, vol. 6, no. 3, pp. 277–293, 1995.

[133] W. F. Vranken, W. Boucher, T. J. Stevens, R. H. Fogh, A. Pajon, M. Llinas, E. L. Ulrich, J. L. Markley, J. Ionides, and E. D. Laue, "The CCPN data model for NMR spectroscopy: development of a software pipeline.," *Proteins*, vol. 59, pp. 687–696, Jun 2005.

[134] W. Lee, M. Tonelli, and J. L. Markley, "NMRFAM-SPARKY: enhanced software for biomolecular NMR spectroscopy.," *Bioinformatics*, vol. 31, pp. 1325–1327, Apr 2015.

[135] Y. Shen, F. Delaglio, G. Cornilescu, and A. Bax, "TALOS+: a hybrid method for predicting protein backbone torsion angles from NMR chemical shifts.," *J Biomol NMR*, vol. 44, pp. 213–223, Aug 2009.

[136] Y. Shen and A. Bax, "SPARTA+: a modest improvement in empirical NMR chemical shift prediction by means of an artificial neural network.," *J Biomol NMR*, vol. 48, pp. 13–22, Sep 2010.

[137] M. Niklasson, R. Otten, A. Ahlner, C. Andresen, J. Schlagnitweit, K. Petzold, and P. Lundström, "Comprehensive analysis of NMR data using advanced line shape fitting," *Journal of Biomolecular NMR*, vol. 69, no. 2, pp. 93–99, 2017.

[138] G. Zhu, Y. Xia, L. K. Nicholson, and K. H. Sze, "Protein dynamics measurements by TROSY-based NMR experiments.," *J Magn Reson*, vol. 143, pp. 423–426, Apr 2000.

[139] L. E. Kay, D. A. Torchia, and A. Bax, "Backbone dynamics of proteins as studied by nitrogen-15 inverse detected heteronuclear NMR spectroscopy: application to staphylococcal nuclease," *Biochemistry*, vol. 28, pp. 8972–8979, 11 1989.

[140] Schrödinger, LLC, "The PyMOL molecular graphics system, version 1.8." November 2015.

[141] P. Pernot, P. Theveneau, T. Giraud, R. N. Fernandes, D. Nurizzo, D. Spruce, J. Surr, S. McSweeney, A. Round, F. Felisaz, L. Foedinger, A. Gobbo, J. Huet, C. Villard, and F. Cipriani, "New beamline dedicated to solution scattering from biological macromolecules at the ESRF," *Journal of Physics: Conference Series*, vol. 247, p. 012009, oct 2010.

[142] C. E. Blanchet, A. Spilotros, F. Schwemmer, M. A. Graewert, A. Kikhney, C. M. Jeffries, D. Franke, D. Mark, R. Zengerle, F. Cipriani, S. Fiedler, M. Roessle, and D. I. Svergun, "Versatile sample environments and automation for biological solution X-ray scattering experiments at the P12 beamline (PETRA III, DESY)," *Journal of applied crystallography*, vol. 48, pp. 431–443, 03 2015.

[143] P. V. Konarev, V. V. Volkov, A. V. Sokolova, M. H. J. Koch, and D. I. Svergun, "*PRIMUS*: a Windows PC-based system for small-angle scattering data analysis," *Journal of Applied Crystallography*, vol. 36, pp. 1277–1282, Oct 2003.

[144] D. Svergun, C. Barberato, and M. H. J. Koch, "CRYSOL - a program to evaluate X-ray solution scattering of biological macromolecules from atomic coordinates," *Journal of Applied Crystallography*, vol. 28, pp. 768–773, 2020/02/11 1995.

[145] J. Trewhella, A. P. Duff, D. Durand, F. Gabel, J. M. Guss, W. A. Hendrickson, G. L. Hura, D. A. Jacques, N. M. Kirby, A. H. Kwan, J. Pérez, L. Pol-

lack, T. M. Ryan, A. Sali, D. Schneidman-Duhovny, T. Schwede, D. I. Svergun, M. Sugiyama, J. A. Tainer, P. Vachette, J. Westbrook, and A. E. Whitten, "2017 publication guidelines for structural modelling of small-angle scattering data from biomolecules in solution: an update," *Acta crystallographica. Section D, Structural biology*, vol. 73, pp. 710–728, 09 2017.

[146] K. L. Sarachan, J. E. Curtis, and S. Krueger, "Small-angle scattering contrast calculator for protein and nucleic acid complexes in solution," *Journal of Applied Crystallography*, vol. 46, pp. 1889–1893, Dec 2013.

[147] D. Franke, M. V. Petoukhov, P. V. Konarev, A. Panjkovich, A. Tuukkanen, H. D. T. Mertens, A. G. Kikhney, N. R. Hajizadeh, J. M. Franklin, C. M. Jeffries, and D. I. Svergun, "*ATSAS 2.8*: a comprehensive data analysis suite for small-angle scattering from macromolecular solutions," *Journal of Applied Crystallography*, vol. 50, pp. 1212–1225, Aug 2017.

[148] A. T. Brunger, "Version 1.2 of the Crystallography and NMR system," *Nature Protocols*, vol. 2, no. 11, pp. 2728–2733, 2007.

[149] M. Sonntag, P. K. A. Jagtap, B. Simon, M.-S. Appavou, A. Geerlof, R. Stehle, F. Gabel, J. Hennig, and M. Sattler, "Segmental, domain-selective perdeuteration and small-angle neutron scattering for structural analysis of multi-domain proteins," *Angewandte Chemie (International ed. in English)*, vol. 56, pp. 9322—9325, August 2017.

[150] G. A. Stoll, S.-I. Oda, Z.-S. Chong, M. Yu, S. H. McLaughlin, and Y. Modis, "Structure of KAP1 tripartite motif identifies molecular interfaces required for retroelement silencing.," *Proc Natl Acad Sci U S A*, vol. 116, pp. 15042–15051, Jul 2019.

[151] A. A. McCarthy, R. Barrett, A. Beteva, H. Caserotto, F. Dobias, F. Felisaz, T. Giraud, M. Guijarro, R. Janocha, A. Khadrouche, M. Lentini, G. A. Leonard, M. Lopez Marrero, S. Malbet-Monaco, S. McSweeney, D. Nurizzo, G. Papp, C. Rossi, J. Sinoir, C. Sorez, J. Surr, O. Svensson, U. Zander, F. Cipriani, P. Theveneau, and C. Mueller-Dieckmann, "ID30B – a versatile beamline for macromolecular crystallography experiments at the ESRF," *Journal of Synchrotron Radiation*, vol. 25, pp. 1249–1260, Jul 2018.

[152] W. Kabsch, "*XDS*," *Acta Crystallographica Section D*, vol. 66, pp. 125–132, Feb 2010.

[153] G. Bunkóczi, N. Echols, A. J. McCoy, R. D. Oeffner, P. D. Adams, and R. J. Read, "Phaser.mrage: automated molecular replacement," *Acta crystallographica. Section D, Biological crystallography*, vol. 69, pp. 2276–2286, 11 2013.

[154] N. Stein, "*CHAINSAW*: a program for mutating pdb files used as templates in molecular replacement," *Journal of Applied Crystallography*, vol. 41, pp. 641–643, Jun 2008.

[155] J. Gabadinho, A. Beteva, M. Guijarro, V. Rey-Bakaikoa, D. Spruce, M. W. Bowler, S. Brockhauser, D. Flot, E. J. Gordon, D. R. Hall, B. Lavault, A. A. McCarthy, J. McCarthy, E. Mitchell, S. Monaco, C. Mueller-Dieckmann, D. Nurizzo, R. B. G. Ravelli, X. Thibault, M. A. Walsh, G. A. Leonard, and S. M. McSweeney, "*MxCuBE*: a synchrotron beamline control environment customized for macromolecular crystallography experiments," *Journal of Synchrotron Radiation*, vol. 17, pp. 700–707, Sep 2010.

[156] M. Cianci, G. Bourenkov, G. Pompidor, I. Karpics, J. Kallio, I. Bento, M. Roessle, F. Cipriani, S. Fiedler, and T. R. Schneider, "P13, the EMBL macromolecular crystallography beamline at the low-emittance PETRA III ring for high- and low-energy phasing with variable beam focusing," *Journal of Synchrotron Radiation*, vol. 24, pp. 323–332, Jan 2017.

[157] G. N. Murshudov, A. A. Vagin, and E. J. Dodson, "Refinement of Macromolecular Structures by the Maximum-Likelihood Method," *Acta Crystallographica Section D*, vol. 53, pp. 240–255, May 1997.

[158] P. Emsley and K. Cowtan, "*Coot*: model-building tools for molecular graphics," *Acta Crystallographica Section D*, vol. 60, pp. 2126–2132, Dec 2004.

[159] J. Schindelin, I. Arganda-Carreras, E. Frise, V. Kaynig, M. Longair, T. Pietzsch, S. Preibisch, C. Rueden, S. Saalfeld, B. Schmid, J.-Y. Tinevez, D. J. White, V. Hartenstein, K. Eliceiri, P. Tomancak, and A. Cardona, "Fiji: an open-source platform for biological-image analysis," *Nature Methods*, vol. 9, pp. 676 EP –, 06 2012.

[160] F. Madeira, Y. M. Park, J. Lee, N. Buso, T. Gur, N. Madhusoodanan, P. Basutkar, A. R. N. Tivey, S. C. Potter, R. D. Finn, and R. Lopez, "The EMBL-EBI search and sequence analysis tools APIs in 2019.," *Nucleic Acids Res*, vol. 47, pp. W636–W641, Jul 2019.

[161] I. Letunic and P. Bork, "Interactive Tree Of Life (iTOL): an online tool for phy-

logenetic tree display and annotation.," *Bioinformatics*, vol. 23, pp. 127–128, Jan 2007.

[162] V. Sklenář and A. Bax, "Spin-echo water suppression for the generation of pure-phase two-dimensional NMR spectra," *Journal of Magnetic Resonance (1969)*, vol. 74, no. 3, pp. 469 – 479, 1987.

[163] G. Bodenhausen and D. J. Ruben, "Natural abundance nitrogen-15 NMR by enhanced heteronuclear spectroscopy," *Chemical Physics Letters*, vol. 69, no. 1, pp. 185 – 189, 1980.

[164] I. R. Kleckner and M. P. Foster, "An introduction to NMR-based approaches for measuring protein dynamics," *Biochimica et biophysica acta*, vol. 1814, pp. 942–968, 08 2011.

[165] H. Lin, M. Jiang, L. Liu, Z. Yang, Z. Ma, S. Liu, Y. Ma, L. Zhang, and X. Cao, "The long noncoding RNA Lnczc3h7a promotes a TRIM25-mediated RIG-I antiviral innate immune response.," *Nat Immunol*, vol. 20, pp. 812–823, Jul 2019.

[166] V. H. Meller and B. P. Rattner, "The roX genes encode redundant male-specific lethal transcripts required for targeting of the MSL complex," *The EMBO journal*, vol. 21, pp. 1084–1091, 03 2002.

[167] A. S. Goryunov, "H/D isotope effects on protein hydration and interaction in solution.," *Gen Physiol Biophys*, vol. 25, pp. 303–311, Sep 2006.

[168] D. S. Wishart and B. D. Sykes, "The 13C Chemical-Shift Index: A simple method for the identification of protein secondary structure using 13C chemical-shift data," *Journal of Biomolecular NMR*, vol. 4, no. 2, pp. 171–180, 1994.

[169] K. Onomoto, M. Jogi, J.-S. Yoo, R. Narita, S. Morimoto, A. Takemura, S. Sambhara, A. Kawaguchi, S. Osari, K. Nagata, T. Matsumiya, H. Namiki, M. Yoneyama, and T. Fujita, "Critical role of an antiviral stress granule containing RIG-I and PKR in viral detection and innate immunity," *PloS one*, vol. 7, no. 8, pp. e43031–e43031, 2012.

[170] S. Jain, J. R. Wheeler, R. W. Walters, A. Agrawal, A. Barsic, and R. Parker, "ATPase-modulated stress granules contain a diverse proteome and substructure," *Cell*, vol. 164, pp. 487–498, 01 2016.

[171] S. Markmiller, S. Soltanieh, K. L. Server, R. Mak, W. Jin, M. Y. Fang, E.-C. Luo, F. Krach, D. Yang, A. Sen, A. Fulzele, J. M. Wozniak, D. J. Gonzalez, M. W.

Kankel, F.-B. Gao, E. J. Bennett, E. Lécuyer, and G. W. Yeo, "Context-dependent and disease-specific diversity in protein interactions within stress granules," *Cell*, vol. 172, pp. 590–604.e13, 01 2018.

[172] G. Chen, L.-C. Ma, S. Wang, R. L. Woltz, E. M. Grasso, G. T. Montelione, and R. M. Krug, "A double-stranded RNA platform is required for the interaction between a host restriction factor and the NS1 protein of influenza A virus.," *Nucleic Acids Res*, vol. 48, pp. 304–315, Jan 2020.

[173] J. G. Sanchez, J. J. Chiang, K. M. Sparrer, S. L. Alam, M. Chi, M. D. Roganowicz, B. Sankaran, M. U. Gack, and O. Pornillos, "Mechanism of trim25 catalytic activation in the antiviral rig-i pathway," *Cell reports*, vol. 16, pp. 1315–1325, 08 2016.

[174] C. Weinert, D. Morger, A. Djekic, M. G. Grütter, and P. R. E. Mittl, "Crystal structure of TRIM20 C-terminal coiled-coil/B30.2 fragment: implications for the recognition of higher order oligomers," *Scientific Reports*, vol. 5, no. 1, p. 10819, 2015.

[175] K. J.-L. Riley and r. Maher, L James, "p53 RNA interactions: new clues in an old mystery," *RNA (New York, N.Y.)*, vol. 13, pp. 1825–1833, 11 2007.

[176] B. Elenbaas, M. Dobbelstein, J. Roth, T. Shenk, and A. J. Levine, "The MDM2 oncoprotein binds specifically to RNA through its RING finger domain," *Molecular medicine (Cambridge, Mass.)*, vol. 2, pp. 439–451, 07 1996.

[177] T. H. Shen, H.-K. Lin, P. P. Scaglioni, T. M. Yung, and P. P. Pandolfi, "The mechanisms of PML-nuclear body formation," *Mol. Cell*, vol. 24, pp. 331–339, Nov 2006.

[178] K.-S. Inn, M. U. Gack, F. Tokunaga, M. Shi, L.-Y. Wong, K. Iwai, and J. U. Jung, "Linear ubiquitin assembly complex negatively regulates RIG-I- and TRIM25-mediated type i interferon induction," *Molecular cell*, vol. 41, pp. 354–365, 02 2011.

[179] V. Hornung, J. Ellegast, S. Kim, K. Brzozka, A. Jung, H. Kato, H. Poeck, S. Akira, K.-K. Conzelmann, M. Schlee, S. Endres, and G. Hartmann, "5'-triphosphate RNA is the ligand for RIG-I," *Science*, vol. 314, pp. 994–997, Nov 2006.

[180] M. U. Gack, E. Nistal-Villán, K.-S. Inn, A. García-Sastre, and J. U. Jung, "Phosphorylation-mediated negative regulation of RIG-I antiviral activity," *Jour-*

nal of Virology, vol. 84, no. 7, pp. 3220–3229, 2010.

[181] C. Lai, L. Liu, Q. Liu, S. Cheng, K. Wang, L. Zhao, M. Xia, C. Wang, H. Gu, Y. Duan, Z. Zhao, L. Zhang, Z. Liu, J. Luo, J. Song, P. Yang, R. Chen, and X. Wang, "Long noncoding rna *AVAN* promotes antiviral innate immunity by interacting with trim25 and enhancing the transcription of foxo3a," *bioRxiv*, p. 623132, 01 2019.

[182] P. D. Uchil, A. Hinz, S. Siegel, A. Coenen-Stass, T. Pertel, J. Luban, and W. Mothes, "TRIM protein-mediated regulation of inflammatory and innate immune signaling and its association with antiretroviral activity.," *J Virol*, vol. 87, pp. 257–272, Jan 2013.

[183] C. Zhao, M. Jia, H. Song, Z. Yu, W. Wang, Q. Li, L. Zhang, W. Zhao, and X. Cao, "The E3 ubiquitin ligase TRIM40 attenuates antiviral immune responses by targeting MDA5 and RIG-I," *Cell Reports*, vol. 21, no. 6, pp. 1613 – 1623, 2017.

[184] H. Oshiumi, M. Miyashita, M. Matsumoto, and T. Seya, "A distinct role of Riplet-mediated K63-linked polyubiquitination of the RIG-I repressor domain in human antiviral innate immune responses.," *PLoS Pathog*, vol. 9, no. 8, p. e1003533, 2013.

[185] M. W. Hentze, A. Castello, T. Schwarzl, and T. Preiss, "A brave new world of RNA-binding proteins," *Nat. Rev. Mol. Cell Biol.*, vol. 19, p. 327, 01 2018.

[186] W.-C. Hsin, C.-H. Chang, C.-Y. Chang, W.-H. Peng, C.-L. Chien, M.-F. Chang, and S. C. Chang, "Nucleocapsid protein-dependent assembly of the RNA packaging signal of Middle East respiratory syndrome coronavirus," *Journal of Biomedical Science*, vol. 25, no. 1, p. 47, 2018.

[187] C. L. Parks, S. E. Witko, C. Kotash, S. L. Lin, M. S. Sidhu, and S. A. Udem, "Role of V protein RNA binding in inhibition of measles virus minigenome replication," *Virology*, vol. 348, no. 1, pp. 96 – 106, 2006.

[188] N. J. Greenfield, "Using circular dichroism spectra to estimate protein secondary structure," *Nature protocols*, vol. 1, no. 6, pp. 2876–2890, 2006.